

**THE USE OF PUMPING TESTS TO MEASURE THE VERTICAL
HYDRAULIC PROPERTIES OF SEDIMENTARY ROCK
FORMATIONS**

by

Jessica Marjorie Worley

A thesis submitted to the Department of Civil Engineering

In conformity with the requirements for
the degree of Master of Applied Science

Queen's University

Kingston, Ontario, Canada

(August, 2012)

Copyright © Jessica Marjorie Worley, 2012

Abstract

An analytical model is presented for the interpretation of pumping tests conducted in a fractured rock aquifer. The solution accommodates multiple horizontal fractures intersecting pumping and observation wells with interconnecting vertical fracture features. The uppermost horizontal fracture is connected via this fracture network to a free surface boundary. Wellbore storage is included at the pumping and observation wells using an approximate superposition technique and the solution is derived using the Laplace transform method. Evaluation is performed by numerical inversion using the Talbot algorithm. Sensitivity of the model to the governing hydraulic parameters for both pumping and observation well data is presented for a realistic range of values for fractured rock. A field example is given to demonstrate the application of the model and to explore the uniqueness of the interpreted values. Based on the results obtained using the present analytical model, estimation of unique values of the vertical hydraulic parameters in a sedimentary rock setting may not be possible using pumping test results.

Subsequently, measuring aquifer properties from various testing methods was investigated to explore the significance of fracture heterogeneities relative to tested volumes and to determine which testing methods were capable of producing reliable parameter estimates. The hydrogeological study was performed in a fractured sedimentary rock aquifer using four different field testing methods: constant head tests, pulse interference tests, 12-hour isolated interval pumping tests and 48-hour open-hole pumping tests. Particular emphasis was placed on the reliable estimation of vertical hydraulic parameters in this setting. The evaluation of the pumping test data was performed using the analytical model derived earlier to determine whether the new pumping test model could produce confident estimates of vertical hydraulic parameters. While estimates of horizontal hydraulic conductivity measurements were not affected by test method, open-well pumping tests do not appear able to predict values of vertical hydraulic

conductivity and specific yield. Alternatively, pulse interference tests may be a less time-intensive option to constant head injection tests for determining vertical parameters in a sedimentary rock setting.

Acknowledgements

This manuscript would never have been completed without the help of a few notable individuals. First, I would like to thank my supervisor, Kent Novakowski, who patiently guided me through this entire process and offered invaluable insight and advice every step of the way. I also wish to thank Chris Jungkunz for his help, constant enthusiasm and company during the long hours of field work, as well as the Hamilton Conservation authority for granting me access to the Fletcher Creek Ecological Preserve. Thanks to my fellow graduate students, especially those I shared an office with in Ellis 222. I will smile when I think of the friends I have made and the memories I share with you, both in and out of the office.

Last, I am grateful to my parents, my brothers and my sister for their unwavering encouragement and my friends who have provided endless support and inspiration through this writing process. I will thank each of you in person.

Forward

This document has been created in accordance with the requirements for a manuscript format thesis. Chapter 1 provides an introduction to the motivation of the study and a critical review of previous research on the topic. The manuscripts comprising Chapters 2 and 3 have been submitted for publication. Chapter 2 has been submitted to *Advances in Water Resources*, and Chapter 3 has been submitted to the *Journal of Hydrology*. Chapter 4 discusses the results obtained from the second and third chapters, and Chapter 5 presents the conclusions of the study. Appendix A contains a detailed derivation of the analytical model that was developed in Chapter 2. Appendix B contains the implementation of the observation well solution in FORTRAN. Appendix C contains the implementation of the source well solution in FORTRAN. Appendix D contains detailed hydraulic parameter estimates from various hydraulic tests conducted at the Fletcher Creek field site. Appendix E contains additional results of the sensitivity analysis performed on the pumping test model derived in Chapter 2 and Appendix F contains the results of the sensitivity analysis performed using the Elmhirst and Novakowski (2012) solution for a pulse interference test.

Table of Contents

Abstract.....	ii
Acknowledgements.....	iv
Forward.....	v
Chapter 1 Introduction.....	1
1.1 Literature cited.....	5
Chapter 2 Interpretation of open-well pumping tests conducted in a fractured rock aquifer: Estimating specific yield and vertical hydraulic conductivity	7
2.1 Introduction.....	8
2.2 Model derivation.....	11
2.3 Sensitivity of model parameters to pumping test response.....	17
2.4 Field study.....	19
2.4.1 Testing procedure.....	20
2.4.2 Fitting to field data.....	20
2.5 Model results and discussion	22
2.6 Conclusions and recommendations.....	25
2.7 List of abbreviations	27
2.8 Literature cited.....	29
Chapter 3 Comparison of methods for measuring vertical hydraulic properties in a sedimentary rock aquifer.....	40
3.1 Introduction.....	41
3.2 Field setting and previous studies	44
3.3 Test methodology.....	46
3.4 Analysis and results	47
3.4.1 Constant head tests.....	48
3.4.2 Pumping tests conducted using isolated zones.....	50
3.4.3 Pulse interference tests.....	51
3.4.4 Pumping tests	52
3.5 Discussion.....	53
3.5.1 Horizontal hydraulic conductivity	53
3.5.2 Vertical hydraulic conductivity.....	54
3.5.3 Specific storage.....	55
3.5.4 Specific yield	56

3.6 Conclusions and recommendations.....	57
3.7 List of abbreviations	59
3.8 Literature cited.....	60
Chapter 4 Discussion	77
4.1 Literature cited.....	79
Chapter 5 Conclusion.....	80
Appendix A Detailed derivation of the pumping test solution	81
Appendix B Pumping test solution observation well Fortran code.....	93
Appendix C Pumping test solution source well Fortran code.....	103
Appendix D Hydraulic parameter estimates from Fletcher Creek field site	113
Appendix E Sensitivity of model parameters to pumping test response.....	125
Appendix F Sensitivity of the source and interference responses to the Elmhirst and Novakowski (2012) solution for a pulse interference test.....	136

List of Figures

Figure 2.1 Conceptual model of the fractured rock aquifer. The datum is set at $z=0$ which is also considered the no flow boundary (Elmhirst and Novakowski, 2012a).....	33
Figure 2.2 Effect of specific yield on the pumping test observation well response. Base case values in Table 2.1 were held fixed while four separate model runs were conducted with values of S_y ranging between 10^{-3} and 10^{-6}	34
Figure 2.3 Effect of vertical hydraulic conductivity on the pumping test observation well response. Base case values in Table 2.1 were held fixed while four separate model runs were conducted with values of K' ranging between 2.0×10^{-6} and 10^{-11}	35
Figure 2.4 Location map of Fletcher Creek Conservation Area in southern Ontario.	36
Figure 2.5 Plan view of borehole locations at the Fletcher Creek Conservation Area field site. ...	37
Figure 2.6 Pumping test response in observation well FC-1 to pumping in source well FC-9 using the present model. Table 2.3 presents the parameter estimation results.	38
Figure 2.7 Pumping test response in FC-1 to pumping in FC-9 with the present model and the Moench (1997) solution. Table 2.3 presents parameter estimations obtained from both models..	39
Figure 3.1 Location map of Fletcher Creek Conservation Area in southern Ontario.	66
Figure 3.2 Plan view of borehole locations at the Fletcher Creek Conservation Area field site. ...	67
Figure 3.3 Transmissivity profile with depth for well FC-3 and a packer spacing of 0.5 m.	68
Figure 3.4 Example of isolated intervals for 12-hour pumping test performed by Lapcevic, et al. (1993).....	69
Figure 3.5 Sensitivity analysis of observation well response to various values of S_s' as determined by the Elmhirst and Novakowski (2012) solution for a pulse interference test.	70
Figure 3.6 Pulse interference test response in observation well FC-1 to slug injection in FC-9. ...	71
Figure 3.7 Log-log plot of geometric mean hydraulic conductivity results and standard deviations obtained from various tests with respect to measurement duration.	72
Figure 3.8 Log-log plot of geometric mean vertical hydraulic conductivity results and standard deviations obtained from various tests with respect to measurement duration.....	73
Figure 3.9 Log-log plot of arithmetic mean specific storage results and standard deviations obtained from various tests with respect to measurement duration.	74
Figure 3.10 Log-log plot of arithmetic mean vertical specific storage results and standard deviations obtained from various tests with respect to measurement duration.....	75
Figure 3.11 Log-log plot of arithmetic mean specific yield results and standard deviations obtained from various tests with respect to measurement duration.	76

List of Tables

Table 2.1 Base case values used in the sensitivity analysis	32
Table 2.2 Comparison of estimated hydraulic parameters between the Moench (1997) and present pumping test solution.	32
Table 2.3 Estimate of hydraulic parameters predicted by both the Moench (1997) and present model solutions for the pumping test response in FC-1 to pumping FC-9.	32
Table 2.4 Sensitivity of vertical hydraulic conductivity to fixed values of specific yield using present pumping test model.	33
Table 3.1 Specific yield estimates from constant head test data analysis.	63
Table 3.2 Base case values used in the sensitivity analysis.	64
Table 3.3 Comparison of mean (standard deviation) for various tests and hydraulic parameters.	65

Chapter 1

Introduction

Fractured rock aquifers are important sources of drinking water in many parts of the world yet can be particularly susceptible to contamination. This inherent vulnerability is due to the preponderance of low rock matrix porosities that make up the bulk of the aquifer, and the fracture conduits which allow for fluid to move at relatively high velocities. In these settings, quantifying bulk hydraulic parameters in the field from aquifer tests and applying these parameters to determine water availability can be difficult (Abbey and Allen, 2000). Issues arise in the ability to analytically determine how high-permeability fractures transmit the majority of the water and how the lower-permeability fractures and matrix provides the storage capacity.

Since the process of identifying, isolating and testing individual fractures can be a labour-intensive, time-consuming and expensive process (Le Borgne, et al., 2006), the relatively simple pumping test is preferred for obtaining representative bulk parameter values. A typical pumping test is conducted by extracting water from a well at a constant rate while monitoring hydraulic head in the source well and in nearby observation wells. Since the first mathematical analysis of drawdown in a well by Theis (1935), analytical models for pumping tests have been developed to better represent a range of formation characteristics and boundary conditions. In particular, the ability to obtain representative vertical hydraulic parameter values has become a focus as these are important for the estimation of groundwater recharge, determining the susceptibility to aquifer contamination from surface sources, and for aquifer remediation.

Accordingly, the first goal of this study is to develop an analytical pumping test model that will improve hydraulic characterization in a fractured rock setting. Most analytical models used at

present were initially developed for homogeneous porous media. In current practice however, these porous media models are applied to heterogeneous fractured rock settings by assuming an equivalent porous media over a certain volume of aquifer (e.g. Raven, 1986; Barrash and Ralston, 1991; Peffer, 1991; Lee et al., 1992; McConnell, 1993). However as shown in Muldoon and Bradbury (2005), bulk hydraulic conductivity values obtained from open-hole pumping tests in a carbonate aquifer with a dense network of fractures could not adequately describe the differences in groundwater travel times observed from separate tests on isolated fractures. Thus while porous media analytical models may be adequate given a highly fractured setting (e.g., Bair and Roadcap, 1992; Podgorney and Ritzi, 1997), the accuracy of parameter estimates has proven to be unreliable in some cases where a few large fractures dominate the flow network (Muldoon and Bradbury, 2005).

Numerous studies have been conducted to explore hydraulic parameter estimates in the horizontal orientation using different tests in a sedimentary rock setting. Parameters such as effective porosity (e.g., Ii, 1995; Bernard et al., 2006), hydraulic conductivity (e.g., Rovey, 1994; Ii, 1995; Nastev et al., 2004; Hunt, 2006), transmissivity (e.g., Abbey and Allen, 2000; Nastev et al., 2004) and storativity (e.g., Rovey, 1998; Abbey and Allen, 2000) have been studied. To date, there have been only a few limited studies conducted on estimating vertical hydraulic conductivity, K' (Reichart, 1992; Hart, 2006; Lemieux et al, 2006) and to the author's knowledge, none on estimating specific yield (S_y) in a sedimentary rock environment. This is despite the fact that accurate estimation of vertical hydraulic conductivity and specific yield is important for projections of regional municipal water supply (Eaton et al., 2007).

In fact few detailed groundwater studies have been published for fractured sedimentary rock, and more specifically, aquifers in fractured dolostone. Of the few, the role of bedding plane fractures for groundwater flow has been illustrated by Novakowski and Lapcevic (1988) in dolostones of

the Niagara Peninsula in Ontario, Canada, by Michalski and Britton (1997) in the Newark Basin, New Jersey, USA and by Lemieux et al. (2006) in St-Eustache, Québec, Canada. In these studies, the importance of using several characterization methods to locate the horizontal bedding planes, identified as the controlling factor for flow, was advised to properly understand groundwater movement in this setting.

In this thesis, an analytical model for pumping tests is derived that accounts for permeable fractures which connect wells, and for fractures distributed vertically. The utility of this model is then explored by application to the interpretation of several pumping tests conducted in an unconfined limestone aquifer. A comparison is also made to other methods of characterization particularly those used for the estimation of vertical hydraulic properties.

In Chapter 2, the mathematical development for an open-hole pumping test solution is presented. The new model incorporates groundwater contribution from the vertical fracture domain to an uppermost horizontal fracture, and accommodates for additional horizontal fractures occurring at depth interconnected by additional vertical fractures. Horizontal bedding planes are likely the most important feature to identify in a sedimentary rock setting due to their potentially high permeability and great lateral extent (Novakowski et al., 1999; Lemieux, et al., 2006). The water table is described as a moving free boundary and wellbore storage and skin effects are accounted for. The model also incorporates a relaxation coefficient, α_1 , developed by Moench (1995, 1997) based on concepts presented in Boulton (1954, 1963) for delayed drainage. As the Moench (1997) solution can make accurate estimations of specific yield and vertical hydraulic conductivity from pumping tests conducted in unconfined porous media, it will be used to compare the accuracy of the model developed in this paper for a fractured rock aquifer.

Discrepancies between small and large-scale hydraulic testing procedures are common in fractured rock due to the natural spatial variability of fractures. These variances are particularly important to consider in development of groundwater models or when resource constraints limit discrete fracture testing. In many instances, the use of small-scale values for predicting large-scale properties may be unrepresentative of the geologic setting as a whole. Chapter 3 evaluates the applicability of the model developed in Chapter 2 for an open-hole pumping test in a fractured sedimentary rock aquifer. This is done by comparing four different field testing methods: constant head tests, pulse interference tests, 12-hour isolated interval pumping tests and 48-hour open-hole pumping tests. As in Chapter 2, particular emphasis is placed on the accurate estimation of vertical hydraulic parameters.

Following the comparison of hydraulic testing methods in Chapter 3, Chapter 4 presents a discussion of the results obtained in Chapters 2 and 3, and Chapter 5 describes the conclusions and implications of the study performed.

1.1 Literature cited

- Abbey, D. G., & Allen, D. M. (2000). Fracture zones, aquifer testing, and scale effects: Considerations in fractured bedrock aquifers of southwestern British Columbia. Proceedings of the 53rd Canadian Geotechnical Conference, Montréal, Québec.
- Bair, E. S., & Roadcap, G. S. (1992). Comparison of flow models used to delineate capture zones of wells: 1. leaky-confined fractured-carbonate aquifer *Ground Water*, 30(2), 199.
- Bernard, S., Delay, F., & Porel, G. (2006). A new method of data inversion for the identification of fractal characteristics and homogenization scale from hydraulic pumping tests in fractured aquifers. *Journal of Hydrology*, 328(3–4), 647-658.
- Barrash, W., & Ralston, D. R. (1991). Analytical modeling of a fracture zone in the Brule formation as an aquifer receiving leakage from water-table and elastic aquitards *Journal of Hydrology*, 125(1-2), 1.
- Boulton, N. S. (1954). Unsteady radial flow to a pumped well allowing for delayed yield from storage. *Intern Assoc Sci Hydrol Publ*, 37, 472-477.
- Boulton, N. S. (1963). Analysis of data from non-equilibrium pumping tests allowing for delayed yield from storage. *Proc Inst of Civil Engineers*, 26(3), 469-482.
- Eaton, T. T., Anderson, M. P., & Bradbury, K. R. (2007). Fracture control of ground water flow and water chemistry in a rock aquitard *Ground Water*, 45(5), 601-615.
- Hart, D. J., Bradbury, K. R., & Feinstein, D. T. (2006). The vertical hydraulic conductivity of an aquitard at two spatial scales. *Ground Water*, 44(2), 201-211.
- Hunt, A. G. (2006). Scale-dependent hydraulic conductivity in anisotropic media from dimensional cross-over *Hydrogeology Journal*, 14(4), 499.
- Li, H. (1995). Effective porosity and longitudinal dispersivity of sedimentary rocks determined by laboratory and field tracer tests *Environmental Geology*, 25(2), 71.
- Le Borgne, T., Bour, O., Paillet, F. L., & Caudal, J. (2006). Assessment of preferential flow path connectivity and hydraulic properties at single-borehole and cross-borehole scales in a fractured aquifer *Journal of Hydrology*, 328(1-2), 347-359.
- Lee, R. R., Ketelle, R. H., Bownds, J. M., & Rizk, T. A. (1992). Aquifer analysis and modeling in a fractured, heterogeneous medium *Ground Water*, 30(4), 589.
- Lemieux, J., Therrien, R., & Kirkwood, D. (2006). Small scale study of groundwater flow in a fractured carbonate-rock aquifer at the St-Eustache quarry, Québec, Canada *Hydrogeology Journal*, 14(4), 603-612.
- McConnell, C. L. (1993). Double porosity well testing in the fractured carbonate rocks of the Ozarks. *Ground Water*, 31(1), 75.

- Michalski, A., & Britton, R. (1997). The role of bedding fractures in the hydrogeology of sedimentary bedrock-evidence from the Newark basin, New Jersey *Ground Water*, 35(2), 318.
- Moench, A. F. (1995). Combining the Neuman and Boulton models for flow to a well in an unconfined aquifer *Ground Water*, 33(3), 378-384.
- Moench, A. F. (1997). Flow to a well of finite diameter in a homogeneous, anisotropic water table aquifer *Water Resources Research*, 33(6), 1397.
- Muldoon, M.A., & Bradbury, K. R. (2005). Site characterization in densely fractured dolomite: Comparison of methods *Ground Water*, 43(6), 863-876.
- Nastev, M., Savard, M. M., Lapcevic, P., Lefebvre, R., & Martel, R. (2004). Hydraulic properties and scale effects investigation in regional rock aquifers, south-western Québec, Canada *Hydrogeology Journal*, 12(3).
- Novakowski, K. S., Lapcevic, P., Bickerton, G., Voralek, J., Zanini, L., & Talbot, C. (1999). The development of a conceptual model for contaminant transport in the dolostone underlying Smithville, Ontario (Final Report Submitted to the Smithville Phase IV Bedrock Remediation Program 175 pp.
- Novakowski, K. S., & Lapcevic, P. A. (1988). Regional hydrogeology of the Silurian and Ordovician sedimentary rock underlying Niagara falls, Ontario, Canada *Journal of Hydrology*, 104(1-4), 211.
- Peffer, J. R. (1991). Complex aquifer-aquitard relationships at an Appalachian plateau site. *Ground Water*, 29(2), 209.
- Podgorney, R. K., & Ritzi, R. W. (1997). Capture zone geometry in a fractured carbonate aquifer. *Ground Water*, 35(6), 1040-1049.
- Raven, K. (1986). Hydraulic characterization of a small ground-water flow system in fractured monzonitic gneiss. National Hydrology Research Institute Scientific Series, 149(30), 133.
- Reichart, T. M. (1992). Influence of vertical fractures in horizontally-stratified rocks. (Master of Science, University of Waterloo).
- Rovey II, C. W. (1994). Assessing flow systems in carbonate aquifers using scale effects in hydraulic conductivity *Environmental Geology*, 24(4), 244.
- Rovey II, C. W. (1998). Digital simulation of the scale effect in hydraulic conductivity *Hydrogeology Journal*, 6(2), 216.
- Theis, C. V. (1935). The relation between the lowering of the piezometric surface and the rate and duration of discharge of a well using ground-water storage *Eos, Transactions, American Geophysical Union*, 16, 519-524.

Chapter 2

Interpretation of open-well pumping tests conducted in a fractured rock aquifer: Estimating specific yield and vertical hydraulic conductivity

Chapter summary

An analytical model is presented for the interpretation of pumping tests conducted in a fractured rock aquifer. The solution accommodates multiple horizontal fractures intersecting pumping and observation wells with interconnecting vertical fracture features. The uppermost horizontal fracture is connected via this fracture network to a free surface boundary. Wellbore storage is included at the pumping and observation wells using an approximate superposition technique and the solution is derived using the Laplace transform method. Evaluation is performed by numerical inversion using the Talbot algorithm. Sensitivity of the model to the governing hydraulic parameters for both pumping and observation well data is presented for a realistic range of values for fractured rock. A field example is given to demonstrate the application of the model and to explore the uniqueness of the interpreted values. Based on the results obtained using the present analytical model, estimation of unique values of the vertical hydraulic parameters in a sedimentary rock setting may not be possible using pumping test results.

2.1 Introduction

In homogeneous porous media, pumping tests conducted in open wells have traditionally been a reliable method for determining the hydraulic characteristics of the bulk aquifer. In fractured media however, the geometry and permeability of fractures largely influence the drawdown in the aquifer. As a result, pumping test interpretation from data collected with open holes can yield estimates of hydraulic properties that may not be representative of the true rock properties (Tiedeman and Hsieh, 2001; Muldoon et al., 2001).

Fractured rock aquifers are often described as having zones of high permeability embedded within a low permeability rock matrix (NRC, 1996). This heterogeneity can create non-uniform flow paths that may involve substantial vertical components. In some settings, such as where sources of contamination at surface are present (Levison and Novakowski, 2009) or where estimates for recharge are required (Muldoon et al., 2001), it is necessary to characterize the vertical hydraulic conductivity, vertical specific storage, and the specific yield of the unconfined bedrock aquifer. A reliable and widely utilised method for estimating the hydraulic characteristics of individual boreholes in fractured rock is to measure transmissivity with depth using a straddle packer system and constant head injection tests (Karasaki et al, 1988; Shapiro and Nicholas, 1989; Zanini et al., 1999). To measure vertical hydraulic properties in particular, pumping tests conducted where identified fracture features are isolated in both the pumping and observation wells using packer systems may be utilised (Lapcevic et al, 1993). While such testing methods are essential for determining the permeability of individual fractures or local-scale properties, to understand the flow characteristics at a site or regional scale requires that separate tests on many different wells be performed. As these methods are time consuming and costly, to perform the number of constant head tests or isolated zone pumping tests necessary is not always an option due to resource constraints. For this reason, performing a simple open-well pumping test is often

more preferable despite the uncertainty in parameter estimation expected from such a test (Tiedeman and Hsieh, 2001).

The interpretation of pumping test data is generally based on mathematical models that relate the drawdown response in an observation well to discharge from a source well. Analytical models that account for wellbore storage and skin effects have been developed to quantify the vertical permeability of a layered system (Neuman and Witherspoon, 1968, 1969; Earlougher, 1980; Ehlig-Economides and Ayoub, 1984). Other models have incorporated the double-porosity concept (Raven, 1986; Barrash and Ralston, 1991; Peffer, 1991; Lee et al., 1992; McConnell, 1993), where to simplify the flow problem the water table was fixed as a constant head boundary during testing. In nature, the water table is a free moving boundary and cannot be assumed to be static, especially when the specific yield is small and drawdown is large. Moench (1995; 1997) built on expressions developed by Boulton (1954; 1963) for delayed drainage of water from the unsaturated zone, and incorporated these into the solution developed by Neuman (1972; 1974). The Neuman (1972; 1974) model accounted for the unconfined condition by assuming the occurrence of instantaneous drainage from the unsaturated zone above the falling water table. By taking into account both the unconfined condition and the non-instantaneous drainage of water from the unsaturated zone, the Moench (1997) solution can provide accurate estimates of specific yield and vertical hydraulic conductivity from pumping tests conducted in unconfined porous media (Elmhirst and Novakowski, 2012a; Levison and Novakowski, 2012). The validity of the Moench (1997) solution for a pumping test conducted in an unconfined bedrock aquifer, however, has not been explored.

Smaller-scale pulse interference test solutions have been developed to predict unique values of vertical hydraulic parameters in a fractured rock environment (a unique value refers to a single outcome or result, without alternative possibilities). For example, Stephenson and Novakowski

(2006) examined different boundary conditions involving vertical fractures to develop several pulse interference test models for an environment dominated by bedding plane fractures. The solution obtained for a constant head boundary was found to estimate unique values of horizontal zone transmissivity and vertical hydraulic conductivity; however, values of horizontal storativity and vertical specific storage could not be uniquely determined. Elmhirst and Novakowski (2012a) developed a pulse interference test model which incorporates a connection from an uppermost horizontal fracture feature to a moving free surface boundary at the water table for an open-hole test. While the model was not capable of uniquely estimating specific storage, unique values of transmissivity, storativity, vertical hydraulic conductivity and specific yield were obtained from application to a field example. As pulse interference tests are relatively local-scale (Stephenson and Novakowski, 2006), it is unclear if more site scale estimates (equally as unique) might be obtained using a pumping test interpreted using an analytical model based on the discrete fracture approach given in Elmhirst and Novakowski (2012a). As specific yield estimates obtained from pumping tests in fractured rock are sometimes claimed to be inaccurate (Bardenhagen, 2000), a careful examination of uniqueness and sensitivity is also warranted.

The primary objective of this study is to develop an analytical model for an open-hole pumping test that can reliably estimate specific yield and vertical hydraulic conductivity in a fractured rock formation. Using the new model, the second objective of this study is to explore the uniqueness of pumping test results in fractured rock. As noted by Healy and Cook (2002), it is incorrect to assume that if a theoretical curve matches an experimental drawdown curve, that the aquifer follows the assumptions inherent to the development of that theoretical curve. For that reason, special attention is paid to the uniqueness of values of specific yield and vertical hydraulic conductivity, in particular. This is explored using the results of an open-well pumping test conducted in a sedimentary rock formation.

2.2 Model derivation

The mathematical basis for this model is built on similar assumptions to those presented in Elmhirst and Novakowski (2012a) for a pulse interference test in a fractured rock setting. The model incorporates mathematical expressions developed by Moench (1995; 1997) and by Novakowski and Bickerton (1997) that accommodate water table fluctuations and the occurrence of multiple horizontal fractures, respectively. The effects of vertical flow are included in the matrix of the upper rock slab based on expressions developed by Stephenson and Novakowski (2006) and in the lower matrix slabs similar to Novakowski and Bickerton (1997). Figure 2.1 illustrates a conceptual model from which the boundary value problem is developed.

Prior to pumping, the elevation of the water table in the formation is assumed to be constant. During the test, flow in vertical fractures is assumed to be linear and flow in horizontal fractures is in the radial direction. Flow into both source and observation wells is assumed to be from horizontal fractures only.

Transient groundwater flow in horizontally fractured media can be described by the following governing equation given in dimensioned form as:

$$\frac{\partial^2 h}{\partial r^2} + \frac{1}{r} \frac{\partial h}{\partial r} - q = \frac{S}{T} \frac{\partial h}{\partial t} \quad r \geq r_w \quad 2.1$$

where h is the hydraulic head, r is the radial distance from the source well, q is the total groundwater contribution between vertical and horizontal fracture domains, S is horizontal fracture storativity, T is the horizontal fracture transmissivity, and r_w is the wellbore radius.

If a formation has n_f horizontal fractures that interconnect source and observation wells, then the total contribution q into the horizontal fracture domain is the summation of q_t and q_f where q_t

defines the water contribution into the topmost fracture and q_f defines the water contribution into remaining (n_f-1) horizontal fractures. Thus:

$$q = (n_f - 1)q_f + q_t \quad 2.2$$

The total contribution of groundwater (q_t) into the top horizontal fracture feature from its adjacent vertical domain is described by the contribution of water across the upper and lower top horizontal fracture interface:

$$q_t = q_{tu} + q_{tl} \quad 2.3$$

where q_{tu} represents the groundwater contribution across the upper fracture interface and q_{tl} the contribution across the lower interface of the top horizontal fracture. For each additional horizontal fracture, the groundwater contribution is described by:

$$q_f = q_{fu} + q_{fl} \quad 2.4$$

where q_{fu} and q_{fl} represent the upper and lower components of groundwater contribution, respectively.

The upper contribution is assumed to originate at the fracture centre and behave according to Darcy's law at the interface of the horizontal fracture and the vertical domain. Based on this, the following expression is developed:

$$q_{tu} = \frac{-K'}{T} \frac{\partial h_m}{\partial z} \Big|_{z=0} = 0; \quad 0 \leq z \leq L_w \quad 2.5$$

where K' is the hydraulic conductivity of the vertical fracture domain, h_m is the hydraulic head in the vertical fracture domain, z is the vertical distance from the centreline of the horizontal fracture and L_w is the vertical distance from the centre of the horizontal fracture to the water table.

Similarly, if the upper and lower groundwater contributions across the interface of each additional horizontal fracture are equal, then

$$q_{tl} = q_{fu} = q_{fl} = \frac{-K' \partial h_m}{T \partial z} \Big|_{z=0} = 0; \quad 0 \leq z \leq L_n \quad 2.6$$

where Darcy's law still applies, contribution once again is assumed to originate from the centre of each additional horizontal fracture and L_n is the half spacing between each horizontal fracture.

Flow in the vertical fracture system is expressed using the one-dimensional diffusion equation:

$$\frac{\partial^2 h_m}{\partial r^2} = \frac{S'_s \partial h}{K' \partial t}; z \geq 0 \quad 2.7$$

where S'_s is the specific storage of the vertical fracture system.

The outer boundary condition is based on the assumption that the horizontal fracture zone is infinite in extent and is described in terms of hydraulic head as:

$$h(\infty, t) = 0 \quad 2.8$$

A continuity relationship is used to link the horizontal and vertical fracture domains:

$$h(r, t) = h_m(r, 0, t) \quad 2.9$$

Fluctuations of the water table are accounted for using the expression developed by Moench (1995; 1997):

$$K' \frac{\partial h_m}{\partial z} \Big|_{z=L_w} = -\alpha_1 S_y \int_0^t \frac{\partial h_m(r, L_w, \tau)}{\partial \tau} \exp\{-\alpha_1(t - \tau)\} \partial \tau \quad 2.10$$

where S_y is the specific yield of the vertical fracture zone and α_1 is the relaxation coefficient that controls the exponential rate of drainage from the unsaturated zone.

The following boundary condition applies to the centre of each rock slab that contributes equal quantities of water to the horizontal fractures that bound it:

$$\left. \frac{\partial h_m}{\partial z} \right|_{z=L_n} = 0 \quad 2.11$$

The initial conditions that describe hydraulic head in both horizontal and vertical fracture domains are:

$$h(r, 0) = 0 \quad 2.12$$

$$h_m(r, z, 0) = 0 \quad 2.13$$

To incorporate the effects of wellbore storage in source and observation wells, an approximate solution method (Tongpenyai and Raghavan, 1981; Ogbe and Brigham, 1984; Novakowski, 1989; Stephenson and Novakowski, 2006; Elmhirst and Novakowski, 2012a) was used. This technique involves the superposition of the response at a point in the formation due to the influence of wellbore storage in each well. To begin, the inner boundary condition applied to the horizontal fracture features at the source well is specified as:

$$2\pi r_w T \left. \frac{\partial h}{\partial r_1} \right|_{r_1=r_w} = \pi r_s^2 \frac{\partial h_s}{\partial t} - Q \quad 2.14$$

where h_s is the hydraulic head in the source well, r_s is the radius of the source well casing, and r_1 is the radial distance from the source well to the point in the formation used in the approximate solution method.

Correspondingly, the inner boundary condition applied to the horizontal fracture features at the observation well is expressed as:

$$2\pi r_w T \left. \frac{\partial h}{\partial r_2} \right|_{r_2=r_w} = \pi r_{ob}^2 \frac{\partial h_{ob}}{\partial t} \quad 2.15$$

where h_{ob} is the hydraulic head in the observation well, r_{ob} is the radius of the well casing, and r_2 is the radial distance from the observation well to the point in the formation used in the approximate solution method.

Continuity between the horizontal fracture zone and source and observation wells is achieved using the following:

$$h_s(t) = h(r_w, t) \quad 2.16$$

$$h_{ob}(t) = h(r_w, t) \quad 2.17$$

The initial drawdown in the source well, prior to the initiation of pumping is:

$$h_s(0) = 0 \quad 2.18$$

and similarly in the observation well, the initial drawdown is described as follows:

$$h_{ob}(0) = 0 \quad 2.19$$

Taking the Laplace transforms of equations [2.15] through [2.19] and applying them to the particular solution generates the solution in Laplace space for the hydraulic head in the horizontal fracture domain:

$$\bar{h} = \frac{QK_0(r(\phi^{1/2}))K_0(r_2(\phi^{1/2})) - Q\xi_5K_0(r_1(\phi^{1/2}))}{p\gamma_3} \quad 2.20$$

where

$$\gamma_3 = K_0(r(\phi^{1/2}))^2 - \xi_5\xi_6 \quad 2.21$$

$$\varepsilon_5 = \frac{C_{ob}pK_0(r_w(\phi^{1/2})) + \lambda_w\phi^{1/2}K_1(r_w(\phi^{1/2}))}{C_{ob}p} \quad 2.22$$

$$\varepsilon_6 = \frac{C_s p K_0(r_w(\phi^{1/2})) + \lambda_w \phi^{1/2} K_1(r_w(\phi^{1/2}))}{C_s p} \quad 2.23$$

$$C_{ob} = \pi r_{ob}^2 \quad 2.24$$

$$C_s = \pi r_s^2 \quad 2.25$$

$$\lambda_w = 2\pi r_w T \quad 2.26$$

And the overbar indicates a Laplace transformed parameter. The hydraulic head in the source well is given by:

$$\bar{h}_s = \frac{1}{p} \left(\frac{Q}{p} + \frac{Q\xi_5 \lambda \phi^{1/2} K_1(r_w(\phi^{1/2}))}{p^2 \gamma_3 C_s} \right) \quad 2.27$$

and in the observation well it is given by:

$$\bar{h}_{ob} = \frac{-Q\lambda\phi^{1/2}K_1(r_w(\phi^{1/2}))K_0(r(\phi^{1/2}))}{p^3\gamma_3C_{ob}} \quad 2.28$$

The Laplace space solutions were numerically inverted using the Talbot (1979) algorithm. This inversion method has been successfully applied to similar problems (e.g., Barker and Black, 1983; Novakowski, 1989; Elmhirst and Novakowski, 2012a).

Verification of the solution was done algebraically, reducing the model to the Moench (1997) solution by reducing the number of fractures to one;

$$n_f=1 \quad 2.30$$

by increasing the thickness of the lower matrix slab until it became infinitely large (i.e. lower boundary is impermeable);

$$L_n \rightarrow \infty \quad 2.31$$

and by reducing the contribution entering the horizontal fracture domain from the vertical domain to an infinitesimally small number. The Moench (1997) solution is applicable to both pumped and observation well data.

2.3 Sensitivity of model parameters to pumping test response

An informal sensitivity analysis on the source and interference responses of the pumping test model was performed to determine whether unique values of specific yield and vertical hydraulic conductivity could be predicted. The parameter sensitivities were evaluated by varying base case values specified in Table 2.1 over a practical range given the geologic setting, and the variation in curve response was observed. The initial case values were chosen based on numbers presented in Stephenson and Novakowski (2006) for a sedimentary rock setting, and from Elmhirst and Novakowski (2012a) for the initial values of n_f , L_n , S_y and α_1 . T and S were specified to be two orders of magnitude greater than the vertical domain hydraulic conductivity and specific storage to reflect the dominance of the horizontal fracture zone that is typical of sedimentary rock formation (Stephenson and Novakowski, 2006). The Moench (1995; 1997) relaxation coefficient, α_1 was set to 1.0×10^9 to reflect instantaneous drainage from the unsaturated zone to the aquifer. Both studies cited above performed a similar sensitivity analysis and satisfactorily determined model performance in this way. The model and its sensitivities were calculated in the Laplace domain followed by numerical inversion to the time domain with responses presented as dimensionless hydraulic head (H/H_0) versus time in a log-log format.

The results of the entire sensitivity analysis relative to each hydraulic parameter are explored in Appendix E. The results of the sensitivity analysis to the parameters specific yield and vertical hydraulic conductivity are presented below.

The effect of specific yield on the observation well response is presented in Figure 2.2. The range of values shown is representative of the reported values in a similar geologic setting (Healy and Cook, 2002). Values of specific yield below 1.0×10^{-6} had little effect on the shape of the curve response; however, such small values are unlikely to be found in practice (Elmhirst and Novakowski, 2012a). At an elapsed time of 10^3 seconds, the differences in amplitude between curves A (1.0×10^{-3}) and D (1.0×10^{-6}) was 40% where at a later time this discrepancy widened to 64%, indicating greater sensitivity to specific yield with test progression and insensitivity at its earliest stages. This supports the contention in Novakowski et al. (2007) that longer tests are required for more accurate estimation of specific yield in these settings.

The effect of vertical hydraulic conductivity on the pumping test response is illustrated in Figure 2.3. The K' value of curve A is representative of a fractured rock setting with essentially no groundwater exchange between horizontal and vertical fracture zones. Values below 10^{-11} had minimal effect on the shape of the drawdown curve. A maximum K' value of 10^{-6} is representative of a highly fractured rock formation; increasing the value of vertical hydraulic conductivity from an impervious rock to that for a highly fractured rock results in a reduction in amplitude of 37 %.

Near-well aquifer properties can also be estimated by interpretation of drawdowns in a single pumped well in a porous media setting. Using the same range of specific yield values as used for Figure 2.2, however, the curves for drawdown in the pumping well were found to completely overlap. Similarly, a range of K' the same as used for Figure 2.2 also resulted in overlapping pumping well curves. Thus, the analytical model is unable to estimate unique values of specific yield and vertical hydraulic conductivity from drawdown versus time data obtained from the pumped well.

2.4 Field study

During the summer of 2011 a field investigation was completed in the Fletcher Creek Conservation Area, Puslinch Township in southern Ontario (Figure 2.4). The site was initially selected for a characterization study by Reichart (1992) due to the presence of an adjacent quarry that permitted correlation between fracture mapping and borehole data, while minimal overburden reduced drilling costs.

At the site, a thin layer of drift consisting of glacial till varies in thickness from approximately 0.5 to 2 meters. Underlying the till is the fractured dolostone of the Middle-Silurian Guelph and Amabel submembers of the Lockport Formation (Reichart, 1992). The stratigraphy is mostly flat-lying with a slight south-westward dip of approximately 4 to 6 metres per kilometer (Liberty, 1981). The Guelph submember is about 9 metres thick, while the Amabel submember is about 60 metres thick. The fracture permeability of the formation sustains domestic and moderate industrial and municipal water supplies.

In previous field investigations of the Fletcher Creek site, both inclined and vertical boreholes were drilled to investigate the three-dimensional interconnection of the larger scale fracture features present in the rock (Figure 2.5). Holes were diamond-drilled to a depth of approximately 30 meters using a 76 millimeter NQ diamond coring bit. Wells were completed as open hole construction to total depth with NX casing from ground surface to the top of the rock (between 1 and 2 meters in depth) (Reichart, 1992). In total, nine boreholes were drilled in a 75 m×100 m area to intersect two vertical fracture sets oriented at 20° and 110°, the former set displaying a slightly higher frequency of occurrence. Of the nine boreholes, six (FC-1 through FC-6) were inclined at approximately 45° from the ground surface and drilled orthogonal to the main vertical fracture sets. Boreholes FC-7 through FC-9 were drilled vertically to allow for cross-hole hydraulic testing. From the information obtained from core logs and quarry mapping, vertical

fracture spacing in the Guelph submember ranges between 2.5 and 5 meters with a median of approximately 3.5, and the spacing of vertical fractures in the Amabel ranges between 0.5 to 2 meters, with a median of around 1.5.

2.4.1 Testing procedure

A 48-hour long pumping test was conducted using a low capacity pump to obtain large-scale estimates of transmissivity, storativity, specific yield, vertical hydraulic conductivity, and vertical specific storage. The length of test duration was chosen based on Novakowski et al. (2007) in which it was found that pumping tests shorter than 48 hours are insensitive to estimates of specific yield in a fractured rock formation using the Moench (1997) solution. For the test, water from borehole FC-9 was pumped at a constant rate of 9.4 L/min (± 0.24 L/min) while the non-pumped wells (FC-1 through FC-8) were used as monitoring wells. Water levels were monitored in both the pumping and observation wells using pressure transducers accurate to 0.001% (± 30 mm). Water level measurements were taken every 10 seconds for the first hour, every 30 seconds for the second hour, every minute for the third hour, and every 5 minutes for the fourth hour. From the fifth hour until the cessation of pumping, measurements were taken at 10 minute intervals. The discharge rate of pumped groundwater was measured manually and the pumping rate adjusted throughout the duration of the test to ensure that a constant flow was maintained. Recovery of the aquifer was monitored for 24 hours following the cessation of pumping with the water level measurement schedule recommencing at 10 seconds and continuing as above until the end of the test.

2.4.2 Fitting to field data

To analyse the data, a curve-matching procedure was undertaken using the model developed herein. The process was assisted by the use of PEST (Doherty et al., 1994), an automated parameter estimation program. With PEST, differences between computer-generated drawdowns (from estimated hydraulic parameters) and measured drawdowns were minimized using an

objective function based on a weighted sum of squared errors. The use of the parameter estimation program required a degree of refinement through trial and error. For example, it was important to select appropriate initial parameter estimates and to determine whether logarithmic parameter transforms were necessary. In some instances, visual matches were made by running the model manually when PEST could not complete the optimization. The following strategy was developed when a visual match was required: first, vertical parameters were held fixed and transmissivity and storativity were allowed to float. Since these parameters are most sensitive to curve fitting, they often produced a reasonable fit (visually) themselves. When optimal values of transmissivity and storativity were determined with PEST, they were in turn held fixed and the vertical parameters then allowed to float. PEST was re-run which allowed the less sensitive vertical parameters to optimize to the field data. If this strategy failed to produce a satisfactory visual fit, PEST was not used and parameter values were manually altered prior to individual model runs. In this manner, parameter values were continually altered until a good visual fit was achieved. An example fit of the present model to observation well drawdown data is illustrated in Figure 2.6. This response is representative of the response observed in other observation wells during the pumping test.

The same pumping test data was also analyzed with the Moench (1997) solution implemented in the program Aqtesolv Pro 4.0 (Duffield, 2007) so as to compare the interpretation using the present model to that based on an isotropic, porous media environment. As the delayed-yield response looks similar to the dual-porosity response of a fractured aquifer, in limited cases, it has been employed to determine the hydraulic characteristics of densely fractured crystalline rock settings (Moench 1995; Elmhirst and Novakowski, 2012b).

Model results and discussion

Table 2.2 compares the hydraulic parameter estimates obtained from both the present model and the Moench (1997) solution. The estimated values include horizontal and vertical hydraulic conductivity, horizontal specific storage, and specific yield and the standard deviations obtained for the fits.

The horizontal parameter values estimated by the Moench (1997) solution were in the range of 1 to 1.5 orders of magnitude smaller than those predicted by the present model solution (specific storage and hydraulic conductivity, respectively). These estimates of K are reasonable, based on the values cited by Reichart (1992) for the same field site. Specific storage estimates predicted by both models are at the lower limit of practicality (using the definition for S_s and a reasonable estimate of aquifer compressibility) which makes their accuracy uncertain. This is with the knowledge that a reduction of the S_s value below 10^{-8} had minimal impact on the observation well response during the sensitivity analysis.

Values of vertical hydraulic conductivity predicted by Moench (1997) were significantly smaller than those predicted by the present model. In addition to this inconsistency, over the course of the data analysis process, it was revealed that the present model was not capable of determining a unique value for vertical hydraulic conductivity. This was contradictory to results from the informal sensitivity analysis that demonstrated a range of sensitivity to this parameter (Figure 2.3). The value of specific yield estimated by the model was slightly lower than the value predicted by the Moench (1997) solution. Based on the informal sensitivity analysis conducted on the present model, values of S_y lower than 10^{-6} did not appear to be sensitive. Since the model predicted a value of S_y lower than this limit, it may not be able to predict values of specific yield in a sedimentary rock setting. However the value of S_y predicted by Moench was also low, suggesting neither analytical model can be used to estimate this parameter. In unconfined aquifers

in porous media, values of specific yield tend to be much higher than those obtained for fractured rock. The non-uniqueness of K' , S_s and S_y in the fitting process may arise from the process of vertical fluid migration during the test where all three parameters are intertwined and govern the rate of fluid movement (which is small). In porous media the value of S_y is so large as to dominate the fluid source allowing for more impact on the drawdown curve and thus more resolution of the individual parameters.

The following example further illustrates the differences observed between the two model solutions and the problems associated with a unique fit. Figure 2.7 presents a log-log plot of the drawdown response in well FC-1 to pumping in FC-9 along with model generated curves to match the field results. At first inspection, both the Moench (1997) and the present model solution matched the field data well; however, the parameter estimates produced from the generated curves are very dissimilar (Table 2.3). While specific storage values are quite comparable between both solutions, the Moench (1997) solution obtains a smaller value of hydraulic conductivity compared to the new model solution by approximately half an order of magnitude. This may be due to the effect of including the contribution of water from the vertical domain to the horizontal fracture domain, where one would expect higher hydraulic conductivities to be estimated. Moreover, this example is an excellent illustration of the inability of both models to predict unique vertical hydraulic conductivity, specific storage, and specific yield values with confidence in this geologic setting. First, the Moench (1997) solution estimated a K' value of 3.1×10^{-9} m/s while PEST derived estimates obtained using the present model provide a K' estimate of 1.4×10^{-6} m/s. Similarly, specific yield values predicted by both models differed by three orders of magnitude for this particular observation well. To test the uniqueness (or lack thereof), K' was fixed at the Moench-derived value of 3.1×10^{-9} m/s and the present model was run using PEST with all other parameter estimates left open to optimization. The results showed that the other parameter estimates remained the same and the curve fit the

field data exactly as it had previously. This illustrates the insensitivity of the present model's solution to K' and the difficulty in predicting the correct value of vertical hydraulic conductivity from open-hole pumping test analytical models in general. The insensitivity is also evidenced by the wide degree of variability in K' values obtained from both solutions for the various fits (see the values of standard deviation shown in Table 2.2).

When the same experiment was conducted for specific yield (the Moench-derived value of 10^{-4} held fixed in the model with all other parameters allowed to range), the curve changed substantially and a fit to the data could not be achieved. Based on the definition of specific yield, it is difficult to say with certainty which value of specific yield is more correct, although the Moench-derived value is likely larger than the fracture pore volume and the value derived from the present model is likely less than the pore volume. The standard deviations obtained for estimates of specific yield in

Table 2.2 show a wide variability for both the Moench (1997) and present model solutions. Although this variability is less pronounced in values predicted by the present model, it is difficult to say what an appropriate estimate of S_y is with much certainty, without a clearer understanding of the primary (fracture-based) porosity.

During the analysis of field data, the ability to predict a unique value of vertical hydraulic conductivity appeared to be potentially dependent upon the value of S_y estimated at the same time. Thus an additional experiment was conducted with the present model to explore whether any relationship or dependency existed between predicted values of S_y and K' from an observation well response. A series of model runs was performed with values of K , S_s , and S_s' fixed at their initially optimized values while values of S_y were varied for each set of runs. The value of K' was initially set to its optimized value, but left open to change depending on the value

set for S_y . Trial runs were conducted with drawdown data from observation well FC-1 and source well FC-9. From the results presented in Table 2.4, unique values of K' were obtained when S_y was greater than 1×10^{-5} . Values of S_y smaller than this produced non-unique estimates of K' . Since values of S_y typical of fractured rock settings are low, and based on the observed arithmetic mean values of S_y obtained from the field study (Table 2.2), the analytical model clearly cannot estimate reliable K' values for this setting.

2.5 Conclusions and recommendations

The purpose of this study was to derive an open-well analytical pumping test solution specific for a fractured rock aquifer having a flow system dominated primarily by horizontal bedding plane fractures. A field example was given to demonstrate the application of the model and to explore the uniqueness of the interpreted values. In addition, the overall sensitivity of the system to the governing parameters was investigated by evaluating how variations to a parameter input would influence model output. This was to provide qualitative information about which model parameters could likely be estimated with enough accuracy to yield unique solutions.

Based on the analysis and discussion, the following conclusions can be made:

1. An informal sensitivity analysis of the model derived in this paper found that the hydraulic parameters K , S_s , S_y , and K' all demonstrated a range of sensitivity for an open hole observation well response given the base case conditions specified. The response in the source well, however, was found to be insensitive to estimates of S_y and K' .
2. The sensitivity of the model for values of $S_y < 10^{-5}$ is significantly diminished independent of the value of other parameters.
3. The Moench (1997) solution and the analytical model derived in this paper could not estimate unique values of S_s , S_y and K' in the sedimentary rock setting presented in the

field example. This is believed to be because of the similarity in their values and the interaction between these parameters in providing vertical fluid migration.

4. While pumping test drawdown curves from each monitoring well may be similar in shape and adequately matched using both the Moench (1997) solution for a porous medium and the solution herein, it should be recognised that the parameter estimates obtained by either solution may be inaccurate.
5. Although several strategies were attempted for obtaining a unique solution (thus obtaining reasonable estimates of the vertical hydraulic parameters) for the field example by fixing some parameters and allowing others to optimise, none were successful. This suggests an alternate approach is required to obtain these estimates.

2.6 List of abbreviations

Q (m ³ /s)	flow rate
r_s (m)	radius of the source well casing
H_0 (m)	initial head in source well
h (m)	hydraulic head
r (m)	radial distance from the source well
q (1/m)	total groundwater contribution between the vertical and horizontal domains
S (-)	bulk storativity of the horizontal fracture domain
T (m ² /s)	bulk transmissivity of the horizontal fracture domain
r_w (m)	wellbore radius
t (s)	time elapsed since slug injection
q_t (1/m)	groundwater contribution into the top horizontal fracture
q_f (1/m)	groundwater contribution into any additional horizontal fracture
n_f (-)	number of equally spaced horizontal fractures connecting the wells
q_{tu} (1/m)	vertical groundwater contribution across the upper interface of the top horizontal fracture
q_{tl} (1/m)	vertical groundwater contribution across the lower interface of the top horizontal fracture
q_{fu} (1/m)	upper contribution into each additional horizontal fracture from the vertical domain
q_{fl} (1/m)	lower contribution into each additional horizontal fracture from the vertical domain
h_m (m)	hydraulic head in the vertical domain
z (m)	vertical distance from the center line of the horizontal fracture feature
L_w (m)	vertical distance to the water table from the center of the top horizontal

	fracture feature
K' (m/s)	hydraulic conductivity of the vertical fracture domain
L_n (m)	half spacing between each horizontal fracture
S_S' (1/m)	specific storage of the vertical domain
S_y (-)	specific yield of the vertical domain
α_1 (-)	Moench (1995, 1997) relaxation coefficient that controls the exponential rate of decline of the water table
I_0, K_0, K_1	modified Bessel functions
A_1, B_1, A_2, B_2	constants
p	Laplace variable; overbar denotes that a parameter is in Laplace space
$\Phi, \omega, \Psi, \gamma_1, \gamma_2, \gamma_3,$ $\xi_1, \xi_2, \xi_3, \xi_4, \xi_5,$ $\xi_6, C_{ob}, C_s, \lambda_w$	constants (defined within text of current chapter)
h_s (m)	hydraulic head in the source well
r_1 (m)	radial distance from the source well to a point in the formation
r_2 (m)	radial distance from the observation well to the point in the formation utilized in the approximate solution method
h_{ob} (m)	hydraulic head in the observation well
r_{ob} (m)	radius of the observation well casing

2.7 Literature cited

- Bardenhagen, I. (2000). Groundwater reservoir characterisation based on pumping test curve diagnosis in fractured formation. *Groundwater, Past Achievements and Future Challenges: Proceedings of the XXX IAH Congress on Groundwater*, Cape Town, South Africa. pp. 81-86.
- Barker, J. A., & Black, J. H. (1983). Slug tests in fissured aquifers *Water Resources Research*, 19(6), 1558-1564.
- Barrash, W., & Ralston, D. R. (1991). Analytical modeling of a fracture zone in the Brule Formation as an aquifer receiving leakage from water-table and elastic aquitards *Journal of Hydrology*, 125(1-2), 1-24.
- Boulton, N. S. (1954). Unsteady radial flow to a pumped well allowing for delayed yield from storage. *Intern Assoc Sci Hydrol Publ*, 37, 472-477.
- Boulton, N. S. (1963). Analysis of data from non-equilibrium pumping tests allowing for delayed yield from storage. *Proc Inst of Civil Engineers*, 26(3), 469-482.
- Doherty, J., Brebber, L., & Whyte, P. (1994). PEST: Model-independent parameter estimation. Watermark Numerical Computing.
- Duffield, G.M. (2007). AQTESOLV for Windows version 4.5: HydroSOLVE, Inc., Reston, Va.
- Earlougher Jr., R. (1980). Analysis and design methods for vertical well testing *Journal of Petroleum Technology*, 32(3), 505-514.
- Ehlig-Economides, C. A., & Ayoub, J. A. (1984). Vertical interference testing across a low permeability zone, paper no. 13251. *The Society of Petroleum Engineers 59th Annual Conference*, Houston, Texas.
- Elmhirst, L. M., & Novakowski, K. S. (2012a). The analysis of pulse interference tests conducted in a fractured rock aquifer bounded by a moving free surface *Advances in Water Resources*, 35, 20-29.
- Elmhirst, L. M., & Novakowski, K. S. (2012b). Effects of test scale on the measurement of transmissivity, vertical hydraulic conductivity, storativity and specific yield in a fractured rock setting. *Manuscript Submitted for Publication to Ground Water*.
- Healy, R., & Cook, P. (2002). Using groundwater levels to estimate recharge *Hydrogeology Journal*, 10(1), 91-109.
- Karasaki, K., Long, J., & Witherspoon, P. (1988). A new analytic model for fracture-dominated reservoirs *SPE Formation Evaluation*, 3(1), 242-250.
- Lapcevic, P.A., Reichart, T.M., Novakowski, K.S. (1993). The interpretation of pumping tests conducted in vertically fractured rock using models developed for porous media. *National Ground Water Association Focus Eastern Conference*, pp. 839-849.

- Lee, R. R., Ketelle, R. H., Bownds, J. M., & Rizk, T. A. (1992). Aquifer analysis and modeling in a fractured, heterogeneous medium *Ground Water*, 30(4), 589-597.
- Levison, J. K., & Novakowski, K. S. (2012). Rapid transport from the surface to wells in fractured rock: A unique infiltration tracer experiment. *Journal of Contaminant Hydrology*, 131(1-4), 29-38.
- Levison, J., & Novakowski, K. (2009). The impact of cattle pasturing on groundwater quality in bedrock aquifers having minimal overburden. *Hydrogeology Journal*, 17(3), 559-569.
- Liberty, B. A. (1981). Colossal cataract: The geologic history of Niagara Falls. In I. H. Tesmer (Ed.), *Structural Geology* (pp. 57-62). Albany, N.Y.: State University of New York Press.
- Muldoon, M., Simo, J. (Toni), & Bradbury, K. (2001). Correlation of hydraulic conductivity with stratigraphy in a fractured-dolomite aquifer, northeastern Wisconsin, USA *Hydrogeology Journal*, 9(6), 570 -583.
- McConnell, C. L. (1993). Double porosity well testing in the fractured carbonate rocks of the Ozarks. *Ground Water*, 31(1), 75-83.
- Moench, A. F. (1995). Combining the Neuman and Boulton models for flow to a well in an unconfined aquifer *Ground Water*, 33(3), 378-384.
- Moench, A. F. (1997). Flow to a well of finite diameter in a homogeneous, anisotropic water table aquifer *Water Resources Research*, 33(6), 1397-1407.
- Neuman, S. P. (1972). Theory of flow in unconfined aquifers considering delayed response of the water table, *Water Resources Research*, 8(4), 1031-1045.
- Neuman, S. P. (1974). Effect of partial penetration on flow in unconfined aquifers considering delayed gravity response, *Water Resources Research*, 10(2), 303-312.
- Neuman, S. P., & Witherspoon, P. A. (1969). Theory of flow in a confined two aquifer system. *Water Resources Research*, 5(4), 803-816.
- Neuman, S. P., & Witherspoon, P. A. (1968). Theory of flow in aquicludes adjacent to slightly leaky aquifers, *Water Resources Research*, 4(1), 103-112.
- Novakowski, K. S. (1989). Analysis of pulse interference tests. *Water Resources Research*, 25(11), 2377-2387.
- Novakowski, K. S., & Bickerton, G. S. (1997). Borehole measurement of the hydraulic properties of low-permeability rock *Water Resources Research*, 33(11), 2509-2517.
- Novakowski, K., Milloy, C., Gleeson, T., Praamsma, T., Levison, J., & Hall, K. (2007). Groundwater recharge in a gneissic terrain having minimal drift cover. *Proceedings of the 8th Joint CGS/IAHCNC Groundwater Conference*, Ottawa, Ontario. pp. 280-285.

- NRC Committee on Fracture Characterization, & Fluid Flow (1996). *Rock fractures and fluid flow: Contemporary understanding and applications* The National Academies Press.
- Ogbe, D. O., & Brigham, W. E. (1984). A model for interference testing with wellbore storage and skin effects at both wells. *59th Annual Technical Conference*, Houston, TX.
- Peffer, J. R. (1991). Complex aquifer-aquitard relationships at an Appalachian plateau site, *Ground Water*, 29(2), 209-217.
- Raven, K. (1986). Hydraulic characterization of a small ground-water flow system in fractured monzonitic gneiss. *National Hydrology Research Institute Scientific Series*, 149(30), 133.
- Reichart, T. M. (1992). Influence of vertical fractures in horizontally-stratified rocks. (Master of Science, University of Waterloo).
- Shapiro, A. M., & Nicholas, J. R. (1989). Assessing the validity of the channel model of fracture aperture under field conditions, *Water Resources Research*, 25(5), 817-828.
- Stephenson, K. M., & Novakowski, K. S. (2006). The analysis of pulse interference tests conducted in a fractured rock aquifer bounded by a constant free surface, *Journal of Hydrology*, 319(1-4), 109-122.
- Talbot, A. (1979). The accurate numerical inversion of Laplace transforms *IMA Journal of Applied Mathematics*, 23(1), 97-120.
- Tiedeman, C. R., & Hsieh, P. A. (2001). Assessing an open-well aquifer test in fractured crystalline rock, *Ground Water*, 39(1), 68 -78.
- Tongpenyai, Y., & Raghavan, R. (1981). The effect of wellbore storage and skin on interference test data *Journal of Petroleum Technology*, 33(1), 151-160.
- Zanini, L., Novakowski, K. S., Lapcevic, P., Bickerton, G., Voralek, J., & Talbot, C. (1999). *The development of a conceptual model for contaminant transport in the dolostone underlying Smithville, Ontario* (Final Report Submitted to the Smithville Phase IV Bedrock Remediation Program).

Table 2.1 Base case values used in the sensitivity analysis

T (m/s)	S (-)	S _y (-)	K' (m/s)	S' _s (1/m)	H ₀ (m)	r (m)	r _w (mm)	r _s (mm)	r _{ob} (mm)	L _w	L _n	n _r	α _t
2.0 x 10 ⁻⁴	2.0 x 10 ⁻⁶	1.0 x 10 ⁻⁴	2.0 x 10 ⁻⁷	2.0 x 10 ⁻⁸	1.0	8.0	76.2	76.2	76.2	6.0	2.0	3.0	1.0 x 10 ⁹

Table 2.2 Comparison of estimated hydraulic parameters between the Moench (1997) and present pumping test solution.

Parameter	Moench (1997)		Present model	
	Estimate	Standard deviation	Estimate	Standard deviation
K (m/s)	7.1 x 10 ⁻⁶	2.4 x 10 ⁻⁶	1.6 x 10 ⁻⁵	5.0 x 10 ⁻⁶
S _s (1/m)	4.0 x 10 ⁻⁸	6.6 x 10 ⁻⁸	2.8 x 10 ⁻⁷	3.3 x 10 ⁻⁷
K' (m/s)	1.2 x 10 ⁻⁸	1.4 x 10 ⁻⁵	1.1 x 10 ⁻⁵	1.0 x 10 ⁻⁵
S _y (-)	6.7 x 10 ⁻⁵	1.9 x 10 ⁻⁴	4.7 x 10 ⁻⁶	8.4 x 10 ⁻⁶

Table 2.3 Estimate of hydraulic parameters predicted by both the Moench (1997) and present model solutions for the pumping test response in FC-1 to pumping FC-9.

Parameters	Moench (1997)	Present model
K (m/s)	4.9 x 10 ⁻⁶	1.3 x 10 ⁻⁵
S _s (1/m)	1.7 x 10 ⁻⁷	2.8 x 10 ⁻⁷
S _y (-)	1.0 x 10 ⁻⁴	1.2 x 10 ⁻⁷
K' (m/s)	3.1 x 10 ⁻⁹	1.4 x 10 ⁻⁶

Table 2.4 Sensitivity of vertical hydraulic conductivity to fixed values of specific yield using present pumping test model.

Fixed S_v (-)	Estimate of K' (m/s)
1.18×10^{-3}	1.4×10^{-6}
1.18×10^{-4}	2.1×10^{-6}
1.18×10^{-5}	8.3×10^{-6}
1.18×10^{-6}	7.0×10^{-6}
1.18×10^{-7}	7.0×10^{-6}

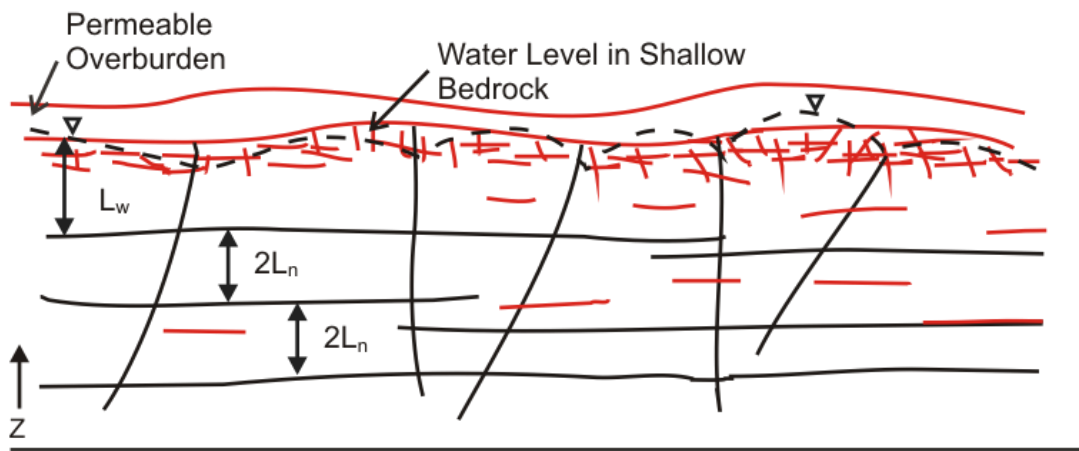


Figure 2.1 Conceptual model of the fractured rock aquifer. The datum is set at $z=0$ which is also considered the no flow boundary (Elmhirst and Novakowski, 2012a).

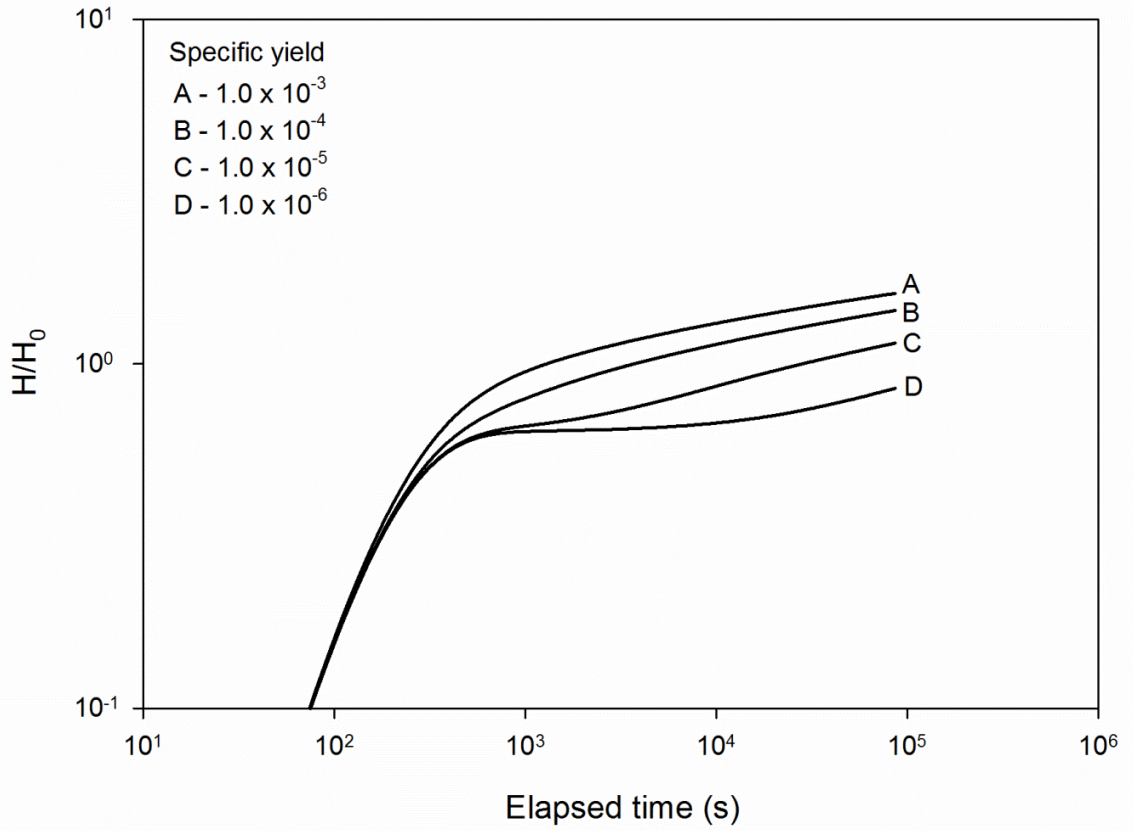


Figure 2.2 Effect of specific yield on the pumping test observation well response. Base case values in Table 2.1 were held fixed while four separate model runs were conducted with values of S_y ranging between 10^{-3} and 10^{-6} .

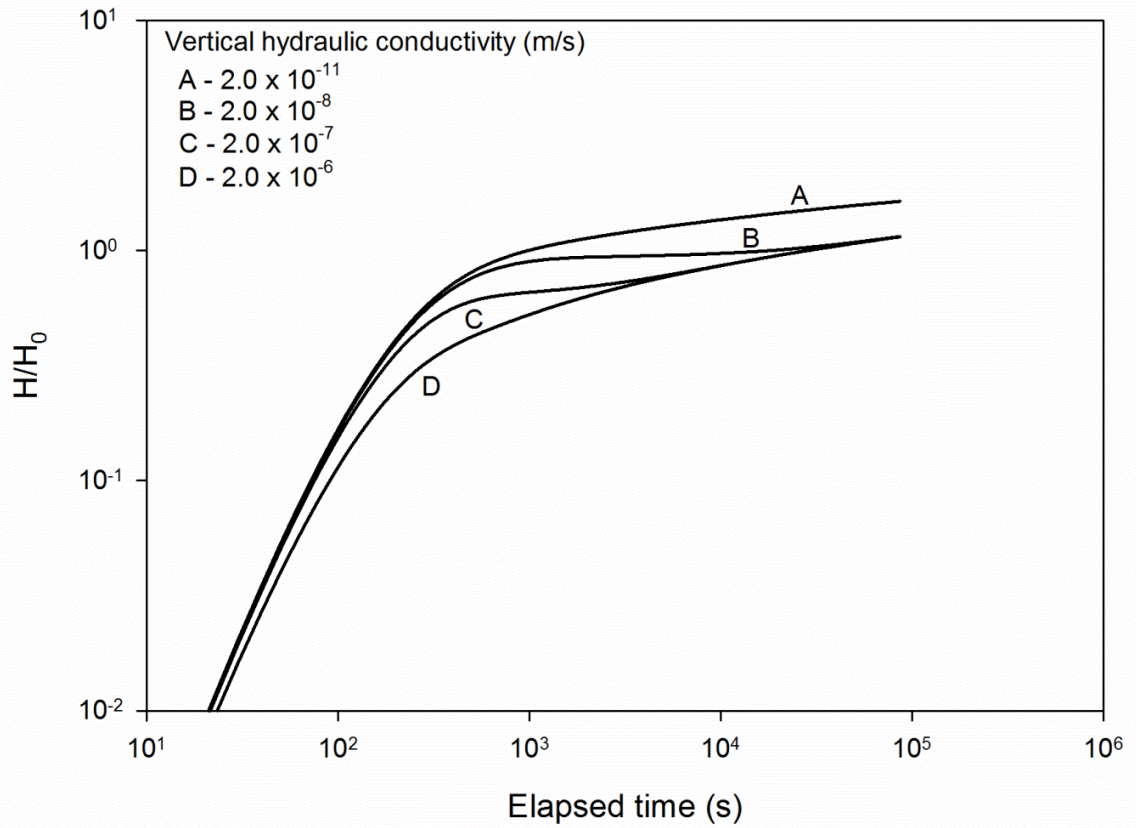


Figure 2.3 Effect of vertical hydraulic conductivity on the pumping test observation well response. Base case values in Table 2.1 were held fixed while four separate model runs were conducted with values of K' ranging between 2.0×10^{-6} and 10^{-11} .



Figure 2.4 Location map of Fletcher Creek Conservation Area in southern Ontario.

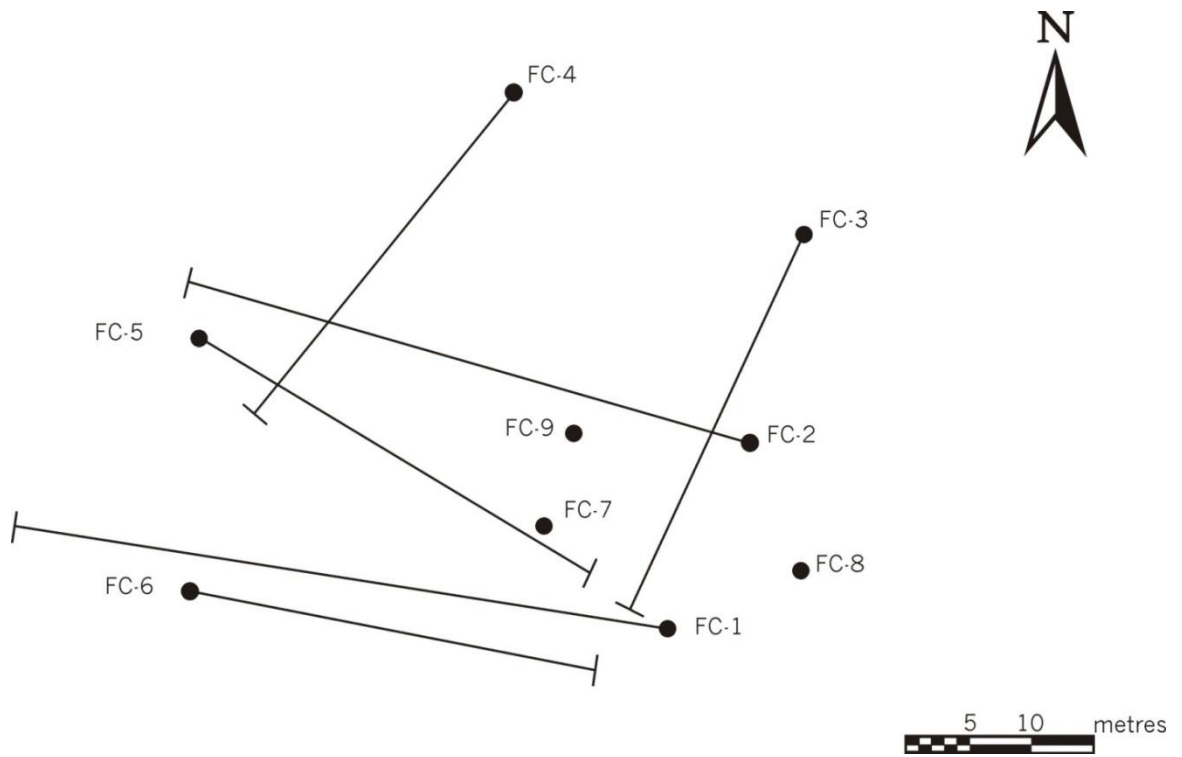


Figure 2.5 Plan view of borehole locations at the Fletcher Creek Conservation Area field site.

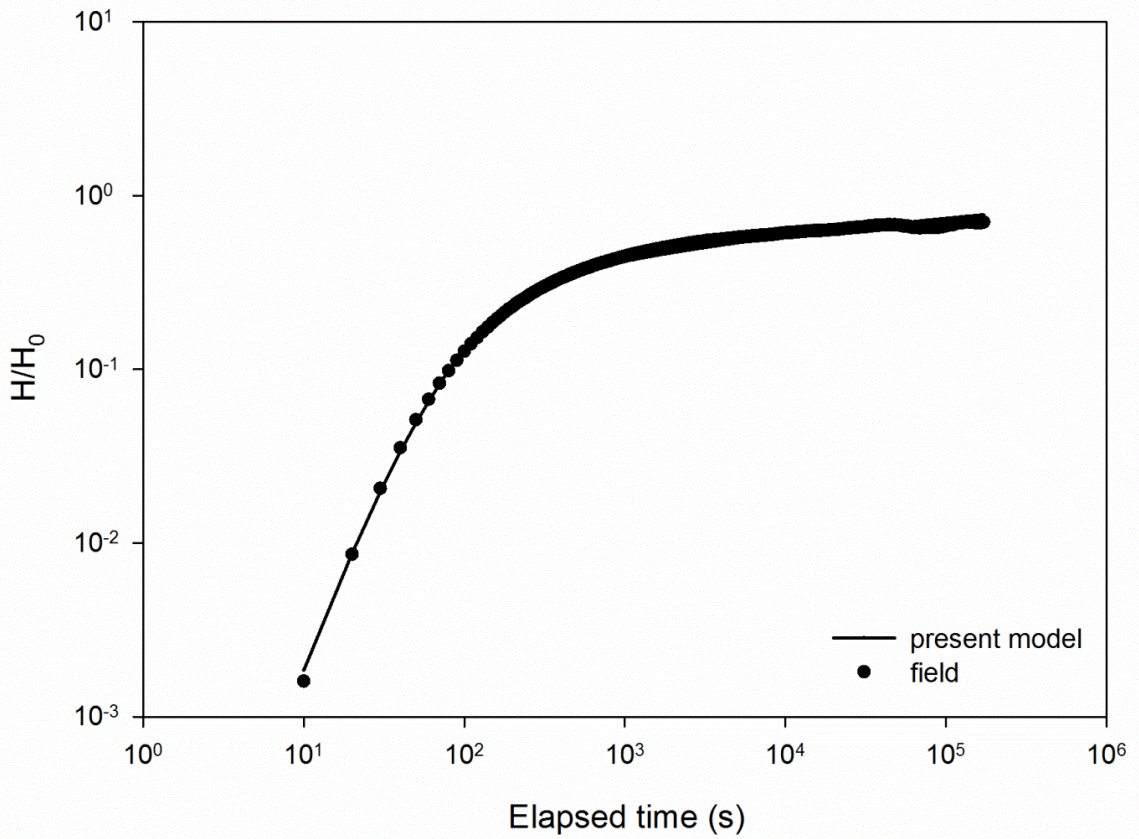


Figure 2.6 Pumping test response in observation well FC-1 to pumping in source well FC-9 using the present model. Table 2.3 presents the parameter estimation results.

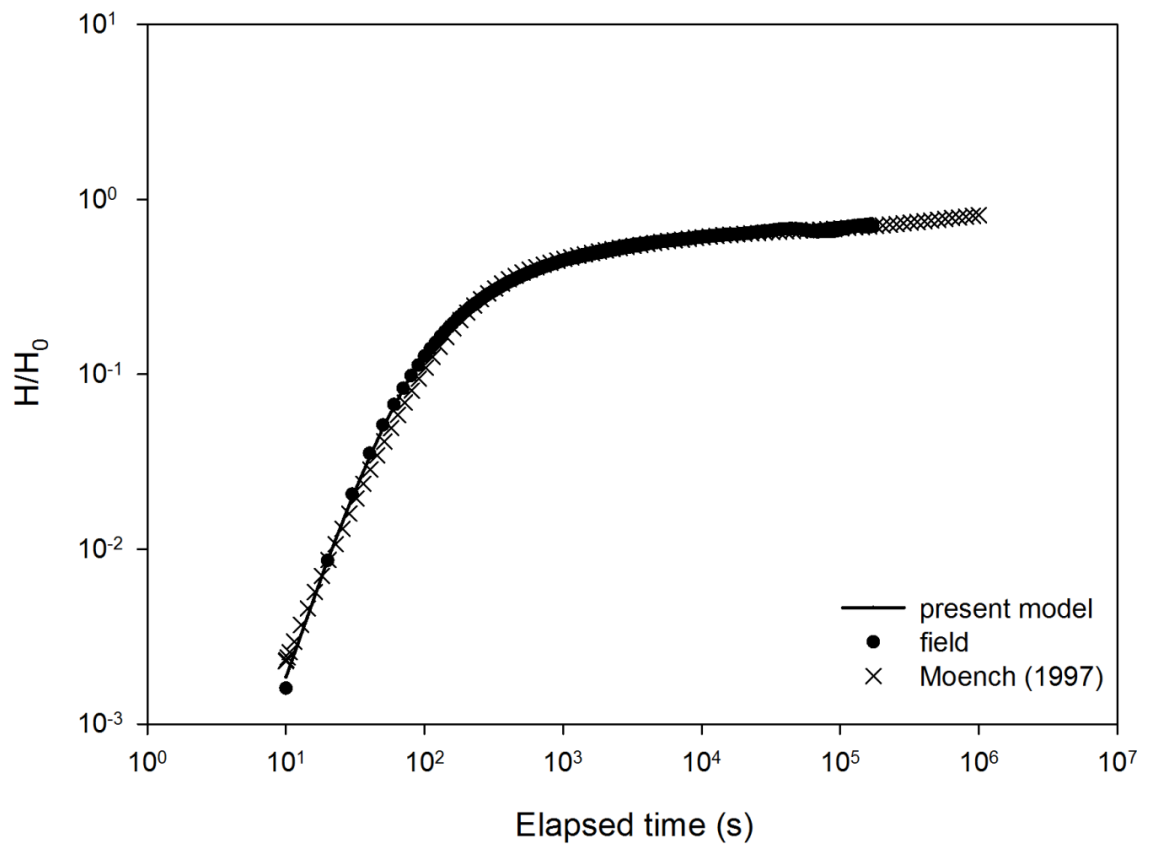


Figure 2.7 Pumping test response in FC-1 to pumping in FC-9 with the present model and the Moench (1997) solution. Table 2.3 presents parameter estimations obtained from both models.

Chapter 3

Comparison of methods for measuring vertical hydraulic properties in a sedimentary rock aquifer

Chapter summary

The characterization of groundwater flow in fractured bedrock aquifers is presently based on a variety of hydraulic testing methods and analytical models. Most models are derived for porous media environments and do not fully represent the complexities of fractured rock settings. In this chapter, measuring aquifer properties using various testing methods allowed for the evaluation of which methods are best capable of producing reliable parameter estimates. The study was performed in a fractured sedimentary rock aquifer using four different field methods: constant head tests conducted using a straddle-packer system, pulse interference tests conducted under open-hole conditions, 12-hour isolated interval pumping tests and 48-hour open-hole pumping tests. Using the results of the constant head tests as the most reliable method for parameter estimation, the results obtained using the other three methods were compared with particular emphasis on the estimation of vertical hydraulic parameters in this setting. The effects of test measurement scale on hydraulic parameter estimates were also investigated. Evaluation of the open-hole pumping test data was performed using the analytical model derived in Chapter 2. The comparison shows that estimates of horizontal hydraulic conductivity were not dependent on test method with all methods providing equivalent results. Open-well pumping tests, however, were confirmed not to reliably estimate values of vertical hydraulic conductivity and specific yield, as was initially discovered in Chapter 2. Alternatively, pulse interference tests conducted under open-hole conditions may offer a less time-intensive option to constant head injection tests for determining vertical hydraulic parameters in a sedimentary rock setting.

3.1 Introduction

In field investigations of fractured rock formations, hydraulic parameters are often determined by analysis of data obtained from single-well or multiple-well tests. Single-well methods, such as constant head tests, can be used to determine the distribution of transmissivity (T) with depth for an individual well (Novakowski et al., 2007). Pulse interference and pumping tests involve multiple wells thereby providing hydraulic information on larger volumes of rock and on the interconnectivity of fracture systems (Rovey, 1994).

Discrepancies between small and large-scale hydraulic testing methods are a common occurrence in fractured rock due to the natural spatial variability of fractures (Sánchez-Vila et al., 1996; Schulze-Makuch et al., 1999). These differences are particularly important to consider in development of groundwater models or when resource constraints limit broad-based, discrete fracture testing (Tiedeman and Hsieh, 2001; Muldoon and Bradbury, 2005). In many cases, the use of small-scale values for predicting large-scale properties may be unrepresentative of the geologic setting as a whole and vice versa (Nastev et al., 2004; Elmhirst, 2011).

In current practice, it is the use of straddle-packer systems for depth-specific hydraulic measurement that provide the most accurate estimate of the hydraulic properties of discrete fracture features at the sub-continuum scale (Lapcevic et al., 1999; Tiedeman and Hsieh, 2001). Testing isolated zones, however, is a time-consuming and costly method that requires specialised equipment (Tiedeman and Hsieh, 2001; Novakowski et al., 2007). Alternatively, if only the bulk hydraulic properties of the flow system are required, pumping from an open well with observation of drawdown in an open observation well may provide reasonable estimates of these properties when evaluated with an appropriate analytical model.

Numerous studies have been performed to estimate hydraulic parameters using different test methods conducted in the horizontal direction in a sedimentary rock setting. The parameters measured include effective porosity (e.g., Li, 1995; Bernard et al., 2006), hydraulic conductivity (K) (e.g., Rovey, 1994; Li, 1995; Nastev et al., 2004; Hunt, 2006), transmissivity (e.g., Abbey and Allen, 2000; Nastev et al., 2004) and storativity (S) (e.g., Rovey, 1998; Abbey and Allen, 2000). To date, there have been only limited studies on estimating vertical hydraulic conductivity (K_v) and specific yield (S_y) from field tests in a sedimentary rock environment (Muldoon and Bradbury, 2005). This is despite the fact that accurate estimation of vertical hydraulic conductivity and specific yield is important for protection of regional municipal water supply (Eaton et al., 2007) and the estimation of groundwater recharge (Healy and Cook, 2002).

Multi-well pumping tests are typically employed for defining the hydraulic parameters at mid-to large-scales in an aquifer and are generally used for predicting specific yield. Determining a value for specific yield requires that the drainage, or emptying of water from rock fractures, is complete, which may require at least 48 hours of pumping in order to obtain a reasonable measurement (Novakowski et al., 2007). In a recent study, however (Chapter 2), the interpretation of pumping tests may not always yield unique and therefore accurate parameter values for a fractured rock aquifer. This was also illustrated by Muldoon and Bradbury (2005) who found inappropriate results from pumping tests analyzed using the Moench (1984) solution in a highly heterogeneous fractured rock setting.

In a study by Tiedeman and Hsieh (2001), an open-well pumping test was used to successfully estimate the hydraulic properties of a fractured rock aquifer when values were compared to results obtained from packer-isolated testing, but only when using a numerical model that accurately represented the fracture heterogeneity in the field setting. The same drawdown data analyzed by application of the Moench (1985) solution for a homogeneous, isotropic leaky

aquifer was found to produce poor matches to drawdowns at most observation wells in the study (Tiedeman and Hsieh, 2001). Similarly, Lemieux, et al. (2006) demonstrated how pumping tests conducted at a representative elementary volume (REV) scale in a fractured dolostone produced hydraulic estimates comparable to a discrete-fracture model. This was only true however when the two high-permeability bedding plane fractures present were explicitly included in the numerical model. Both examples are illustrative of the general need to describe a setting as a non-uniform continuum containing several discrete dominant features (Neuman, 2005). Despite these studies, the analysis of open-well pumping tests using an analytical model remains the practical standard because of cost and time constraints associated with the development of a site-specific numerical model.

To further evaluate the applicability of the model developed in Chapter 2 for an open-hole pumping test in a fractured sedimentary rock aquifer and to determine the most appropriate method for obtaining accurate estimates of the vertical hydraulic properties of these aquifers, the use of constant head tests conducted with straddle packer systems, pulse interference tests conducted in open holes, and pumping tests conducted using intervals isolated with straddle packer systems are compared. The results of the constant head tests are used as reference values for the site as such testing allows for direct measurement of discrete fracture properties, especially when the tests are conducted in both vertical and inclined wells which intersect horizontal and vertical fracture features. The goal of this study is therefore to provide a quantitative analysis of the ability to measure hydraulic parameters, vertical properties in particular, by comparison of hydraulic parameter estimates obtained using different testing methods. A further consideration is the effect of scale on aquifer test data. Scale effects refer to the inconsistencies in parameter estimates that may be observed between small and large-scale hydraulic testing methods. Test scale is therefore a necessary consideration when comparing

these different testing methods and their ability to estimate vertical hydraulic properties in sedimentary rock.

3.2 Field setting and previous studies

To conduct this study, the most simplistic field setting possible in fractured bedrock was selected, that being a sedimentary rock aquifer in level terrain with continuous horizontal fracture features intersected by relatively regular vertical joints. The study area (referred to as the Fletcher Creek site, Figure 3.1) is located in southern Ontario and is underlain by the Guelph and Amabel dolostones of the Lockport Formation. The site was initially selected for a characterization study by Reichart (1992) due to the presence of an adjacent quarry that permitted correlation between fracture mapping and borehole data. The stratigraphy is mostly flat-lying with a slight south-westward dip of approximately 4 to 6 metres per kilometer (Liberty, 1981). The Guelph submember is about 9 metres thick, while the underlying Amabel submember is about 60 metres thick. The fracture permeability of the formation sustains domestic and moderate industrial and municipal water supplies in the vicinity.

In the Reichart (1992) study, both inclined and vertical boreholes were drilled to investigate the three-dimensional interconnection of the larger scale fracture features present in the rock (Figure 3.2). Holes were diamond-drilled to a depth of approximately 30 meters using a 76 millimetre NQ diamond coring bit. Wells were completed as open-hole construction to total depth with NX casing from ground surface to the top of the rock (between 1 and 2 meters in depth). In total, nine boreholes were drilled in an area of about 75 m by 100 m, to intersect two vertical fracture sets oriented at 20° and 110°, the former set displaying a slightly higher frequency of occurrence based on measurements in the local quarry. Of the nine boreholes, six (FC-1 through FC-6) were inclined at approximately 45° from the ground surface and drilled orthogonal to the main vertical fracture sets. Boreholes FC-7 through FC-9 were drilled vertically to allow for cross-hole

hydraulic tests to be performed. From fracture mapping conducted in the quarry and on other exposed bedrock pavements in the immediate vicinity, vertical fracture spacing in the Guelph submember ranged between 2.5 and 5 meters with a median of approximately 3.5. The spacing of vertical fractures in the Amabel ranged between 0.5 to 2 meters, with a median of around 1.5 (Reichart, 1992).

Constant head tests were conducted at the field site by Reichart (1992) using a straddle-packer system to determine the vertical variation of transmissivity in each well with saturated depth (Lapcevic et al., 1999). Packers were first spaced at 1.5 metre intervals for exploratory testing in each borehole, and then at 0.5 metre spacing to isolate individual horizontal and vertical fracture features in the formation. The range of hydraulic conductivity measured with the system used varied from 10^{-4} to 10^{-11} m/s. Four horizontal fracture zones in the upper 30 m of rock with transmissivities ranging from 10^{-4} to 10^{-6} m²/s were identified.

At the same field site, four 12-hour long pumping tests were conducted using straddle packers to isolate specific fracture zones (Lapcevic et al., 1993). For each test, a permeable horizontal fracture zone was isolated and pumped, while nineteen observation intervals were isolated using packers with monitoring of drawdown conducted via pressure transducers. The observation intervals were altered for each test to maximize the number of fracture features studied. An example test configuration is illustrated in Figure 3.4. The tests were analysed using the ratio method (Neuman and Witherspoon, 1972) where interpretation is based on the ratio of drawdown between the pumped fracture zone and the surrounding rock at a given radial distance from the pumped well. The results of interpretation showed that the data from the pumped fracture zone demonstrated the influence of the vertical fractures. In the following we compare the results of these previous studies to the interpretation of pumping tests and pulse interference tests conducted in an open-well configuration at this site.

3.3 Test methodology

To assess the veracity of the estimates of hydraulic conductivity, specific storage, vertical hydraulic conductivity, specific yield, and vertical specific storage obtained from pumping tests conducted in open wells, four types of hydraulic tests were compared. These included constant head tests and isolated interval pumping tests as described above, and pulse interference tests, and long-term pumping tests conducted in open wells.

Pulse-interference tests are a multiple-well method for assessing the hydraulic properties of a geological formation between two wells (Sageev, 1986; Novakowski, 1989). Pulse-interference tests in the slug test format were conducted by instantaneously raising or lowering the water level in a source well, and then monitoring the pressure response to the slug with a transducer in both the source well and in eight observation wells. The range over which the response to the slug source can be detected is considerably greater than for porous media as a result of the low storativity commonly found in fractured rock environments (Novakowski, 1989). An initial displacement (H_0) of approximately 0.5 m in the source well was achieved using a solid cylinder, 41.5 mm in diameter and 1.815 meters in length that was instantaneously lower into or removed from the well. Pressure transducers accurate to 0.001% (± 30 mm) were used to measure the source and observation well responses at a sampling rate of one measurement every 5 s. Multiple tests were conducted in each well to ensure reliability and repeatability of test results. The recorded test data was analyzed using the Elmhirst and Novakowski (2012a) solution where aquifer thickness was taken to be the open length of the borehole. The three most permeable horizontal bedding plane fractures were specified in the solution at depths determined by Reichart (1992). As was shown in Elmhirst and Novakowski (2012a), the solution is insensitive to the number of fractures used.

The 48-hour pumping tests were conducted with a low capacity pump to obtain larger-scale estimates of transmissivity, storativity, vertical hydraulic conductivity, and specific yield. The length of test duration was chosen based on Novakowski et al. (2007) where pumping tests shorter than 48-hours long were determined to be insensitive to estimates of specific yield in a fractured rock formation using the Moench (1997) solution. For the first pumping test, water was removed at a constant rate of 9.4 L/min (± 0.24 L/min) from well FC-9 using a low capacity pump while the non-pumped wells, FC-1 through FC-8, were used as monitoring wells. For the second test, FC-7 was pumped at a rate of 9.1 L/min (± 0.31 L/min) and drawdown was monitored in wells FC-1 through FC-6 and wells FC-8 and FC-9. Monitoring of all wells was conducted using pressure transducers accurate to 0.001% (± 30 mm), and the discharge rate of pumped groundwater was measured manually throughout the duration of the test. Water level measurements were taken every 10 s for the 1st hour, every 30 s for the 2nd hour, every minute for the 3rd hour, and every 5 min for the 4th hour. In the 5th hour, measurements were taken every 10 min until the cessation of pumping. Recovery of the aquifer was monitored for 24 hours following the completion of pumping with the measurement schedule recommencing at 10 s and continuing as above until the end of the test.

3.4 Analysis and results

Single-well constant head tests were used to determine the distribution of transmissivity for each individual well. Multiple-well pulse interference tests were analyzed using the Elmhirst and Novakowski (2012a) solution to determine horizontal and vertical zone hydraulic conductivity and specific storage, as well as specific yield. These same parameters were also determined by analysing pumping test data with the model derived in Chapter 2. Vertical fracture permeability results from the isolated zone pumping tests were interpreted using an analytical model and the

ratio method (Lapcevic et al., 1993). These results were also used in the comparison of parameter estimates to test scale. The analysis performed for each type of test is outlined below.

3.4.1 Constant head tests

Discrete interval transmissivities were obtained from the constant head test data using the Theim equation:

$$T = \frac{Q}{2\pi\Delta h} \ln\left(\frac{r}{r_w}\right) \quad 3.1$$

where Q is the discharge rate of the pumping well, Δh is the drawdown at radial distance r (radius of influence) and r_w refers to the wellbore radius. The radius of influence is assumed to be large in low-storativity media and must be estimated since it is difficult to determine definitively (Doe and Remer, 1981). However, overestimating the radius of influence has only a minor effect on the calculation given that the parameter is a logarithmic variable in Eq. (3.1). A conservative estimate of 10 m for the radius of influence was used by Reichart (1992) based on guidance from Bliss and Rushton (1984). The Theim equation is based on a confined aquifer which is a reasonable supposition to make if the fractures in the test section are mainly vertical or mainly horizontal in orientation. An example distribution of transmissivity with depth is presented in Figure 3.3.

To compare with other test results, transmissivity values were converted into hydraulic conductivity. A representative hydraulic conductivity for the entire well length was obtained from the ratio of the arithmetic sum of the discrete interval transmissivities to the tested borehole length. Since flow only occurs in the fractured portion of each test interval, this hydraulic conductivity is representative of fracture permeability and not total rock mass permeability, which for this setting is typically $< 1 \times 10^{-9}$ m/s and thus contributes little to bulk K (Domenico and Schwartz, 1990).

To determine the hydraulic conductivity of vertical fractures from the constant head test data, the location of vertical fractures known from the isolated zone pumping tests were identified, and correlated to the same zones isolated for the constant head tests. The K' from the constant head tests in these zones was then calculated using:

$$K' = (2b)^3 \frac{\rho g}{12\mu} \frac{1}{(b)} \quad 3.2$$

where $2b$ is the equivalent single fracture aperture as determined from the cubic law relation between $2b$ and T , ρg is the specific weight of groundwater, μ is the dynamic viscosity of water¹ and b is the packer interval spacing. The cubic law expression (Snow, 1968) for this analysis is given by:

$$2b = \left(T \times \frac{12\mu}{\rho g}\right)^{1/3} \quad 3.3$$

While the constant head tests were not conducted under open borehole conditions as were the pulse-interference and pumping tests, the values obtained provide what is likely the best possible estimate of vertical hydraulic parameters as these are direct measurements of the properties of individual vertical features. Therefore if the constant head values are comparable to open-hole pumping and pulse interference values, these later tests could potentially be used in place of the more detailed and costly constant head method.

Although estimates of specific storage cannot be obtained from constant head test analysis conducted using the Thiem equation, specific yield can be estimated by assuming that the cumulative fracture aperture is approximately equivalent to effective porosity (Milloy, 2007; Novakowski et al., 2007). The combined effective porosity of both vertical and horizontal features provides an estimate of specific yield as water is primarily released from both fracture

¹ Equal to 1.39×10^{-3} Pa·s for a groundwater temperature of 8°C.

types with water-level decline (Healy and Cook, 2002). For each inclined borehole, an equivalent fracture aperture ($2b_{eq}$), representative of the total fracture opening, was determined from the total T using the cubic law. Division of $2b_{eq}$ by the tested borehole length provides a value for S_y as presented in Table 3.1.

Constant head tests may be influenced by wellbore skin which can result in an underestimate of transmissivity (Lapcevic et al., 1999). This issue was dismissed through examination of longer-term pumping test data which offered no indication of such effects.

3.4.2 Pumping tests conducted using isolated zones

Values of vertical hydraulic conductivity were determined from isolated zone pumping tests conducted over a 12-hour period by isolating and pumping horizontal fractures and observing drawdown in intervals isolating vertical fractures. Data was analyzed using the ratio method developed by Neuman and Witherspoon (1972) whereby the pumped fracture and surrounding rock, vertical fractures included, were described as an aquifer/aquitard system with flow moving horizontally in the aquifer and vertically in the aquitard. The analysis was then based on the ratio of drawdown between the pumped fracture zone and the surrounding rock at a particular radial distance from the pumping well.

Test data from the observation intervals isolating the pumped fracture zone were interpreted using the Theis solution. The values of transmissivity and storativity determined from type curves were used to determine the vertical hydraulic diffusivity (α'). This parameter can also be defined as:

$$\alpha' = \frac{K'}{S'_s} \quad 3.4$$

where S'_s is the aquitard specific storage. Aquifer specific storage, S_s , was found by dividing S by the packer spacing interval. Since specific storage is assumed to be equivalent between the

aquifer and aquitard ($S'_s = S_s$) then the vertical hydraulic conductivity of the aquitard was determined by rearranging Eq. 3.4.

$$K' = \alpha' S'_s \quad 3.5$$

3.4.3 Pulse interference tests

The Elmhirst and Novakowski (2012a) solution was used to estimate values of transmissivity, storativity, vertical hydraulic conductivity, vertical specific storage, and specific yield from pulse interference tests conducted in open wells. Although the field example in a gneissic formation presented by Elmhirst and Novakowski (2012a) demonstrated that values of vertical specific storage were insensitive to model results, the model is sensitive to this parameter for the sedimentary rock setting explored in this study. The parameter sensitivities were evaluated by varying base case values specified in Table 3.2 over a practical range given the geologic setting, and the variation in curve response was observed. The initial case values were chosen based on numbers presented in Stephenson and Novakowski (2006) for a sedimentary rock setting, and from Elmhirst and Novakowski (2012a) for the initial values of n_f (number of fractures), L_n (half spacing between each horizontal fracture), S_y and α_l (Moench [1995; 1997] relaxation coefficient). An example of the result is illustrated in Figure 3.5. In order to obtain unique fits to the field data, the procedure described in the following paragraph was adopted. The results of the entire sensitivity analysis to the Elmhirst and Novakowski (2012a) solution for pulse interference test data in both source and observation wells are presented in Appendix E.

The data analysis method used with the Elmhirst and Novakowski (2012a) solution involved a curve-matching procedure aided by the use of PEST (Doherty, 1994), an automated parameter estimation program. The proper use of the parameter estimation program often required a degree of refinement through trial and error. In some instances, visual matches were made by running the model manually when PEST could not complete the optimization procedure. The following

strategy was developed when a manual match was required: first, vertical parameters were held fixed and transmissivity and storativity were allowed to range since they were typically most sensitive to curve fitting. When optimal values of T and S were determined with PEST, they were in turn held and the vertical parameters then allowed to range. PEST was re-run which allowed the fit to be refined. If this strategy failed to produce a satisfactory fit to the field data, PEST was not used and parameter values were manually altered prior to individual model runs. In this manner, parameter values were continually altered until a good visual fit was achieved. Following this curve fitting method meant being unable to obtain realistic confidence intervals for each parameter which is why they are not presented for cases where this procedure was done.

Transmissivity and storativity estimates were converted to hydraulic conductivity and specific storage values respectively, by dividing by the vertical test length of each well. An example of an observation well response and best model fit is presented in Figure 3.6.

3.4.4 Pumping tests

The 48-hour open borehole pumping tests were interpreted using the pumping test solution developed in Chapter 2. Horizontal zone transmissivity and storativity estimates obtained by the model were converted to hydraulic conductivity and specific storage estimates respectively, by dividing by the vertical length of each well.

Similar to the data analysis method described in 3.4.3 for pulse interference test analysis, the present pumping test solution developed in Chapter 2 also involved a curve-matching procedure aided by the use of PEST. In cases where PEST failed to optimize, visual matches were made by running the model manually using the strategy described above.

While it is convenient to match pumping test data from all observation wells to a single set of aquifer parameters (composite analysis), the inability to do this is not uncommon in fractured rock because of local scale heterogeneities. For this field setting, hydraulic parameters were determined by analytical methods from drawdown data in each observation well and the mean of these results is reported here as an estimate of overall aquifer parameters.

3.5 Discussion

In the following section, we explore the variation of horizontal and vertical zone hydraulic conductivity, specific yield and horizontal and vertical specific storage estimates obtained with each test method at the Fletcher Creek field site. Table 3.3 summarises the mean values and standard deviations obtained from the different tests. In order to conduct the comparison, a discussion of the results in the context of scale effects is also required. Scale effects, or discrepancies between small-scale and large-scale values of hydraulic properties, can be related to test type where the duration of a test is proportional to the volume of aquifer sampled. The results for each parameter are discussed below.

3.5.1 Horizontal hydraulic conductivity

Table 3.3 and Figure 3.7 compare the values of hydraulic conductivity estimated from pumping tests, pulse interference tests and constant head tests. Estimates from the pumping tests (using the model in Chapter 2) and from the pulse interference tests produced very comparable estimates, 1.6×10^{-5} m/s and 1.8×10^{-5} m/s, respectively. Compared to these values, the geometric mean value of K estimated from the constant head tests was approximately 0.7 orders of magnitude lower; while the mean value estimated using the Moench (1997) pumping test solution was approximately half an order of magnitude lower. If the Moench (1997) results are not considered, there appears to be a slight increase in hydraulic conductivity estimates with increased length of test duration, or scale.

Nastev et al. (2004) found that hydraulic conductivity values obtained from smaller scale tests typically yield lower values compared to larger scale tests in heterogeneous aquifers with scattered zones of highly fractured media interspersed with less heavily fractured zones. This is because when a larger volume of aquifer is disturbed, there is a greater probability of meeting interconnected fracture zones and preferential flow pathways that contribute to higher transmissivities (Rovey, 1994). From the results presented in Figure 3.7, there is only a weak pattern of increased horizontal hydraulic conductivity with increased test scale; for the most part, estimates from each test stay within less than an order of magnitude difference. In the study by Nastev et al. (2004), hydraulic conductivity values were found to range by 2 orders of magnitude from local scale to REV scale tests. Also, log standard deviations amongst the different tests appeared to be more or less consistent. In this study, the standard deviations on K values appear to decrease with increasing measurement scale. However these variations are consistent with the notion that hydraulic tests that sample larger volumes of aquifer tend to have lower standard deviations since a greater degree of heterogeneity is sampled. The lower the standard deviation, the closer the likelihood that the test is estimating a near REV parameter value (Elmhirst, 2011). A reduction in the standard deviation of hydraulic conductivity with test scale as observed in Figure 3.7 is also in agreement with findings by Kurikami et al (2008). Overall, from this field data it does not appear that estimates of horizontal hydraulic conductivity are strongly influenced by test method in a sedimentary rock environment.

3.5.2 Vertical hydraulic conductivity

As illustrated in Figure 3.8, geometric mean estimates of bulk K' remained within half an order of magnitude between constant head, pulse interference and isolated zone pumping tests (3.3×10^{-7} - 7.3×10^{-7} m/s). However, open-well pumping test data provided a geometric mean estimate for the site of 1.7×10^{-5} m/s, over two orders of magnitude higher than values predicted by the other test methods. In addition, analysis of the pumping test data with the Moench (1997) solution

estimated a mean value 1.5-2 orders of magnitude lower than the more local-scale methods. The discrepancy in the geometric mean estimates obtained from the pumping tests between solutions is not surprising given that in Chapter 2, both the Moench (1997) and the derived pumping test solution did not appear to be capable of uniquely estimating K' for one pumping test conducted at the Fletcher Creek field site. Based on the discrepancy observed in this comparison (particularly when compared to the direct measurements obtained using the constant head method), and even with the addition of another pumping test data set, the estimates predicted by both open-hole analytical pumping test models cannot be considered acceptable. This also implies that the other vertical hydraulic parameters estimated using this method are likely to be unreliable.

Log standard deviations for the K' values were smallest for the constant head test measurements; the pulse interference and isolated zone pumping test results produced larger, yet similar standard deviations. A certain degree of heterogeneity was expected from one fracture zone to the next and therefore provides a reasonable explanation for the variability in K' estimates. Despite this observed variability, it is worthy to note that the pulse interference tests, constant head tests and isolated zone pumping tests produced comparable geometric mean estimates. Therefore if resource constraints limit the performance of constant head tests in multiple wells, the more simple to conduct and less expensive pulse interference test evaluated with the Elmhirst and Novakowski (2012a) solution could potentially provide a reasonable vertical hydraulic conductivity estimate if values are averaged over the site-scale to provide a bulk K' value. It is important to consider however that the agreement observed here in geometric mean K' could be particular to this field setting.

3.5.3 Specific storage

Specific storage of a saturated aquifer is defined as the volume of water that a unit volume of aquifer releases from storage under unit decline in hydraulic head (Freeze and Cherry, 1979).

Separate horizontal and vertical specific storage values were calculated to reflect the difference in spacing and orientation of fractures and hence storage values that may be directionally dependent. From the field study, values of horizontal specific storage (S_s) and vertical specific storage (S_s') (Figure 3.9 and Figure 3.10, respectively) were compared using pulse interference tests and isolated zone pumping tests. Estimates of horizontal specific storage decreased by a little less than two orders of magnitude between the isolated zone pumping test and the pulse interference test scale, while estimates of vertical specific storage decreased by less than one order of magnitude (when estimates from pulse interference tests in wells FC-7 and FC-9 are averaged). In part this is an artefact of the ratio method used to analyse the isolated zone tests, whereby the S_s and S_s' are equated in order to calculate K' . Considering that unique solutions were achieved with the pulse-interference test solution using the strategy described in the methods sections, more credence must be given to the estimates obtained for S_s and S_s' using this method.

Standard deviation in estimates of vertical specific storage for the pulse interference tests was large, demonstrating the broad range in values of arithmetic mean obtained for each observation well for these tests. Although it is possible that such a range in values may occur in this setting, this may also be an artefact of the fitting process. As no direct measurement can be obtained for this parameter for comparison, further examination of this issue is warranted.

3.5.4 Specific yield

The arithmetic mean estimates of specific yield amongst pulse interference and constant head tests are presented in Table 3.3. As can be seen visually in Figure 3.11, values of S_y vary by approximately half an order of magnitude between constant head and pulse interference tests.

Comparison of specific yield estimates among different testing methods in fractured rock has not been studied. This is in part because aquifer tests in fractured rock may be viewed as unreliable

for estimating S_y (Healy and Cook, 2002). To date, only one study on the scale effects associated with S_y in a fractured rock environment has been conducted. Elmhirst (2011) found that in a crystalline rock setting, no definitive scale effect could be detected after review of mean data from constant head tests, pulse interference tests and long term pumping tests (analysed with the Moench [1997] model). In fact, mean values of S_y varied by less than half an order of magnitude between tests. Based on the findings here, there does not appear to be a discernible scale effect between site scale arithmetic mean values of S_y estimated from constant head injection tests and pulse interference tests. Similar to the comparison of K' values obtained from constant head tests and pulse interference tests, it appears that in a sedimentary rock setting, pulse interference tests can be used in the place of the more resource and cost intensive constant head tests to obtain satisfactory bulk estimates of S_y .

3.6 Conclusions and recommendations

A broad-based comparison of various hydraulic testing methods was carried out in a sedimentary rock aquifer located near Cambridge, Ontario, Canada. Constant head injection tests, pulse interference tests, and two types of pumping tests were performed on nine wells, six of which are inclined at approximately 45 degrees to ground surface. The aim of this study was to explore the use of a simple open-hole pumping test in providing confident site-scale estimates of hydraulic parameters, those in the vertical orientation in particular, when compared to other testing methods. The following conclusions can be made:

1. Open-well pumping tests are capable of providing an accurate bulk estimate of horizontal K in a sedimentary rock setting. From the constant head test scale up to the pumping test scale, K increased by approximately half an order of magnitude, indicative of little if any scale effect present.
2. Geometric mean estimates of bulk K' remained within half an order of magnitude between constant head, pulse interference and isolated zone pumping tests. Similarly,

arithmetic mean estimates of bulk S_y values varied by half an order of magnitude between constant head injection tests and pulse interference tests. Since variations between half an order of magnitude are not indicative of a significant scale effect, this suggests that pulse interference tests can be used as an alternative to the more expensive and difficult constant head injection tests for determining K' and S_y in a sedimentary rock setting.

3. In order to obtain unique results for K' and S_y , a specific strategy is required when using a parameter estimation procedure, whereby values of the horizontal hydraulic parameters are first determined using fixed estimates of the vertical parameters, following which the vertical parameters are determined using the values for the horizontal parameters obtained in the previous step.
4. Although unique estimates of horizontal and vertical specific storage were obtained using the open-hole pulse interference tests, as there are no direct measurements to compare to, the accuracy of these values are uncertain. Further investigation of this issue is warranted.
5. Even with the addition of more pumping test data, the interpretation of open-well pumping tests with either the analytical model developed in Chapter 2, or the Moench (1997) solution remained uncertain, with non-uniqueness significantly prevalent in the vertical hydraulic parameters.

3.7 List of abbreviations

T (m ² /s)	bulk transmissivity of the horizontal fracture domain
Q (m ³ /s)	flow rate
h (m)	hydraulic head
r (m)	radial distance from the source well
r_w (m)	wellbore radius
K' (m/s)	hydraulic conductivity of the vertical fracture domain
K (m/s)	hydraulic conductivity of the horizontal fracture domain
$2b$ (m)	fracture aperture spacing
$2b_{eq}$ (m)	equivalent fracture aperture
P (kg/m ³)	density of water
g (m/s ²)	acceleration due to gravity
μ (Ns/m ²)	dynamic viscosity of water
H_0 (m)	initial head in source well
b (m)	packer interval spacing
n_f	number of horizontal fractures
S_s (1/m)	specific storage of the horizontal domain
S_s' (1/m)	specific storage of the vertical domain
S_y (-)	specific yield of the vertical domain
α'	vertical hydraulic diffusivity
L_n (m)	half spacing between each horizontal fracture
S (-)	storativity of the horizontal fracture domain
REV	representative elementary volume

3.8 Literature cited

- Abbey, D. G., & Allen, D. M. (2000). Fracture zones, aquifer testing, and scale effects: Considerations in fractured bedrock aquifers of southwestern British Columbia. *Proceedings of the 53rd Canadian Geotechnical Conference*, Montréal, Québec.
- Bernard, S., Delay, F., & Porel, G. (2006). A new method of data inversion for the identification of fractal characteristics and homogenization scale from hydraulic pumping tests in fractured aquifers. *Journal of Hydrology*, 328(3–4), 647-658.
- Bliss, J. C., & Rushton, K. R. (1984). The reliability of packer tests for estimating the hydraulic conductivity of aquifers *Quarterly Journal of Engineering Geology and Hydrogeology*, 17(1), 81.
- Doe, T. W., & Remer, J. (1981). Analysis of constant-head tests in non-porous fractured rock. *Third Invitational Well-Testing Symposium: Well Testing in Low Permeability Environments* Berkeley, California. pp. 84-89.
- Doherty, J., Brebber, L., & Whyte, P. (1994). PEST: Model-independent parameter estimation. Watermark Numerical Computing.
- Domenico, P. A., & Schwartz, F. W. (1990). *Physical and chemical hydrogeology*. New York: John Wiley & Sons.
- Eaton, T. T., Anderson, M. P., & Bradbury, K. R. (2007). Fracture control of ground water flow and water chemistry in a rock aquitard *Ground Water*, 45(5), 601-615.
- Elmhirst, L. M. (2011). The use of pulse interference tests for the determination of specific yield in fractured rock settings. (Master of Applied Science, Queen's University).
- Elmhirst, L. M., & Novakowski, K. S. (2012a). The analysis of pulse interference tests conducted in a fractured rock aquifer bounded by a moving free surface *Advances in Water Resources*, 35, 20.
- Elmhirst, L. M., & Novakowski, K. S. (2012b). Effects of test scale on the measurement of transmissivity, vertical hydraulic conductivity, storativity and specific yield in a fractured rock setting. *Manuscript Submitted for Publication*.
- Freeze, R. A., & Cherry, J. F. (1979). *Groundwater*. Englewood Cliffs, N.J.: Prentice-Hall.
- Healy, R., & Cook, P. (2002). Using groundwater levels to estimate recharge *Hydrogeology Journal*, 10(1), 91.
- Hunt, A. G. (2006). Scale-dependent hydraulic conductivity in anisotropic media from dimensional cross-over *Hydrogeology Journal*, 14(4), 499.
- Ii, H. (1995). Effective porosity and longitudinal dispersivity of sedimentary rocks determined by laboratory and field tracer tests *Environmental Geology*, 25(2), 71.

- Kurikami, H., Takeuchi, R., & Yabuuchi, S. (2008). Scale effect and heterogeneity of hydraulic conductivity of sedimentary rocks at Horonobe URL site. *Physics and Chemistry of the Earth*, 33, S37-S44.
- Lapcevic, P.A., Reichart, T.M., Novakowski, K.S. (1993). The interpretation of pumping tests conducted in vertically fractured rock using models developed for porous media. *National Ground Water Association Focus Eastern Conference*, pp. 839-849.
- Lapcevic, P. A., Novakowski, K. S., & Sudicky, E. A. (1999). Groundwater flow and solute transport in fractured media. In J. W. Delleur (Ed.), *The handbook of groundwater engineering* (). Boca Raton: CRC Press LLC.
- Lemieux, J., Therrien, R., & Kirkwood, D. (2006). Small scale study of groundwater flow in a fractured carbonate-rock aquifer at the St-Eustache quarry, Québec, Canada *Hydrogeology Journal*, 14(4), 603-612.
- Liberty, B. A. (1981). Colossal cataract: The geologic history of Niagara falls. In I. H. Tesmer (Ed.), *Structural geology* (pp. 57-62). Albany, N.Y.: State University of New York Press.
- Lloyd, J. W. (1999). *Water resources of hard rock aquifers in arid and semi-arid zones* No. 58). Paris: UNESCO.
- Milloy, C. A. (2007). Measurement of hydraulic head for the evaluation of groundwater recharge to discrete fracture zones in a crystalline bedrock aquifer. (M.Sc thesis. Queen's University).
- Moench, A. F. (1984). Double-porosity models for a fissured groundwater reservoir with fracture skin *Water Resources Research*, 20(7), 831.
- Moench, A. F. (1985). Transient flow to a large-diameter well in an aquifer with storative semiconfining layers. *Water Resources Research*, 21(8), 1121-1131.
- Moench, A. F. (1995). Combining the Neuman and Boulton models for flow to a well in an unconfined aquifer *Ground Water*, 33(3), 378-384.
- Moench, A. F. (1997). Flow to a well of finite diameter in a homogeneous, anisotropic water table aquifer *Water Resources Research*, 33(6), 1397.
- Muldoon, M., & Bradbury, K. R. (2005). Site characterization in densely fractured dolomite: Comparison of methods *Ground Water*, 43(6), 863-876.
- Nastev, M., Savard, M. M., Lapcevic, P., Lefebvre, R., & Martel, R. (2004; 2004). Hydraulic properties and scale effects investigation in regional rock aquifers, south-western Québec, Canada *Hydrogeology Journal*, 12(3).
- Neuman, S. P. (2005). Trends, prospects and challenges in quantifying flow and transport through fractured rocks. *Hydrogeology Journal*, 13(1), 124-147.

- Neuman, S. P., & Witherspoon, P. A. (1972). Field determination of the hydraulic properties of leaky multiple aquifer systems. *Water Resources Research*, 8(5), 1284-1298.
- Novakowski, K. S. (1989). Analysis of pulse interference tests. *Water Resources Research*, 25(11), 2377-2387.
- Novakowski, K., Milloy, C., Gleeson, T., Praamsma, T., Levison, J., & Hall, K. (2007). Groundwater recharge in a gneissic terrain having minimal drift cover. *Proceedings of the 8th Joint CGS/IAHCNC Groundwater Conference*, Ottawa, Ontario. pp. 280-285.
- Reichart, T. M. (1992). Influence of vertical fractures in horizontally-stratified rocks. (Master of Science, University of Waterloo).
- Rovey II, C. W. (1994). Assessing flow systems in carbonate aquifers using scale effects in hydraulic conductivity *Environmental Geology*, 24(4), 244.
- Rovey II, C. W. (1998). Digital simulation of the scale effect in hydraulic conductivity *Hydrogeology Journal*, 6(2), 216.
- Sageev, A. (1986). Slug test analysis, *Water Resour. Res.*, 22(8):1323-1333.
- Sánchez-Vila, X., Carrera, J., & Girardi, J. P. (1996). Scale effects in transmissivity. *Journal of Hydrology*, 183(1-2), 1-22.
- Schulze-Makuch, D., Carlson, D. A., Cherkauer, D. S., & Malik, P. (1999). Scale dependency of hydraulic conductivity in heterogeneous media *Ground Water*, 37(6), 904.
- Snow, D. T. (1968). Rock fracture spacings, openings and porosities. Proceedings from the American Society of Civil Engineers, 94. pp. 73-91.
- Stephenson, K. M., & Novakowski, K. S. (2006). The analysis of pulse interference tests conducted in a fractured rock aquifer bounded by a constant free surface, *Journal of Hydrology*, 319(1-4), 109-122.
- Tiedeman, C. R., & Hsieh, P. A. (2001). Assessing an open-well aquifer test in fractured crystalline rock. *Ground Water*, 39(1), 68-78.

Table 3.1 Specific yield estimates from constant head test data analysis.

Borehole	Total T (m ² /s)	2b(m)	Tested borehole length (m)	S _y (-)
FC-1	9.3 x 10 ⁻⁵	5.4 x 10 ⁻⁴	22.68	2.4 x 10 ⁻⁵
FC-2	2.0 x 10 ⁻⁴	7.0 x 10 ⁻⁴	21.08	3.3 x 10 ⁻⁵
FC-3	1.1 x 10 ⁻⁴	5.7 x 10 ⁻⁴	15.96	3.6 x 10 ⁻⁵
FC-4	3.0 x 10 ⁻⁴	8.0 x 10 ⁻⁴	13.76	5.8 x 10 ⁻⁵
FC-5	1.4 x 10 ⁻⁴	6.2 x 10 ⁻⁴	8.46	7.3 x 10 ⁻⁵
FC-6	9.6 x 10 ⁻⁵	5.5 x 10 ⁻⁴	9.41	5.8 x 10 ⁻⁵
FC-7	9.9 x 10 ⁻⁵	5.5 x 10 ⁻⁴	9.19	6.0 x 10 ⁻⁵
FC-8	3.4 x 10 ⁻⁵	3.9 x 10 ⁻⁴	12.18	3.2 x 10 ⁻⁵

Table 3.2 Base case values used in the sensitivity analysis.

T (m/s)	S (-)	S_y (-)	K' (m/s)	S'_s (1/m)	Ho (m)	r (m)	r_w (mm)	r_s (mm)	r_{ob} (mm)	L_w	L_n	n_r	α_t
2.0 x 10 ⁻⁵	2.0 x 10 ⁻⁶	1.0 x 10 ⁻⁴	2.0 x 10 ⁻⁷	2.0 x 10 ⁻⁸	1.0	8.0	76.2	76.2	76.2	6.0	2.0	3.0	1.0 x 10 ⁹

Table 3.3 Comparison of mean (standard deviation) for various tests and hydraulic parameters.

Parameter	Source well	Monitored wells	Pumping test: Moench (1997)	Pumping test: Present model	Pulse interference test	Isolated zone pumping test	Constant head test
K (m/s)	FC-9	FC-1 - FC-8	7.1×10^{-6} (2.4×10^{-6})	1.6×10^{-5} (5.0×10^{-6})	1.8×10^{-5} (1.3×10^{-5})	(-)	4.6×10^{-6} (4.2×10^{-6}) ^d
	FC-7	FC-1 - FC-6, FC-8,9	6.6×10^{-6} (2.4×10^{-6})	9.3×10^{-6} (4.4×10^{-6})	1.1×10^{-5} (7.5×10^{-6})		
S _s (1/m)	FC-9	FC-1 - FC-8	4.0×10^{-8} (6.6×10^{-8})	2.8×10^{-7} (3.3×10^{-7})	2.7×10^{-6} (5.7×10^{-6})	8.9×10^{-5} (9.1×10^{-5}) ^a	(-)
	FC-7	FC-1 - FC-6, FC-8,9	5.1×10^{-7} (5.4×10^{-7})	1.0×10^{-6} (1.2×10^{-6})	1.9×10^{-6} (4.6×10^{-6})		
K' (m/s)	FC-9	FC-1 - FC-8	1.2×10^{-8} (1.4×10^{-5})	1.1×10^{-5} (1.0×10^{-5})	1.4×10^{-6} (2.6×10^{-5})	5.8×10^{-7} (1.8×10^{-5}) ^b	3.8×10^{-7} (5.2×10^{-7}) ^e
	FC-7	FC-1 - FC-6, FC-8,9	3.0×10^{-9} (4.3×10^{-6})	2.6×10^{-5} (4.7×10^{-5})	5.9×10^{-7} (3.7×10^{-6})		
S _y (-)	FC-9	FC-1 - FC-8	6.7×10^{-5} (1.9×10^{-4})	4.7×10^{-6} (8.4×10^{-6})	9.3×10^{-5} (1.6×10^{-4})	(-)	4.7×10^{-5} (1.8×10^{-5}) ^f
	FC-7	FC-1 - FC-6, FC-8,9	7.1×10^{-2} (2.1×10^{-1})	6.3×10^{-5} (1.2×10^{-4})	1.6×10^{-4} (2.0×10^{-4})		
S _s ' (1/m)	FC-9	FC-1 - FC-8		3.9×10^{-7} (5.1×10^{-7})	5.5×10^{-5} (1.2×10^{-4})	8.9×10^{-5} (9.1×10^{-5}) ^c	(-)
	FC-7	FC-1 - FC-6, FC-8,9		2.4×10^{-6} (2.5×10^{-6})	1.9×10^{-6} (2.5×10^{-6})		

^a Individual horizontal fracture storativities (interpreted using the ratio method and multiple aquifer model) divided by the test interval spacing.

^b Individual vertical fracture transmissivities (interpreted using the ratio method and multiple aquifer model) divided by the test interval spacing.

^c Individual vertical fracture storativities (interpreted using the ratio method and multiple aquifer model) divided by the test interval spacing where S_s is assumed equivalent to S_s'.

^d Summation of transmissivity (obtained using the Theim equation) divided by tested borehole length.

^e Tests isolating vertical fractures were identified and K' calculated using the cubic law and dividing by test interval spacing.

^f For each borehole an equivalent fracture aperture (2b) was determined from the total transmissivity using the cubic law. Division of 2b by the tested borehole length provides a value for S_y.

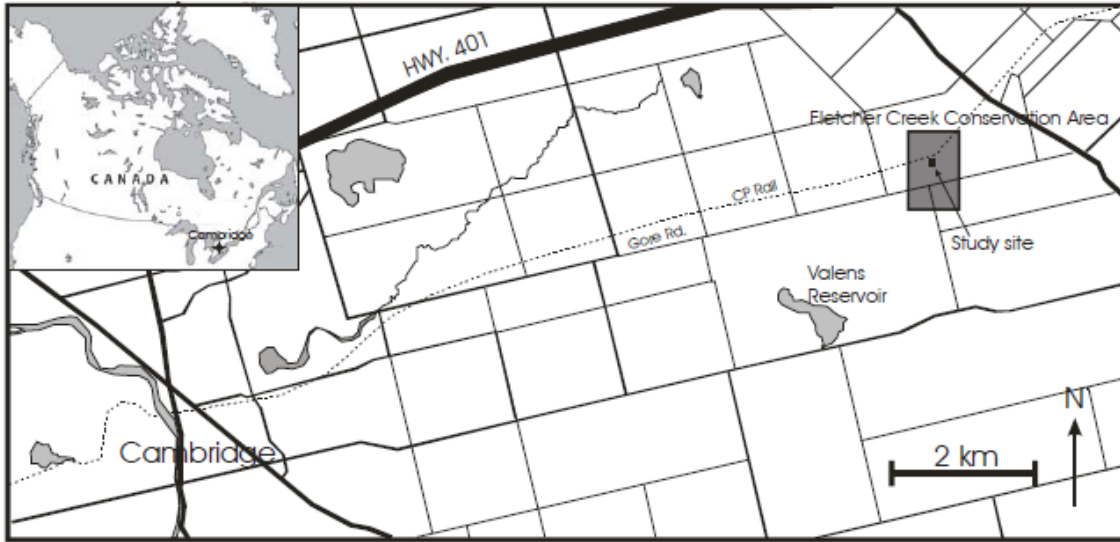


Figure 3.1 Location map of Fletcher Creek Conservation Area in southern Ontario.

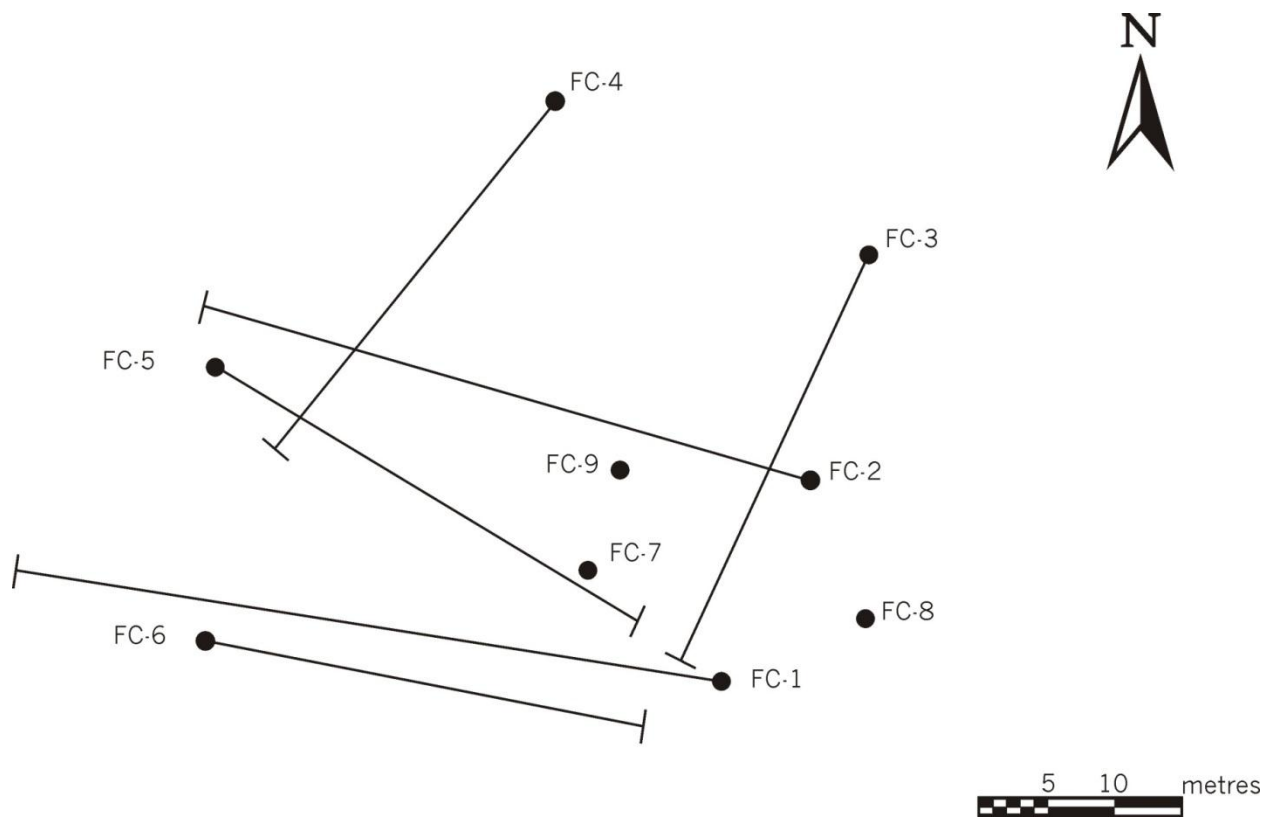


Figure 3.2 Plan view of borehole locations at the Fletcher Creek Conservation Area field site.

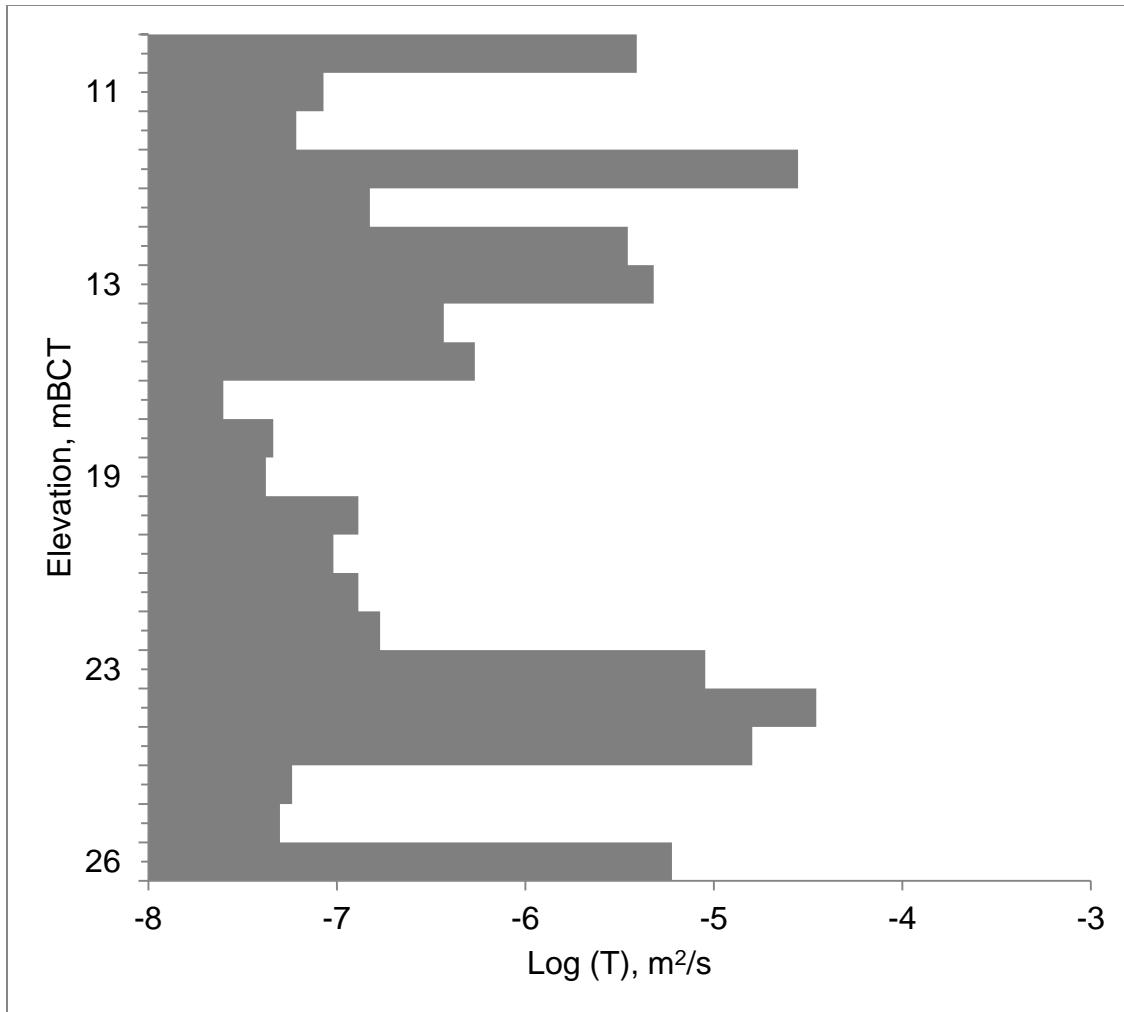


Figure 3.3 Transmissivity profile with depth for well FC-3 and a packer spacing of 0.5 m.

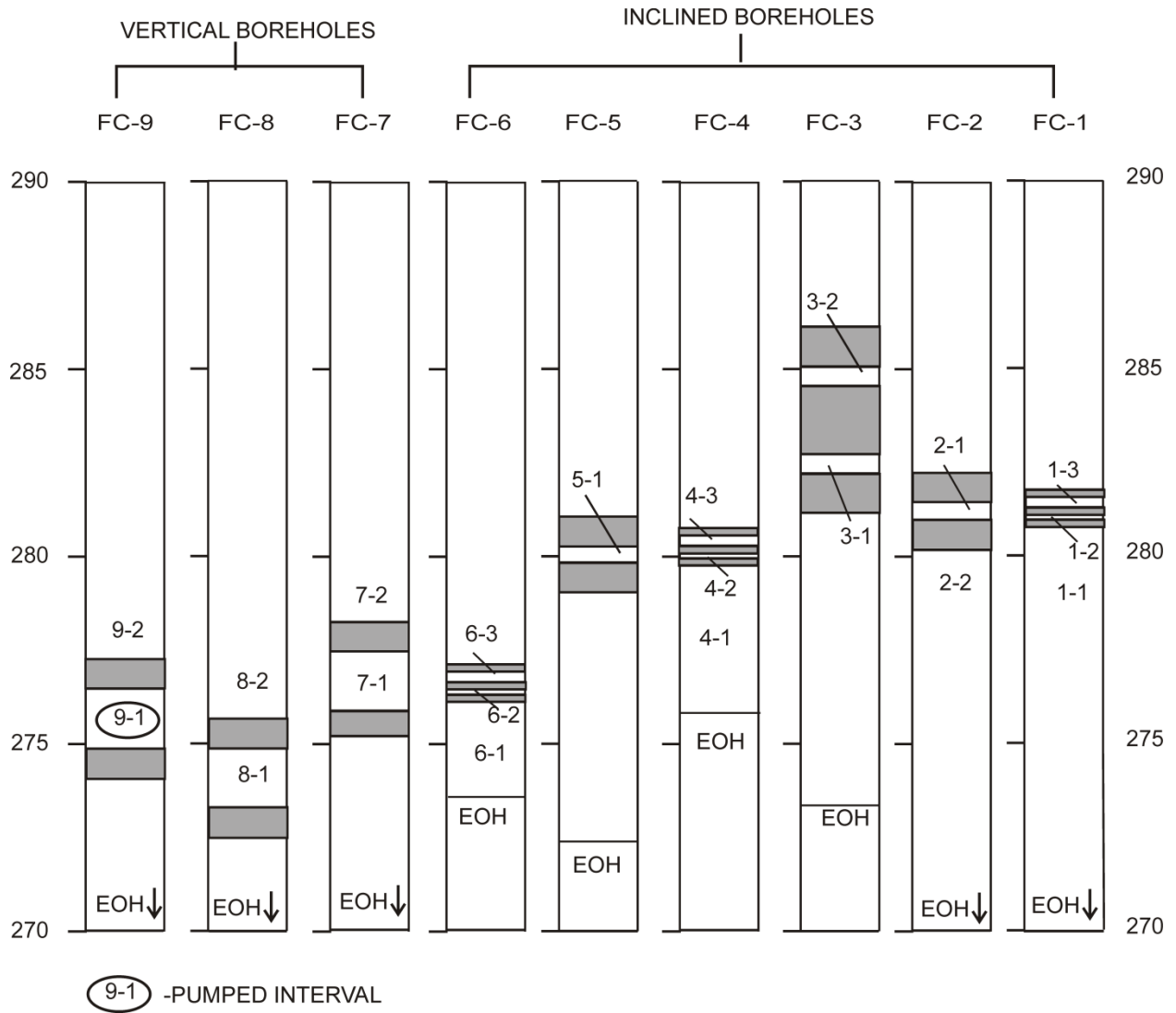


Figure 3.4 Example of isolated intervals for 12-hour pumping test performed by Lapcevic, et al. (1993).

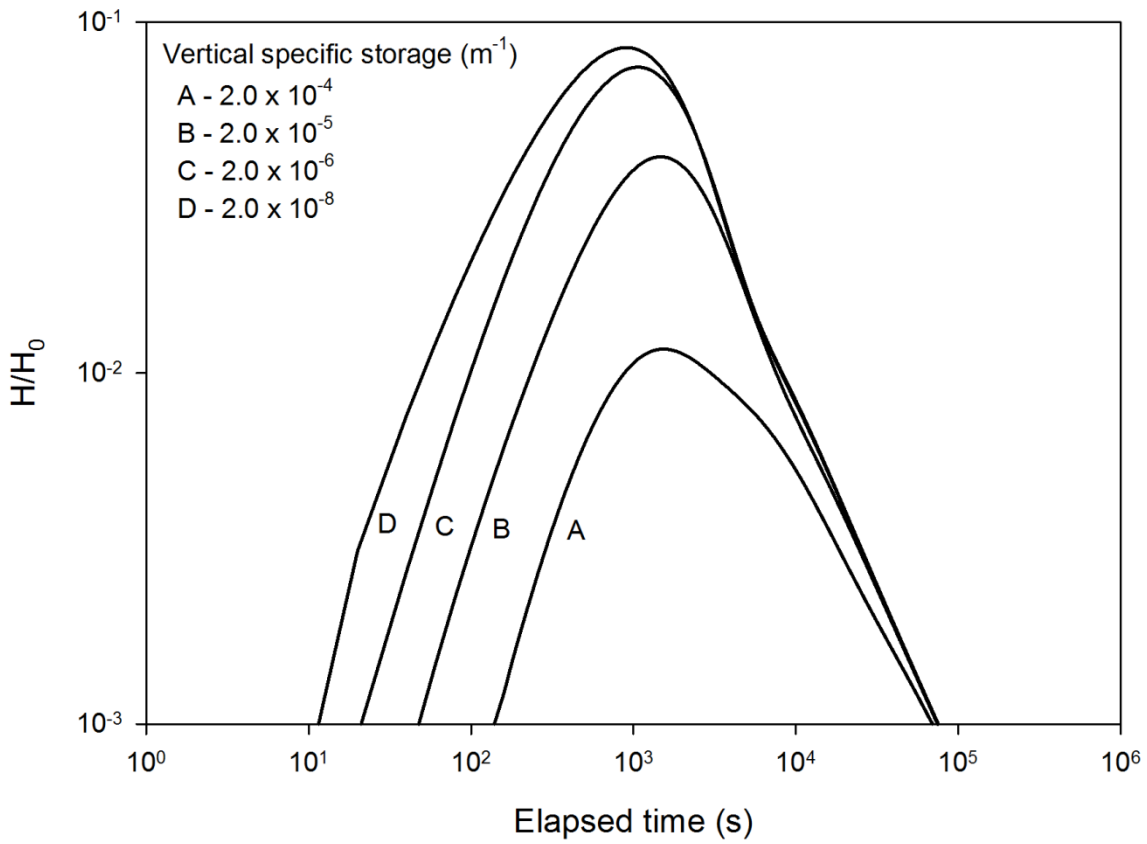


Figure 3.5 Sensitivity analysis of observation well response to various values of S_s' as determined by the Elmhirst and Novakowski (2012) solution for a pulse interference test.

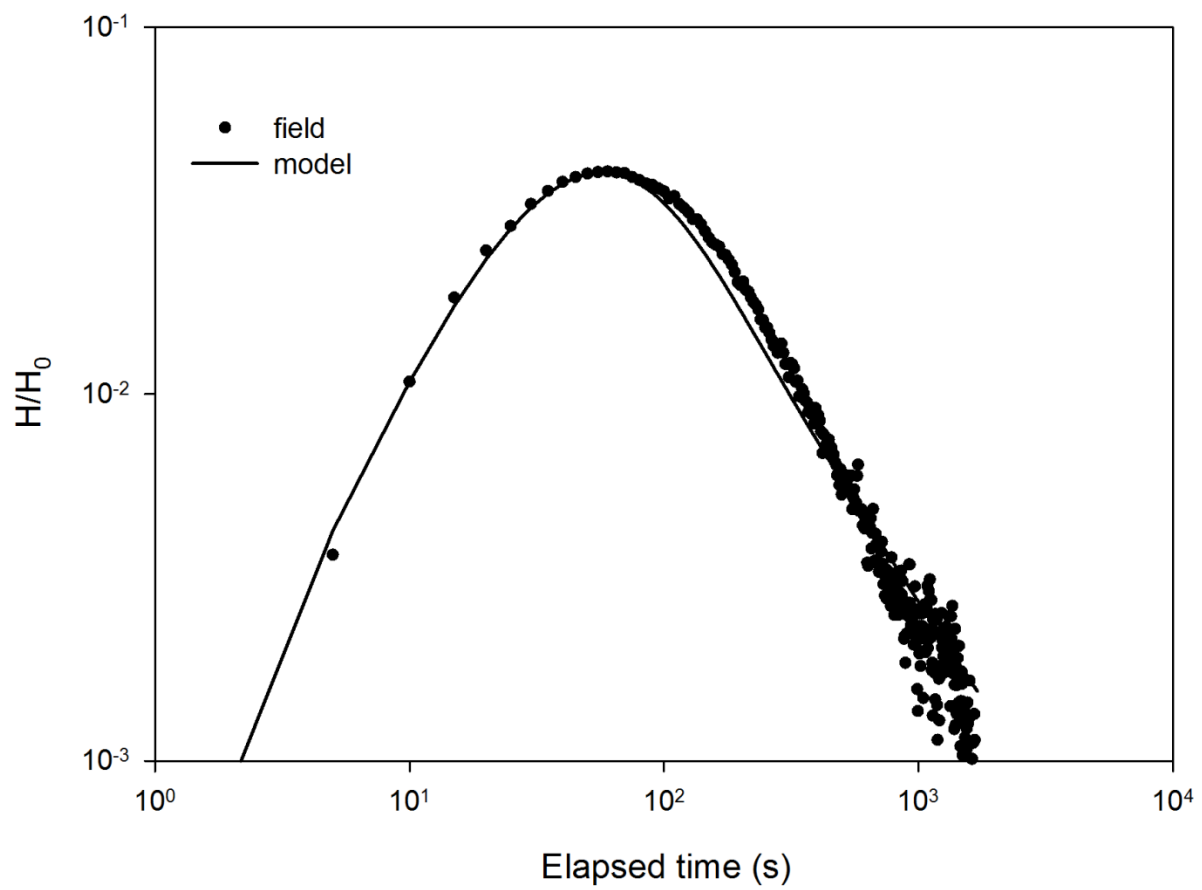


Figure 3.6 Pulse interference test response in observation well FC-1 to slug injection in FC-9.

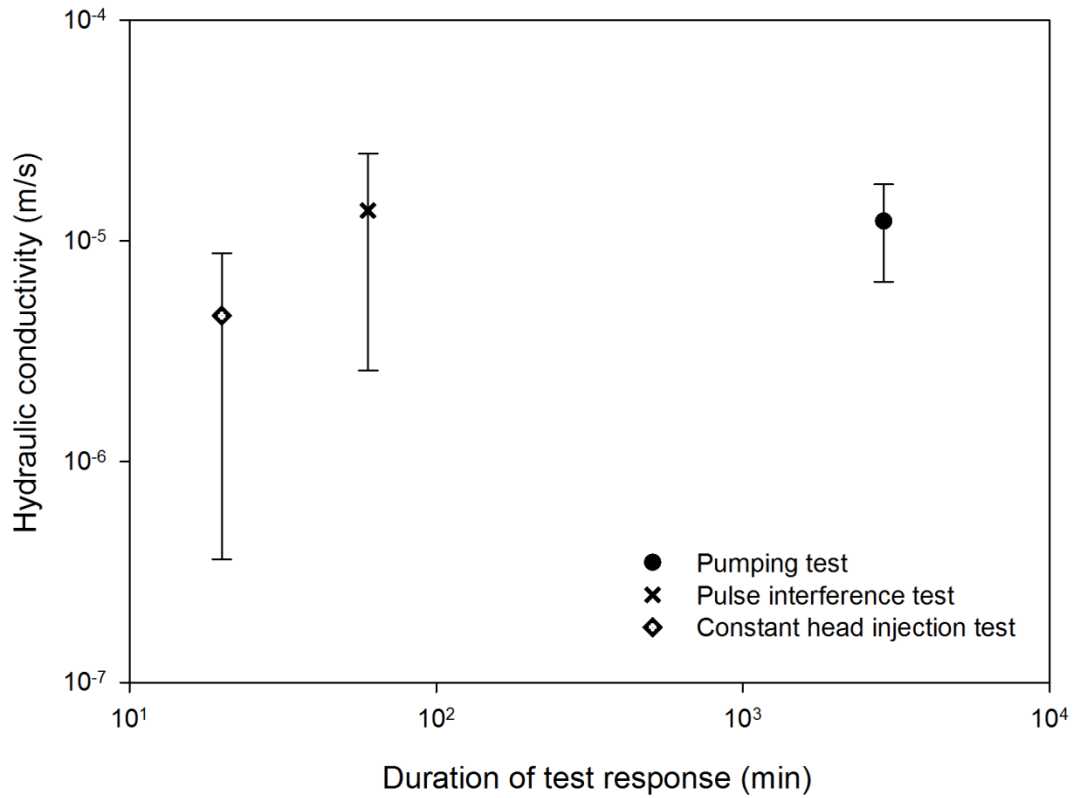


Figure 3.7 Log-log plot of geometric mean hydraulic conductivity results and standard deviations obtained from various tests with respect to measurement duration.

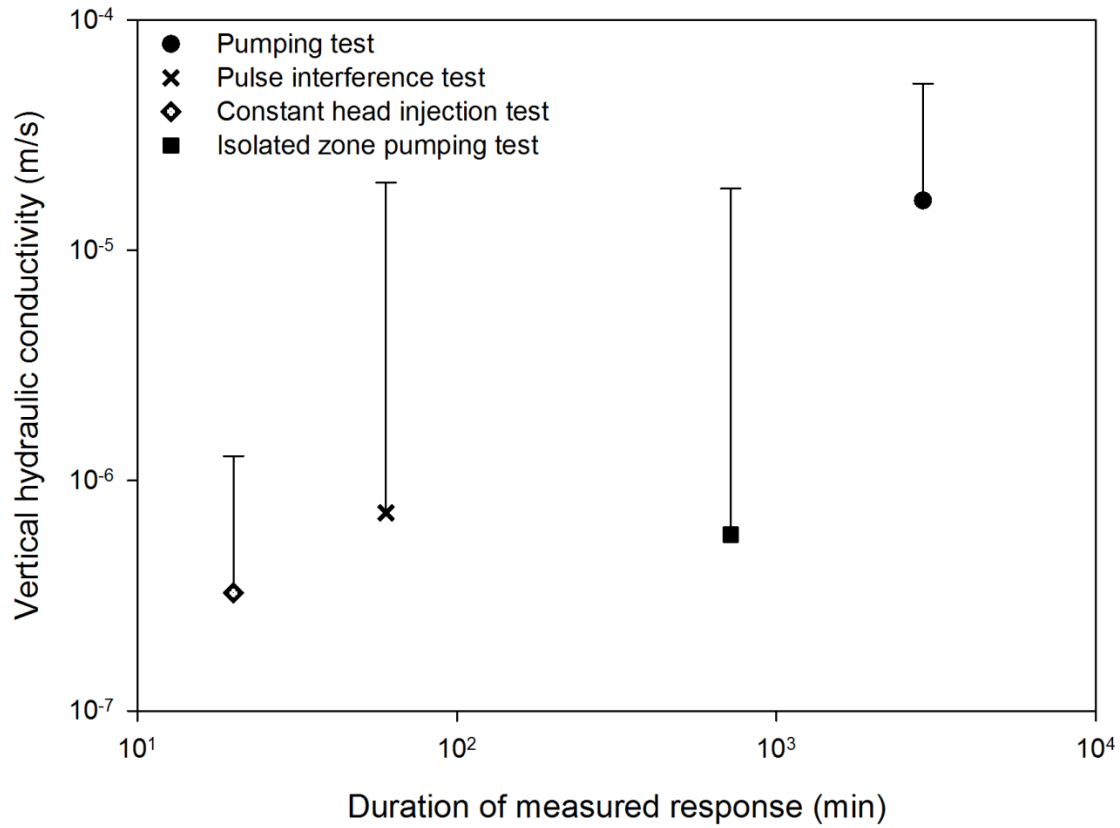


Figure 3.8 Log-log plot of geometric mean vertical hydraulic conductivity results and standard deviations obtained from various tests with respect to measurement duration.

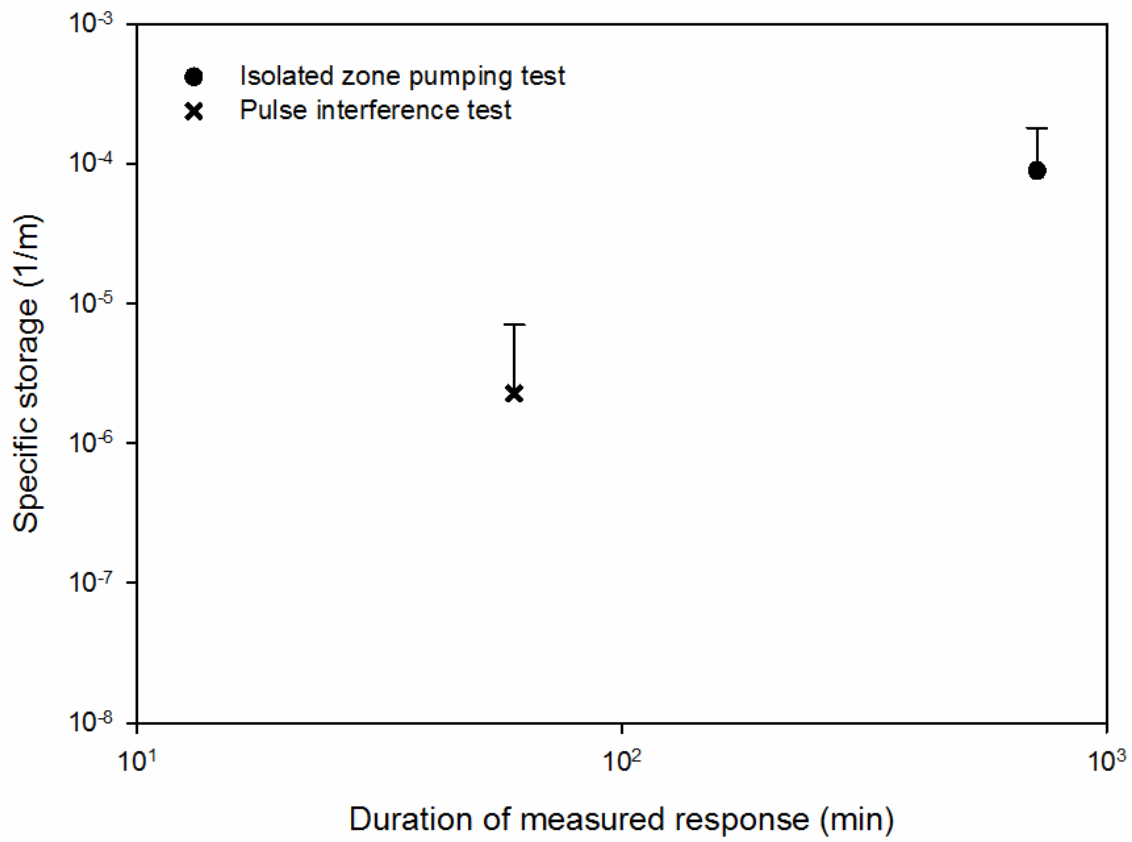


Figure 3.9 Log-log plot of arithmetic mean specific storage results and standard deviations obtained from various tests with respect to measurement duration.

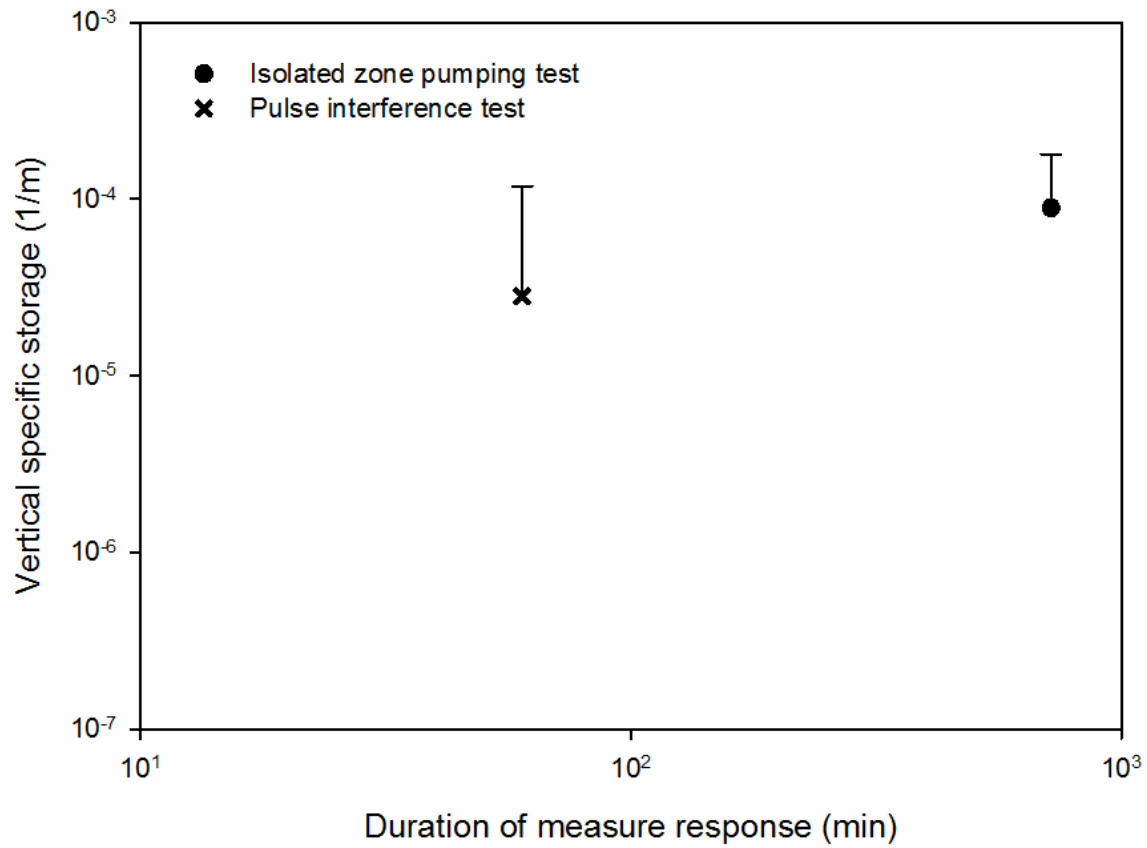


Figure 3.10 Log-log plot of arithmetic mean vertical specific storage results and standard deviations obtained from various tests with respect to measurement duration.

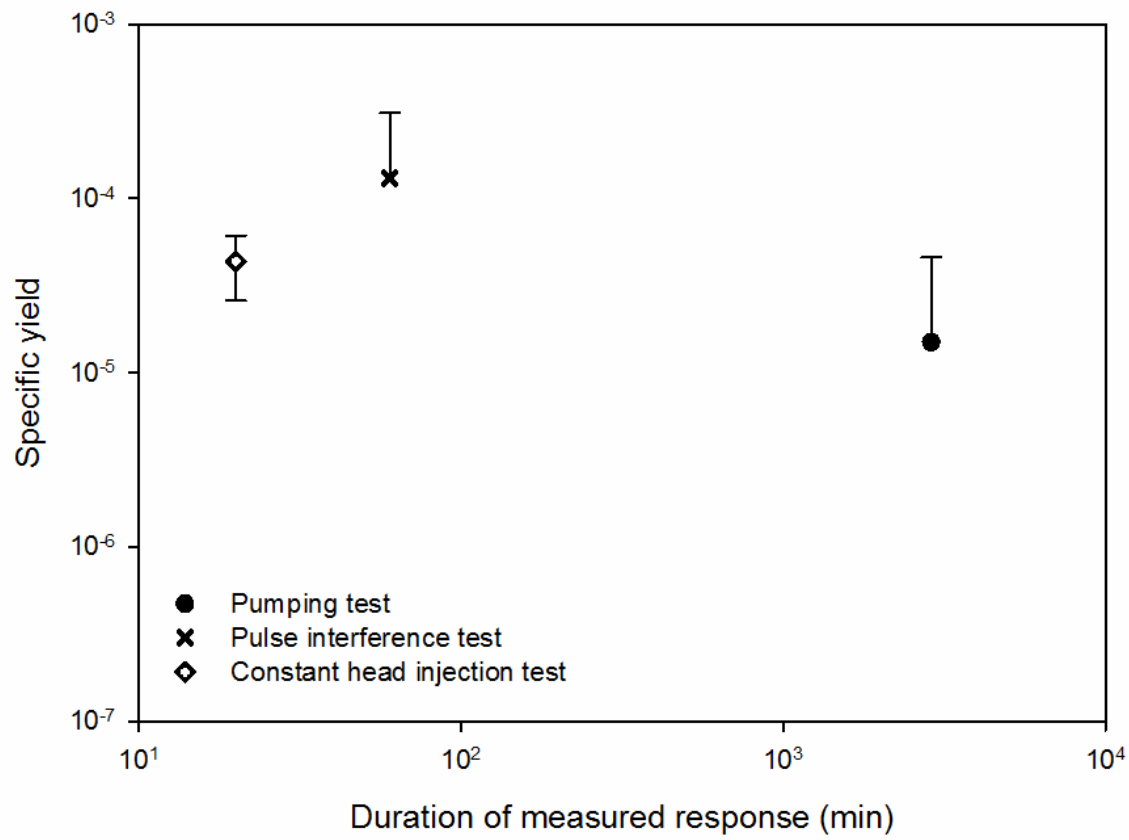


Figure 3.11 Log-log plot of arithmetic mean specific yield results and standard deviations obtained from various tests with respect to measurement duration.

Chapter 4

Discussion

Both the analytical pumping test model that was presented in Chapter 2 and the Moench (1997) solution could not estimate unique values of specific storage, specific yield and vertical hydraulic conductivity in the sedimentary rock setting presented in the field example. This is believed to be because of the similarity in their values and the interaction between these parameters in providing vertical fluid migration. For instance, it was found that the sensitivity of the model for values of specific yield below 10^{-5} was significantly diminished independent of the value of other parameters. This was a concern in the field setting given that estimates of specific yield were near this value. Additionally, while pumping test drawdown curves from each monitoring well could be similar in shape and adequately matched using both the Moench (1997) solution and the solution derived in Chapter 2, the parameter estimates obtained by either solution were not necessarily accurate.

Following the development of the pumping test model, a comparison of various hydraulic testing methods was carried out in the same sedimentary rock field setting. The results of the study found that open-well pumping tests were capable of providing an accurate bulk estimate of hydraulic conductivity in a sedimentary rock setting. From the constant head test scale up to the pumping test scale, hydraulic conductivity increased by approximately half an order of magnitude, indicative of little if any scale effect present. Geometric mean estimates of bulk vertical hydraulic conductivity remained within half an order of magnitude between constant head, pulse interference and isolated zone pumping tests. Similarly, arithmetic mean estimates of bulk

specific yield values varied by half an order of magnitude between constant head injection tests and pulse interference tests. Since variations of half an order of magnitude are not indicative of a significant scale effect, this may show that pulse interference tests can be used as an alternative to the more expensive and difficult constant head injection tests for determining vertical hydraulic conductivity and specific yield in a sedimentary rock setting.

In order to obtain unique results for K' and S_y , a specific strategy was required when using a parameter estimation procedure; values of the horizontal hydraulic parameters were first determined using fixed estimates of the vertical parameters, then the vertical parameters were determined using the values for the horizontal parameters obtained in the previous step. Although unique estimates of horizontal and vertical specific storage were obtained using the open-hole pulse interference tests, since there are no direct measurements to compare to, the accuracy of these values remains uncertain and further investigation of this issue is warranted. Even with the addition of more pumping test data, the interpretation of open-well pumping tests with either the analytical model developed in Chapter 2, or the Moench (1997) solution remained uncertain, with non-uniqueness significantly prevalent in the vertical hydraulic parameters.

4.1 Literature cited

Moench, A. F. (1997). Flow to a well of finite diameter in a homogeneous, anisotropic water table aquifer *Water Resources Research*, 33(6), 1397.

Chapter 5

Conclusion

Open-well pumping tests evaluated with an analytical model are not able to uniquely predict vertical hydraulic parameters in a sedimentary rock formation. Although several strategies were attempted to obtain unique solutions for the field example, results suggest that an alternate approach is required to obtain these estimates.

By examining a range of hydraulic field investigation techniques to characterize vertical parameters in a sedimentary rock aquifer, it was found that pulse interference tests may be able to determine a value of vertical hydraulic conductivity and specific yield comparable to estimates from constant head testing. This may suggest that pulse interference tests may be a less time-intensive and cost effective alternative to constant head tests for hydrogeological site characterization. However, given that the sensitivity analysis performed on the model derived in this paper found that vertical and horizontal hydraulic conductivity, specific storage, and specific yield all demonstrated a range of sensitivity for an open-hole observation well response, this model may perhaps still provide unique estimates of these parameters in an alternative field setting.

Appendix A

Detailed derivation of the pumping test solution

The Laplace transform applied to equations [A1] through [A11]:

$$\mathcal{L}[A. 1]: \frac{\partial^2 \bar{h}}{\partial r^2} + \frac{1}{r} \frac{\partial \bar{h}}{\partial r} = \frac{S}{T} p \bar{h} - \bar{q} \quad A.14$$

$$\mathcal{L}[A. 2]: \bar{q} = (n_f - 1) \bar{q}_f + \bar{q}_t \quad A.15$$

$$\mathcal{L}[A. 3]: \bar{q}_t = \bar{q}_{tu} + \bar{q}_{tl} \quad A.16$$

$$\mathcal{L}[A. 4]: \bar{q}_f = \bar{q}_{fu} + \bar{q}_{fl} \quad A.17$$

$$\mathcal{L}[A. 5]: \bar{q}_{tu} = \frac{-K' \partial \bar{h}_m}{T \partial z} \Big|_{z=0} \quad A.18$$

$$\mathcal{L}[A. 6]: \bar{q}_{tl} = \bar{q}_{fu} = \bar{q}_{fl} = \frac{-K' \partial \bar{h}_m}{T \partial z} \Big|_{z=0} \quad A.19$$

$$\mathcal{L}[A. 7]: \frac{\partial^2 \bar{h}_m}{\partial z^2} = \frac{S'_s}{K'} p \bar{h}_m \quad A.20$$

$$\mathcal{L}[A. 8]: \bar{h}(r, p) = \bar{h}_m(r, 0, p) \quad A.21$$

$$\mathcal{L}[A. 9]: \bar{h}(\infty, p) = 0 \quad A.22$$

Using the theory of convolution,

$$\mathcal{L}[A. 10]: K' \frac{\partial \bar{h}_m}{\partial z} \Big|_{z=L_w} = -\alpha_1 S_y \frac{p \bar{h}_m(r, L_w, p)}{p + \alpha_1} \quad A.23$$

$$\mathcal{L}[A. 11]: \frac{\partial \bar{h}_m}{\partial z} \Big|_{z=L_n} = 0 \quad A.24$$

Solving equation A.20 for \bar{h}_m :

Factor equation A.20:

$$\bar{h}_m (D_z + (\Psi p)^{1/2}) (D_z - (\Psi p)^{1/2}) = 0 \quad A.25$$

where

$$D_z^n = \frac{\partial^n}{\partial z^n}$$

$$\Psi = \frac{S'_s}{K'}$$

The general solution for Eq. [A.25] becomes:

$$\bar{h}_m = A_1 \exp\left(-z(\Psi p)^{\frac{1}{2}}\right) + B_1 \exp\left(z(\Psi p)^{\frac{1}{2}}\right) \quad A.26$$

where A_1 and B_1 are constants.

Applying [A.24] to the derivative of [A.26] with respect to z :

$$\left. \frac{\partial \bar{h}_m}{\partial z} \right|_{z=L_n} = (\Psi p)^{\frac{1}{2}} (B_1 \xi_4 - A_1 \xi_3) = 0 \quad \text{A.27}$$

where

$$\xi_3 = \exp(-L_n(\Psi p)^{1/2})$$

$$\xi_4 = \exp(L_n(\Psi p)^{1/2})$$

Solving Eq. [A.27] for A_1 :

$$A_1 = B_1 \frac{\xi_4}{\xi_3} \quad \text{A.28}$$

Applying Eq. [A.28] to Eq. [A.26] yields the particular solution of [A.20] in terms of \bar{h}_m :

$$\bar{h}_m = B_1 \left[\frac{\xi_3}{\xi_4} \exp\left(-z(\Psi p)^{\frac{1}{2}}\right) + \exp\left(z(\Psi p)^{\frac{1}{2}}\right) \right] \quad \text{A.29}$$

Solving Eq. [A.19] for the contribution, \bar{q} :

Apply the derivative of Eq. [A.29] with respect to z to Eq. [A.19]:

$$\begin{aligned} \bar{q}_{tl} = \bar{q}_{fu} = \bar{q}_{fl} = \frac{-K'}{T} (\Psi p)^{1/2} B_1 \left[\frac{\xi_3}{\xi_4} \exp\left(-z(\Psi p)^{\frac{1}{2}}\right) \right. \\ \left. + \exp\left(z(\Psi p)^{\frac{1}{2}}\right) \right] \end{aligned} \quad \text{A.30}$$

Remove the B_1 term from [A.30] by multiplying by $\frac{\bar{h}}{Eq.[A.29]}$:

$$\bar{q}_{tl} = \bar{q}_{fu} = \bar{q}_{fl} = \frac{-K'}{T} \bar{h} (\Psi p)^{1/2} \frac{\xi_3 - \xi_4}{\xi_3 + \xi_4} \quad \text{A.31}$$

Solve Eq. [A.18] for \bar{q}_{tu} :

The general solution of [A.25] is:

$$\bar{h}_m = A_2 \exp\left(-z(\Psi p)^{\frac{1}{2}}\right) + B_2 \exp\left(z(\Psi p)^{\frac{1}{2}}\right) \quad \text{A.32}$$

where A_2 and B_2 are constants.

To obtain the particular solution of \bar{h}_m , determine the value of the constants A_2 and B_2 .

Apply Eq. A.23 to Eq. A.32

$$\begin{aligned} & \lambda_2 \left[B_2 \exp\left(L_w(\Psi p)^{\frac{1}{2}}\right) - A_2 \xi_1 \right] \\ & = -\lambda_1 \left[B_2 \exp\left(L_w(\Psi p)^{\frac{1}{2}}\right) + A_2 \xi_1 \right] \end{aligned} \quad \text{A.33}$$

where

$$\begin{aligned} \lambda_1 &= \frac{\alpha_1 S_y p}{p + \alpha_1} \\ \lambda_2 &= K'(\Psi p)^{\frac{1}{2}} \\ \xi_1 &= \exp\left(-L_w(\Psi p)^{\frac{1}{2}}\right) \end{aligned}$$

Isolating A_2 by rearranging Eq. A.33 gives:

$$A_2 = B_2 \frac{\xi_2}{\xi_1} \quad \text{A.34}$$

where

$$\xi_2 = \frac{\lambda_1 + \lambda_2}{\lambda_1 - \lambda_2} \exp\left(L_w(\Psi p)^{\frac{1}{2}}\right)$$

Substitute Eq. A.34 into Eq. A.32:

$$\bar{h}_m = B_2 \left[\frac{\xi_2}{\xi_1} \exp\left(-z(\Psi p)^{\frac{1}{2}}\right) + \exp\left(z(\Psi p)^{\frac{1}{2}}\right) \right] \quad \text{A.35}$$

Solve Eq. A.18 for \bar{q}_{tu}

First, apply the derivative of Eq. A.35 with respect to z to Eq. A.18 to give:

$$\bar{q}_{tu} = \frac{-K'}{T} B_2 (\Psi p)^{\frac{1}{2}} \left(\frac{\xi_1 + \xi_2}{\xi_1 - \xi_2} \right) \quad \text{A.36}$$

The B_2 term is eliminated by multiplying Eq. A.36 by $\frac{\bar{h}}{Eq.A.35}$ to yield:

$$\bar{q}_{tu} = \frac{-K'}{T} \bar{h} (\Psi p)^{\frac{1}{2}} \left(\frac{\xi_1 + \xi_2}{\xi_1 - \xi_2} \right) \quad \text{A.37}$$

Substituting Eq. A.31 and Eq. A.37 into Eq. A.16 provides an expression for \bar{q}_t :

$$\bar{q}_t = \frac{-K'}{T} \bar{h} (\Psi p)^{\frac{1}{2}} \left[\left(\frac{\xi_3 - \xi_4}{\xi_3 + \xi_4} \right) + \left(\frac{\xi_1 + \xi_2}{\xi_1 - \xi_2} \right) \right] \quad \text{A.38}$$

where

$$\xi_3 = \exp\left(-L_n(\Psi p)^{\frac{1}{2}}\right)$$

$$\xi_4 = \exp\left(L_n(\Psi p)^{\frac{1}{2}}\right)$$

Solve for \bar{q}_f by applying Eq. A.31 to Eq. A.17:

$$\bar{q}_f = -2 \frac{K'}{T} \bar{h} (\Psi p)^{\frac{1}{2}} \left(\frac{\xi_3 - \xi_4}{\xi_3 + \xi_4} \right) \quad \text{A.39}$$

Solve for \bar{q} by applying Eq. A.38 and Eq. A.39 to Eq. A.15

$$\bar{q} = \frac{-K'}{T} \bar{h} (\Psi p)^{\frac{1}{2}} \left[(2n_f - 1) \left(\frac{\xi_3 - \xi_4}{\xi_3 + \xi_4} \right) + \left(\frac{\xi_1 + \xi_2}{\xi_1 - \xi_2} \right) \right] \quad \text{A.40}$$

Substituting Eq. A.40 into Eq. A.14:

$$\begin{aligned} \frac{\partial^2 \bar{h}}{\partial r^2} + \frac{1}{r} \frac{\partial \bar{h}}{\partial r} = \bar{h} \left[\frac{S}{T} p \right. \\ \left. + \frac{K'}{T} (\Psi p)^{\frac{1}{2}} \left[(2n_f - 1) \left(\frac{\xi_3 - \xi_4}{\xi_3 + \xi_4} \right) + \left(\frac{\xi_1 + \xi_2}{\xi_1 - \xi_2} \right) \right] \right] \end{aligned} \quad \text{A.41}$$

The general solution to Eq. A.41 is

$$\bar{h} = C_1 K_0 \left(\Phi^{\frac{1}{2}} r \right) + D_1 I_0 \left(\Phi^{\frac{1}{2}} r \right) \quad \text{A.42}$$

where C_1 and D_1 are constants, K_0 and I_0 are modified Bessel functions and

$$\Phi = \frac{Sp}{T} + \frac{K'}{T} (\Psi p)^{\frac{1}{2}} \left[(2n_f - 1) \left(\frac{\xi_3 - \xi_4}{\xi_3 + \xi_4} \right) + \left(\frac{\xi_1 + \xi_2}{\xi_1 - \xi_2} \right) \right] \quad \text{A.43}$$

Applying the condition of Eq. A.22 to Eq. A.42 produces the following particular solution:

$$\bar{h} = C_1 K_0 \left(\Phi^{\frac{1}{2}} r \right) \quad \text{A.44}$$

To account for the effects of wellbore storage in source and observation wells, an approximate solution method is used (Figure 1). This method was first developed by Tongpenyai and

Raghaven (1981) and has since been successfully employed for both pumping and pulse interference test solutions. The solution is found by superposing the response in the formation to the point P due to the effect of wellbore storage in each well (Novakowski, 1989).

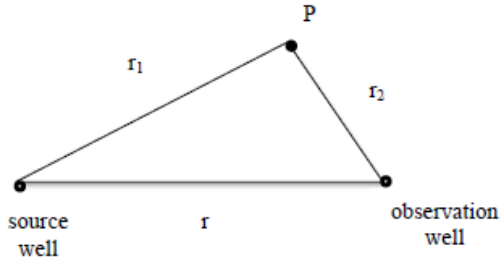


Figure A. 1 The relationship between a source well, observation well, and observation point P used in the approximate solution method.

The inner boundary condition for the source well is:

$$2\pi r_w T \left. \frac{\partial h}{\partial r_1} \right|_{r_1=r_w} = \pi r_s^2 \frac{\partial h_s}{\partial t} - Q \quad \text{A.45}$$

where h_s is the head in the source well, r_s is the radius of the source well casing and r_1 is the radial distance from the source well to the point P. Similarly the inner boundary condition for the observation well is given by:

$$2\pi r_w T \left. \frac{\partial h}{\partial r_2} \right|_{r_2=r_w} = \pi r_{ob}^2 \frac{\partial h_{ob}}{\partial t} \quad \text{A.46}$$

where h_{ob} is the hydraulic head in the observation well, r_{ob} is the radius of the observation well casing and r_2 is the radial distance between the observation well and the point P.

Continuity between the source well and the formation is given by:

$$h_s(t) = h(r_w, t) \quad \text{A.47}$$

and similarly between the observation well and the formation:

$$h_{ob}(t) = h(r_w, t) \quad \text{A.48}$$

The initial conditions in the source and observation wells are as follows:

$$h_{ob}(0) = 0 \quad \text{A.49}$$

$$h_s(0) = 0 \quad \text{A.50}$$

Apply the Laplace transform to Eq.'s A.45 to A.48:

$$\mathcal{L}[A. 45]: 2\pi r_w T \left. \frac{\partial \bar{h}}{\partial r_1} \right|_{r_1=r_w} = \pi r_s^2 \bar{h}_s p - \frac{Q}{p} \quad \text{A.51}$$

$$\mathcal{L}[A. 46]: 2\pi r_w T \left. \frac{\partial \bar{h}}{\partial r_2} \right|_{r_2=r_w} = \pi r_{ob}^2 \bar{h}_{ob} p \quad \text{A.52}$$

$$\mathcal{L}[A. 47]: \bar{h}_s(p) = \bar{h}(r_w, p) \quad \text{A.53}$$

$$\mathcal{L}[A. 48]: \bar{h}_{ob}(p) = \bar{h}(r_w, p) \quad \text{A.54}$$

Applying the superposition principal:

$$h = h_1 + h_2 \quad \text{A.55}$$

Apply the particular solution from Eq. A.44 along r_1 and r_2 to give:

$$\bar{h}_1 = C_1 K_0(\Phi^{\frac{1}{2}} r_1) \quad \text{A.56}$$

$$\bar{h}_2 = C_2 K_0(\Phi^{\frac{1}{2}} r_2) \quad \text{A.57}$$

Apply Eq. A.56 and Eq. A.57 to Eq. A.55 to give:

$$\bar{h} = C_1 K_0(\Phi^{\frac{1}{2}} r_1) + C_2 K_0(\Phi^{\frac{1}{2}} r_2) \quad \text{A.58}$$

Substitute the derivative of Eq. A.56 into Eq. A.51:

$$\bar{h}_s = \frac{Q}{p} - \frac{C_1 \lambda \Phi^{\frac{1}{2}} K_1(\Phi^{\frac{1}{2}} r_w)}{C_s p} \quad \text{A.59}$$

where

$$C_s = \pi r_s^2$$

$$\lambda_w = 2\pi r_w T$$

Substitute the derivative of Eq. A.57 into Eq. A.52:

$$\bar{h}_{ob} = \frac{-C_2 \lambda \Phi^{\frac{1}{2}} K_1(\Phi^{\frac{1}{2}} r_w)}{C_{ob} p} \quad \text{A.60}$$

where

$$C_{ob} = \pi r_{ob}^2$$

Apply Eq. A.53 to Eq. A.58:

Substitute Eq. A.58 and A.59 into A.53:

$$C_2 K_0 \left(\Phi^{\frac{1}{2}} r \right) + C_1 \xi_6 = \frac{Q}{p} \quad \text{A.61}$$

where

$$\xi_6 = \frac{C_s p K_0 \left(r_w \phi^{\frac{1}{2}} \right) + \lambda_w \phi^{\frac{1}{2}} K_1 \left(r_w \phi^{\frac{1}{2}} \right)}{C_s p} \quad \text{A.62}$$

Substitute Eq. A.58 and Eq. A.60 into Eq. A.54:

$$C_1 K_0 \left(\Phi^{\frac{1}{2}} r \right) + C_2 \xi_5 = 0 \quad \text{A.63}$$

where

$$\xi_5 = \frac{C_{ob} p K_0 \left(r_w \phi^{\frac{1}{2}} \right) + \lambda_w \phi^{\frac{1}{2}} K_1 \left(r_w \phi^{\frac{1}{2}} \right)}{C_{ob} p} \quad \text{A.64}$$

use Cramer's rule to solve for the unknowns C_1 and C_2 :

$$C_1 = \frac{\det \begin{vmatrix} \frac{h_o}{p} & K_0 K_0 \left(\Phi^{\frac{1}{2}} r \right) \\ 0 & \xi_5 \end{vmatrix}}{\det \begin{vmatrix} \xi_6 & K_0 \left(\Phi^{\frac{1}{2}} r \right) \\ K_0 \left(\Phi^{\frac{1}{2}} r \right) & \xi_5 \end{vmatrix}}$$

then

$$C_1 = -\frac{Q\xi_5}{p\gamma_3} \quad \text{A.65}$$

where

$$\gamma_3 = \left(K_0 \left(\Phi^{\frac{1}{2}} r \right) \right)^2 - \xi_5 \xi_6 \quad \text{A.66}$$

$$C_2 = -\frac{QK_0 \left(\Phi^{\frac{1}{2}} r \right)}{p\gamma_3} \quad \text{A.67}$$

The solution in Laplace space for the hydraulic head in the source well is obtained by substitution of Eq. A.65 into Eq. A.59 and taking the integral with respect to p:

$$\bar{h}_s = \int_0^p \left(\frac{Q}{p} - \frac{\lambda_w \Phi^{\frac{1}{2}} Q \xi_5 K_1 \left(\Phi^{\frac{1}{2}} r_w \right)}{C_s p^2 \gamma_3} \right) dp \quad \text{A.68}$$

and then

$$\bar{h}_s = \frac{1}{p} \left(\frac{Q}{p} - \frac{\lambda_w \Phi^{\frac{1}{2}} Q \xi_5 K_1 \left(\Phi^{\frac{1}{2}} r_w \right)}{C_s p^2 \gamma_3} \right) \quad \text{A.69}$$

The solution in Laplace space for the hydraulic head in the observation well is obtained by substitution of Eq. A.67 into Eq. A.60 and taking the integral with respect to p:

$$\bar{h}_{ob} = \int_0^p \left(\frac{-Q\lambda\phi^{1/2}K_1(r_w(\phi^{1/2}))K_0(r(\phi^{1/2}))}{p^2\gamma_3C_{ob}} \right) dp \quad \text{A.70}$$

and then

$$\bar{h}_{ob} = \frac{-Q\lambda\phi^{1/2}K_1(r_w(\phi^{1/2}))K_0(r(\phi^{1/2}))}{p^3\gamma_3C_{ob}} \quad \text{A.71}$$

The Laplace space solution for hydraulic head in the horizontal fracture domain is given by applying Eq. A.65 and Eq. A.67 to Eq. A.58:

$$\bar{h} = \frac{QK_0(r(\phi^{1/2}))K_0(r_2(\phi^{1/2})) - Q\xi_5K_0(r_1(\phi^{1/2}))}{p\gamma_3} \quad \text{A.72}$$

Appendix B

Pumping test solution observation well Fortran code

```

PROGRAM ow_pump
!*****
!***** THIS PROGRAM NUMERICALLY INVERTS A SOLUTION FOR A *****
!***** PUMPING TEST INCLUDING STORAGE IN BOTH SOURCE *****
!***** AND OBSERVATION WELLS *****
!***** *****
!***** THIS PROGRAM USES DIMENSIONED GROUPINGS *****
*****
!*****
IMPLICIT REAL*8 (A-H,O-Z)
REAL*8 K1,PI,NUMOBS,LN,LW,NF,NFMULT,QQ
INTEGER N
DOUBLE COMPLEX FS
DIMENSION TIM(6000)

! IDENTIFY INPUT AND OUTPUT FILES
!-----
OPEN(11,FILE='ow_pump.in',STATUS='UNKNOWN')
OPEN(22,FILE='ow_pump.out',STATUS='UNKNOWN')

! READ IN PARAMETER VALUES FROM MULTCH.IN FILE
!-----
READ(11,*) K1
READ(11,*) TR
READ(11,*) SS1
READ(11,*) ST
READ(11,*) SY
READ(11,*) H0
READ(11,*) R
READ(11,*) RW
READ(11,*) RSW
READ(11,*) ROB
READ(11,*) LN
READ(11,*) LW
READ(11,*) ALPHA1
READ(11,*) NF

! READ IN OBSERVATION TIMES
!-----
READ(11,300) NUMOBS
DO 1 I=1,NUMOBS
    READ(11,*) TIM(I)
CONTINUE

! DEFINE CONSTANTS AND PLACE-HOLDER PARAMETERS
!-----

```

1

```

      PI=4.0D+00*DATAN(1.0D+00)
      O=(K1/TR)
      F=(SS1/K1)
      CS=PI*(RSW**2)
      CR=PI*(ROB**2)
      Q=2*(PI)*RW*TR
      QQ=(PI)*RSW*RSW*H0
      NFMULT=2*Nf-1.0

! CALCULATE DIMENSIONLESS HEAD AT EACH OBSERVATION TIME
!-----
      DO 2 I=1,NUMOBS
          TIME=TIM(I)

          !      ASSIGN VALUES TO TALBOT ALGORITHM PARAMETERS
          ALAMDA=6/TIME
          SIGMA=0.0
          ANU=1.0
          N=32

          ! CALCULATE HEAD IN SLUG-TESTED WELL (INVERT FROM LAPLACE
SPACE)
          ! PLEASE NOTE: CODE OUTPUTS DIMENSIONLESS HEAD H/H0 AND
TIME

          CALL
TALBOT(HR, TIME, ALAMDA, SIGMA, ANU, N, R, CR, CS, RW, Q, QQ, H0, ST, TR, O, F, ALPHA1, L
N, LW, NFMULT, SY)

          WRITE(22,*) HR
2          CONTINUE

          ! FORMAT STATEMENTS
          !-----
300          FORMAT(f5.3,/)

          STOP
          END PROGRAM

!*****
!***** FUNCTION FS *****
!***** *****
!***** THIS FUNCTION CALCULATES HEAD IN AN OBSERVATION WELL *****
!***** THAT IS INTERSECTED BY ONE OR MORE HORIZONTAL FRACTURE *****
!***** FEATURES OF WHICH THE UPPERMOST FRACTURE IS CONNECTED *****
!***** TO THE WATER TABLE. A CONSTANT HEAD BOUNDARY CONDITION *****
!***** HAS BEEN APPLIED TO THE WATER TABLE. *****
!***** *****
!***** FUNCTION FS IS THE SOLUTION IN LAPLACE SPACE *****
!***** LAURA M. ELMHIRST, JUNE 2010 *****
!***** MODIFIED BY JESSICA M. WORLEY DECEMBER 2011 *****
!***** QUEEN'S UNIVERSITY, KINGSTON *****
!*****

```

DOUBLE COMPLEX FUNCTION

FS (P, R, CR, CS, RW, Q, QQ, H0, ST, TR, O, F, ALPHA1, LN, LW, NFMULT, SY)

REAL*8 R, O, CR, F, CS, RW, H0, Q, QQ, ST, TR, ALPHA1, LN, LW, NFMULT

REAL*8 EXPMAX, DR, DI, SY

DOUBLE COMPLEX CPI, COMPR, COMEGA, CCR, CFORK, CCS, CBK0, CBK1, P, B22

DOUBLE COMPLEX PHI, ZETA1, ZETA2, DET, Y, CST, CTR, CH0, CRW, CLAM, TDET

DOUBLE COMPLEX CALPHA1, CQLN, CQLW, ONE, CNFMULT, ARGLN, ARGLW, Y1, Y2

DOUBLE COMPLEX LFAC, CQ

! DEFINE CONSTANTS

!-----

EXPMAX=708.

PI=4.0D+00*DATAN(1.0D+00)

! CONVERT PARAMETER TYPES TO DOUBLE COMPLEX

CCR=DCMPLX(CR)

CCS=DCMPLX(CS)

CPI=DCMPLX(PI)

COMPR=DCMPLX(R)

CLAM=DCMPLX(Q)

CH0=DCMPLX(H0)

CQ=DCMPLX(QQ)

CRW=DCMPLX(RW)

CST=DCMPLX(ST)

CSY=DCMPLX(SY)

CTR=DCMPLX(TR)

COMEGA=DCMPLX(O)

CFORK=CDSQRT(DCMPLX(F)*P)

CALPHA1=DCMPLX(ALPHA1)

CNFMULT=DCMPLX(NFMULT)

ONE=DCMPLX(1.0)

! CALCULATE PHI FOR MULTIPLE FRACTURES, THE UPPERMOST FRACTURE
BEING

! CONNECTED TO CONSTANT HEAD BOUNDARY CONDITION AT THE WATER
TABLE

!-----

CQLN=DCMPLX(2.0*LN)*CFORK

CQLW=DCMPLX(2.0*LW)*CFORK

IF(REAL(CQLN).GT.EXPMAX) CQLN=DCMPLX(EXPMAX)

IF(REAL(CQLW).GT.EXPMAX) CQLW=DCMPLX(EXPMAX)

Y1=CFORK*(COMEGA*CTR)

Y2=CALPHA1*CSY*P/(P+CALPHA1)

LFAC=(Y1+Y2)/(Y2-Y1)

ARGLN=(ONE-CDEXP(CQLN))/(ONE+CDEXP(CQLN))

ARGLW=(ONE+LFAC*CDEXP(CQLW))/(ONE-LFAC*CDEXP(CQLW))

```

        PHI=CDSQRT ((CST*P/CTR)-COMEGA*CFORK*(CNFMULT*ARGLN+ARGLW))
! CALCULATE HEAD AT SOURCE WELL IN LAPLACE SPACE
!-----
-----
ZETA1=(CCR*P*CBK0((PHI)*CRW)+CLAM*PHI*CBK1((PHI)*CRW))/(CCR*P)

ZETA2=(CCS*P*CBK0((PHI)*CRW)+CLAM*PHI*CBK1((PHI)*CRW))/(CCS*P)

DET=(CBK0((PHI)*COMPR))*CBK0((PHI)*COMPR)-(ZETA1*ZETA2)

B22=(CBK0(COMPR*(PHI))*CQ)/(DET*P)

! CHECK FOR NON-ZERO ARGUEMENT
DR=REAL(ZETA1)+REAL(ZETA2)
DI=AIMAG(ZETA1)+AIMAG(ZETA2)
DADD=DR+DI

! IF ZERO ARGUMENT FS=0 OTHERWISE, CALCULATE SOURCE WELL
HEAD IN LAPLACE SPACE
IF(DADD.EQ.0.0) THEN
        FS=0.0
ELSE
        FS=(1/P)*(-1*CLAM*B22*(PHI)*CBK1((PHI)*CRW))/(CCR*P)
! OBS WELL

END IF
RETURN
END FUNCTION FS

SUBROUTINE
TALBOT(FT,T,ALAMDA,SIGMA,ANU,N,R,CR,CS,RW,Q,QQ,H0,ST,TR,O,F,ALPHA1,LN,L
W,NFMULT,SY)

! THIS ROUTINE INVERTS THE LAPLACE TRANSFORM FS(S) NUMERICALLY
! TO GIVE FT(T).
! FS(S) IS A COMPLEX*8 FUNCTION OF ITS COMPLEX*8 ARGUEMENT S.
! FOR MOST APPLICATIONS IT IS RECOMENDED THAT:
! SIGMA=0.0, ANU=1.0, ALAMDA=6.0/T, N32
!*****
IMPLICIT REAL*8(A-H,O-Z)
REAL*8 NFMULT,BC,LN,LW
DOUBLE COMPLEX S(1024),DS(1024),ZZ,FS,SUM,B,B1,B2,V2,ARG1
DOUBLE COMPLEX ARG2,CON1,CON2,CLAMDA,CNU,CSIGMA
DOUBLE PRECISION PIBYN,ALPHA,THETA,TAU,PSI,CP,SP,RS
DOUBLE PRECISION RSMAX,RSMEXP
DATA Z/0.0/
PI=3.141592653589732384626433827950D+00
CON1=DCMPLX(0.5,0.0)

```

```

CON2=DCMPLX(2.0,0.0)
CLAMDA=DCMPLX(ALAMDA,Z)
CNU=DCMPLX(ANU,Z)
CSIGMA=DCMPLX(SIGMA,Z)

PIBYN=PI/FLOAT(N)
TAU=DBLE(ALAMDA*T)
ZZ=DCMPLX(Z,Z)
NM1=N-1

DO 10 K=1,NM1
    THETA=FLOAT(K)*PIBYN
    ALPHA=THETA/DTAN(THETA)
    S(K)=DCMPLX(ALPHA,ANU*THETA)
    DS(K)=DCMPLX(ANU,THETA+ALPHA*(ALPHA-1)/THETA)*CON1
10 CONTINUE

PSI=TAU*ANU*PIBYN
CP=2.0*DCOS(PSI)
SP=DSIN(PSI)
B=ZZ
B1=B

DO 20 KA=1,NM1
    K=N-KA
    RS=TAU*DBLE(S(K))
    RSMAX=DMAX1(RS,-50.0)
    RSMEXP=DEXP(RSMAX)
    V2=DCMPLX(RSMEXP,Z)
    B2=B1
    B1=B
    ARG1=CLAMDA*S(K)+CSIGMA

    !RECHEK NEXT LIEN!
    B=DCMPLX(CP,Z)*B1-
B2+V2*DS(K)*FS(ARG1,R,CR,CS,RW,Q,QQ,H0,ST,TR,O,F,ALPHA1,LN,LW,NFMULT,SY)
20 CONTINUE

ARG2=CLAMDA+CSIGMA+ZZ

SUM=DCMPLX(DEXP(TAU),Z)*CNU*FS(ARG2,R,CR,CS,RW,Q,QQ,H0,ST,TR,O,F,
ALPHA1,LN,LW,NFMULT,SY)*CON1+DCMPLX(CP,Z)*B-CON2*(B1-B*DCMPLX(Z,SP))
FT=ALAMDA*EXP(SIGMA*T)*DBLE(SUM)/FLOAT(N)

RETURN
END

! MODIFIED BESSEL FUNCTION K0(X) FOR COMPLEX X
!
```

```

! SEE ABOMOWITZ & STEGUN, HANDBOOK OF METHEMATICAL FUNCTIONS
! PAGE 375 FOR SERIES EXPANSION.
! PROGRAMMED BY: E.A. SUDICKY,
!
!           INSTITUTE FOR GROUNDWATER RESEARCH,
!           UNIVERSITY OF WATERLOO,
!           WATERLOO, ONTARIO N2L 3G1
!           MARCH, 1987.
!
DOUBLE COMPLEX FUNCTION CBK0(X)
IMPLICIT DOUBLE COMPLEX(A-H,O-Z)
DOUBLE PRECISION PI,E,FACT1,Z1
CBK0=(0.0,0.0)
E=0.577215664901533
PI=3.14159265
IF(CDABS(X).LE.1.0E-03) GOTO 200
IF(CDABS(X).GT.50.0) GOTO 99
IF(CDABS(X).GT.5.0) GOTO 100
X2=X/2.0
X3=X*X/4.0
XX=X3
!
!           SUM1 ADDS TO I0(X)
!
SUM1=DCMPLX(1.0,0.0)
SUM2=DCMPLX(0.0,0.0)
SUM3=DCMPLX(0.0,0.0)
FACT1=1.0
N=0
10 N=N+1
Z1=FLOAT(N)
FACT1=FACT1*Z1
TERM1=XX/(FACT1*FACT1)
SUM3=SUM3+1.0/Z1
SUM1=SUM1+TERM1
RUNTRM=TERM1*SUM3
SUM2=SUM2+RUNTRM
XX=XX*X3
IF(CDABS(RUNTRM/SUM2).LT.1.0E-06) GOTO 20
GOTO 10
20 CBI0=SUM1
CBK0=-(CDLOG(X2)+E)*CBI0+SUM2
GOTO 99
!
!           LARGE X
!
100 Z=CDSQRT(X)
CBK0=CDEXP(-X)/Z*DSQRT(PI/2.0)
GOTO 99
!
!           SMALL X
!

```

```

200      U=X/2.0
          CBI0=1.00+U*U
          CBK0=-CDLOG(U)*CBI0-E
99      CONTINUE
          RETURN
END

!      MODIFIED BESSEL FUNCTION K1(X)
!
!      SEE CARSLAW & JAEGER, PG. 489, EQUATION (10) FOR K1 SERIES.
!      SEE GRADSHTEYN & RYZHIK, PG. 961, EQUATION 8.477.2 FOR I1.
!
!      PROGRAMMED BY: E.A. SUDICKY,
!                      INSTITUTE FOR GROUNDWATER RESEARCH,
!                      UNIVERSITY OF WATERLOO,
!                      WATERLOO, ONTARIO, N2L SG1
!                      JANUARY, 1987.
!
!      UPDATE FOR COMPLEX: F.W.LETNIOWSKI
!                      MAY, 1987.
!
DOUBLE COMPLEX FUNCTION CBK1(X)
!
      IMPLICIT DOUBLE COMPLEX(A-H,O-Z)
      DOUBLE PRECISION PI,E,FACT,Z1,Z2
!
      CBK1=DCMPLX(0.0,0.0)
      E=0.577215665
      PI=3.14159265
      IF(CDABS(X).LE.1.0E-03) GOTO 200
      IF(CDABS(X).GT.50.0) GOTO 99
      IF(CDABS(X).GT.5.0) GOTO 100

      X2=X/2.0
      X3=X*X/4.0
      XX=X2*X3

!      SUM1 ADDS TO I1(X)

      SUM1=X2
      SUM2=SUM1
      SUM3=DCMPLX(0.0,0.0)
      FACT=1.0
      N=0
10     N=N+1
          Z1=FLOAT(N)
          Z2=FLOAT(N+1)
          FACT=FACT*Z1*Z2
          TERM1=XX/FACT
          SUM3=SUM3+1.0/Z1
          SUMI=2.0*SUM3+1.0/Z2

```

```

SUM1=SUM1+TERM1
SUM2=SUM2+TERM1*SUMI
XX=XX*X3
IF (CDABS (TERM1*SUM1/SUM2) .LT.1.0E-06) GOTO 20
GOTO 10
20 CBI1=SUM1
CBK1=(CDLOG (X2)+E)*CBI1-0.5*SUM2+1.0/X
GOTO 99

! LARGE X

100 Z=CDSQRT (X)
CBK1=CDEXP (-X)/Z*DSQRT (PI/2.0)*(1.0+3.0/(8.0*X))
GOTO 99

! SMALL X

200 U=X/2.0
CBK1=1.0/X+U*(CDLOG (U)+E)-X/4.0
99 CONTINUE

RETURN
END

! MODIFIED BESSEL FUNCITON I1(X)

! SEE CARSLAW & JAEGER, PG. 489, EQUATION (10) FOR K1 SERIES.
! SEE GRADSHTEYN & RYZHIK, RG. 961, EQUATION 8.447.2 FOR I1.

! PROGRAMMED BY: E.A. SUDICKY,
! INSTITUTE FOR GROUNDWATER RESEARCH,
! UNIVERSITY OF WATERLOO,
! WATERLOO, ONTARIO, N2L 3G1
! JANUARY, 1987.

! UPDATE FOR COMPLEX: F.W. LETNIEWSKI
! MAY, 1987

DOUBLE COMPLEX FUNCTION CBI1 (X)

IMPLICIT DOUBLE COMPLEX (A-H,O-Z)
DOUBLE PRECISION PI,E,FACT,Z1,Z2

CBI1=DCMPLX(0.0,0.0)
E=0.577215665
PI=3.14159265
IF(CDABS (X) .LE.1.0E-03) GOTO 200
IF(CDABS (X) .GT.50.0) GOTO 99
IF(CDABS (X) .GT.5.0) GOTO 100

X2=X/2.0
X3=X*X/4.0

```

```

                XX=X2*X3

!      SUM1 ADDS TO I1(X)
!      SERIES EXPANSION

                SUM1=X2
                SUM2=SUM1
                SUM3=DCMPLX(0.0,0.0)
                FACT=1.0
                N=0
10          N=N+1
                Z1=FLOAT(N)
                Z2=FLOAT(N+1)
                FACT=FACT*Z1*Z2
                TERM1=XX/FACT
                SUM3=SUM3+1.0/Z1
                SUMI=2.0*SUM3+1.0/Z2
                SUM1=SUM1+TERM1
                SUM2=SUM2+TERM1*SUMI
                XX=XX*X3
                IF(CDABS(TERM1*SUM1/SUM2).LT.1.0E-06) GOTO 20
                GOTO 10
20          CBI1=SUM1
                GOTO 99

!      LARGE X
!      ASYMPTOTIC SERIES EXPANSION

100         Z=CDSQRT(X)
                CBI1=CDEXP(X)/Z*DSQRT(PI*2.0)*(1.0-3.0/(8.0*X))
                GOTO 99

!      SMALL X
!      POLYNOMIAL APPROXIMATION

200         U=X/2.0
                T=X/3.75
                CBI1=U+.87890594*T**2*X+.51498869*T**4*X+.15084934*T**6*X
99          CONTINUE
RETURN
END

!      MODIFIED BESSEL FUNCTION I0(X) FOR COMPLEX X

!      SEE ABOMOWITZ & STEGUN, HANDBOOK OF MATHEMATICAL FUNCTIONS
!      PAGE 375 FOR SERIES EXPANSION.

!      PROGRAMMED BY: E.A. SUDICKY,
!                      INSTITUTE FOR GROUNDWATER RESERACH,
!                      UNIVERSITY OF WATERLOO,
!                      WATERLOO, ONTARIO, N2L 3G1
!                      MARCH, 1987.

```

```

DOUBLE COMPLEX FUNCTION CBI0(X)
IMPLICIT DOUBLE COMPLEX (A-H,O-Z)
DOUBLE PRECISION PI,E,FACT1,Z1
CBI0=(0.0,0.0)
E=0.577215664901533
PI=3.14159265
IF(CDABS(X).LE.1.0E-03) GOTO 200
IF(CDABS(X).GT.50.0) GOTO 99
IF(CDABS(X).GT.5.0) GOTO 100
X2=X/2.0
X3=X*X/4.0
XX=X3

!      SUM1 ADDS TO I0(X)

      SUM1=DCMPLX(1.0,0.0)
      SUM2=DCMPLX(0.0,0.0)
      SUM3=DCMPLX(0.0,0.0)
      FACT1=1.0
      N=0
10     N=N+1
      Z1=FLOAT(N)
      FACT1=FACT1*Z1
      TERM1=XX/(FACT1*FACT1)
      SUM3=SUM3+1.0/Z1
      SUM1=SUM1+TERM1
      RUNTRM=TERM1*SUM3
      SUM2=SUM2+RUNTRM
      XX=XX*X3
      IF(CDABS(RUNTRM/SUM2).LT.1.0E-06) GOTO 20
      GOTO 10
20     CBI0=SUM1
      GOTO 99

!      LARGE X

100     Z=CDSQRT(X)
      CBI0=CDEXP(X)/(Z*DSQRT(PI*2.0))
      GOTO 99

!      SMALL X

200     U=X/2.0
      CBI0=1.00+U*U
99     CONTINUE
      RETURN
END

```

Appendix C

Pumping test solution source well Fortran code

```

PROGRAM SW_PUMP
!*****
!***** THIS PROGRAM NUMERICALLY INVERTS A SOLUTION FOR A *****
!***** PUMPING TEST IN A SOURCE WELL INCLUDING STORAGE IN *****
!***** BOTH SOURCE AND OBSERVATION WELLS *****
!***** *****
!***** THIS PROGRAM USES DIMENSIONED GROUPINGS *****
!*****
      IMPLICIT REAL*8 (A-H,O-Z)
      REAL*8 K1,PI,NUMOBS,LN,LW,NF,NFMULT,QQ
      INTEGER N
      DOUBLE COMPLEX FS
      DIMENSION TIM(6000)

! IDENTIFY INPUT AND OUTPUT FILES
!-----
      OPEN(11,FILE='sw_pump.in',STATUS='UNKNOWN')
      OPEN(22,FILE='sw_pump.out',STATUS='UNKNOWN')

! READ IN PARAMETER VALUES FROM MULTCH.IN FILE
!-----
      READ(11,*) K1
      READ(11,*) TR
      READ(11,*) SS1
      READ(11,*) ST
      READ(11,*) SY
      READ(11,*) H0
      READ(11,*) R
      READ(11,*) RW
      READ(11,*) RSW
      READ(11,*) ROB
      READ(11,*) LN
      READ(11,*) LW
      READ(11,*) ALPHA1
      READ(11,*) NF

! READ IN OBSERVATION TIMES
!-----
      READ(11,300) NUMOBS
      DO 1 I=1,NUMOBS
          READ(11,*) TIM(I)
1      CONTINUE

! DEFINE CONSTANTS AND PLACE-HOLDER PARAMETERS
!-----
      PI=4.0D+00*DATAN(1.0D+00)

```

```

O= (K1/TR)
F= (SS1/K1)
CS=PI* (RSW**2)
CR=PI* (ROB**2)
Q=2* (PI) *RW*TR
QQ= (PI) *RSW*RSW*H0
NFMULT=2*Nf-1.0

! CALCULATE DIMENSIONLESS HEAD AT EACH OBSERVATION TIME
!-----
DO 2 I=1, NUMOBS
    TIME=TIM(I)

    ! ASSIGN VALUES TO TALBOT ALGORITHM PARAMETERS
    ALAMDA=6/TIME
    SIGMA=0.0
    ANU=1.0
    N=32

    ! CALCULATE HEAD IN PUMPED WELL (INVERT FROM LAPLACE SPACE)
    ! PLEASE NOTE: CODE OUTPUTS DIMENSIONLESS HEAD H/H0 AND
TIME
    CALL
TALBOT (HR, TIME, ALAMDA, SIGMA, ANU, N, R, CR, CS, RW, Q, QQ, H0, ST, TR, O, F, ALPHA1, L
N, LW, NFMULT, SY)
    WRITE (22, *) HR/H0
2 CONTINUE

! FORMAT STATEMENTS
!-----
300 FORMAT (f5.3, /)

STOP
END

!*****
!***** FUNCTION FS *****
!***** THIS FUNCTION CALCULATES HEAD IN A SOURCE WELL THAT IS *****
!***** INTERSECTED BY ONE OR MORE HORIZONTAL FRACTURE FEATURES *****
!***** OF WHICH THE UPPERMOST FRACTURE IS CONNECTED TO THE *****
!***** WATER TABLE. A CONSTANT HEAD BOUNDARY CONDITION HAS *****
!***** BEEN APPLIED TO THE WATER TABLE. *****
!***** *****
!***** FUNCTION FS IS THE SOLUTION IN LAPLACE SPACE *****
!***** *****
!***** LAURA M. ELMHIRST, JUNE 2010 *****
!***** MODIFIED BY JESSICA M. WORLEY DECEMBER 2011 *****
!***** QUEEN'S UNIVERSITY, KINGSTON *****
!*****

DOUBLE COMPLEX FUNCTION
FS (P, R, CR, CS, RW, Q, QQ, H0, ST, TR, O, F, ALPHA1, LN, LW, NFMULT, SY)

```

```
REAL*8 R, O, CR, F, CS, RW, H0, Q, QQ, ST, TR, ALPHA1, LN, LW, NFMULT
REAL*8 EXPMAX, DR, DI, SY
```

DOUBLE COMPLEX

```
CPI, COMPR, COMEGA, CCR, CFORK, CCS, CBK0, CBK1, P, B2S
```

DOUBLE COMPLEX

```
PHI, ZETA1, ZETA2, DET, Y, CST, CTR, CH0, CRW, CLAM, TDET
```

DOUBLE COMPLEX

```
CALPHA1, CQLN, CQLW, ONE, CNFMULT, ARGLN, ARGLW, Y1, Y2
```

DOUBLE COMPLEX LFAC, CQ

```
! DEFINE CONSTANTS
```

```
!-----
```

```
EXPMAX=708.
PI=4.0D+00*DATAN(1.0D+00)
```

```
! CONVERT PARAMETER TYPES TO DOUBLE COMPLEX
```

```
CCR=DCMPLX(CR)
CCS=DCMPLX(CS)
CPI=DCMPLX(PI)
COMPR=DCMPLX(R)
CLAM=DCMPLX(Q)
CQ=DCMPLX(QQ)
CH0=DCMPLX(H0)
CRW=DCMPLX(RW)
CST=DCMPLX(ST)
CSY=DCMPLX(SY)
CTR=DCMPLX(TR)
COMEGA=DCMPLX(O)
CFORK=CDSQRT(DCMPLX(F)*P)
CALPHA1=DCMPLX(ALPHA1)
CNFMULT=DCMPLX(NFMULT)
ONE=DCMPLX(1.0)
```

```
! CALCULATE PHI FOR MULTIPLE FRACTURES, THE UPPERMOST FRACTURE
BEING ! CONNECTED TO CONSTANT HEAD BOUNDARY CONDITION AT THE WATER
TABLE !-----
```

```
-----
CQLN=DCMPLX(2.0*LN)*CFORK
CQLW=DCMPLX(2.0*LW)*CFORK
```

```
IF(REAL(CQLN).GT.EXPMAX) CQLN=DCMPLX(EXPMAX)
IF(REAL(CQLW).GT.EXPMAX) CQLW=DCMPLX(EXPMAX)
```

```
Y1= CFORK*(COMEGA/CTR)
Y2=CALPHA1*CSY*P/(P+CALPHA1)
LFAC=(Y1+Y2)/(Y2-Y1)
```

```
ARGLN=(ONE-CDEXP(CQLN))/(ONE+CDEXP(CQLN))
```

```

      ARGWLW= (ONE+LFAC*CDEXP (CQLW) ) / (ONE-LFAC*CDEXP (CQLW) )

      PHI=CDSQRT ( (CST*P/CTR) -COMEGA*CFORK* (CNFMULT*ARGLN+ARGWLW) )
!PHI=CDSQRT (CST*P/CTR) !NOVAKOWSKI 1989

! CALCULATE HEAD AT SOURCE WELL IN LAPLACE SPACE
!-----
-----

ZETA1= (CCR*P*CBK0 ( (PHI) *CRW) +CLAM*PHI*CBK1 ( (PHI) *CRW) ) / (CCR*P)

ZETA2= (CCS*P*CBK0 ( (PHI) *CRW) +CLAM*PHI*CBK1 ( (PHI) *CRW) ) / (CCS*P)

DET= (CBK0 ( (PHI) *COMPR) ) * (CBK0 ( (PHI) *COMPR) ) - (ZETA1*ZETA2)

B2S= (ZETA1*CQ) / (DET*P)

! CHECK FOR NON-ZERO ARGUEMENT
DR=REAL (ZETA1) +REAL (ZETA2)
DI=AIMAG (ZETA1) +AIMAG (ZETA2)
DADD=DR+DI

! IF ZERO ARGUMENT FS=0 OTHERWISE, CALCULATE SOURCE WELL
HEAD IN LAPLACE SPACE
  IF (DADD.EQ.0.0) THEN
    FS=0.0
  ELSE

FS= (1/P) * ( (CLAM*B2S* (PHI) *CBK1 ( (PHI) *CRW) ) / (CCS*P) + (CQ/P) )
  END IF
  RETURN
END

!*****

SUBROUTINE
TALBOT (FT, T, ALAMDA, SIGMA, ANU, N, R, CR, CS, RW, Q, QQ, H0, ST, TR, O, F, ALPHA1, LN, L
W, NFMULT, SY)

! THIS ROUTINE INVERTS THE LAPLACE TRANSFORM FS(S) NUMERICALLY
! TO GIVE FT(T) .
! FS(S) IS A COMPLEX*8 FUNCTION OF ITS COMPLEX*8 ARGUEMENT S.
! FOR MOST APPLICATIONS IT IS RECOMENDED THAT:
! SIGMA=0.0, ANU=1.0, ALAMDA=6.0/T, N32
!*****
  IMPLICIT REAL*8 (A-H, O-Z)
  REAL*8 NFMULT, BC, LN, LW, QQ
  DOUBLE COMPLEX S (1024), DS (1024), ZZ, FS, SUM, B, B1, B2, V2, ARG1
  DOUBLE COMPLEX ARG2, CON1, CON2, CLAMDA, CNU, CSIGMA
  DOUBLE PRECISION PIBYN, ALPHA, THETA, TAU, PSI, CP, SP, RS
  DOUBLE PRECISION RSMAX, RSMEXP

```

```

DATA Z/0.0/
PI=3.141592653589732384626433827950D+00
CON1=DCMPLX (0.5,0.0)
CON2=DCMPLX (2.0,0.0)
CLAMDA=DCMPLX (ALAMDA,Z)
CNU=DCMPLX (ANU,Z)
CSIGMA=DCMPLX (SIGMA,Z)

PIBYN=PI/FLOAT (N)
TAU=DBLE (ALAMDA*T)
ZZ=DCMPLX (Z,Z)
NM1=N-1

DO 10 K=1,NM1
    THETA=FLOAT (K) *PIBYN
    ALPHA=THETA/DTAN (THETA)
    S (K) =DCMPLX (ALPHA,ANU*THETA)
    DS (K) =DCMPLX (ANU,THETA+ALPHA* (ALPHA-1) /THETA) *CON1
10 CONTINUE

PSI=TAU*ANU*PIBYN
CP=2.0*DCOS (PSI)
SP=DSIN (PSI)
B=ZZ
B1=B

DO 20 KA=1,NM1
    K=N-KA
    RS=TAU*DBLE (S (K) )
    RSMAX=DMAX1 (RS,-50.0)
    RSMEXP=DEXP (RSMAX)
    V2=DCMPLX (RSMEXP,Z)
    B2=B1
    B1=B
    ARG1=CLAMDA*S (K) +CSIGMA

    B=DCMPLX (CP,Z) *B1-
B2+V2*DS (K) *FS (ARG1,R,CR,CS,RW,Q,QQ,H0,ST,TR,O,F,ALPHA1,LN,LW,NFMULT,SY
)
20 CONTINUE

ARG2=CLAMDA+CSIGMA+ZZ

SUM=DCMPLX (DEXP (TAU) ,Z) *CNU*FS (ARG2,R,CR,CS,RW,Q,QQ,H0,ST,TR,O,F,
ALPHA1,LN,LW,NFMULT,SY) *CON1+DCMPLX (CP,Z) *B-CON2* (B1-B*DCMPLX (Z,SP) )
    FT=ALAMDA*EXP (SIGMA*T) *DBLE (SUM) /FLOAT (N)

RETURN
END

! MODIFIED BESSEL FUNCTION K0 (X) FOR COMPLEX X

```

```
! SEE ABOMOWITZ & STEGUN, HANDBOOK OF METHEMATICAL FUNCTIONS
! PAGE 375 FOR SERIES EXPANSION.
! PROGRAMMED BY: E.A. SUDICKY,
```

```
! INSTITUTE FOR GROUNDWATER RESEARCH,
! UNIVERSITY OF WATERLOO,
! WATERLOO, ONTARIO N2L 3G1
! MARCH, 1987.
```

```
DOUBLE COMPLEX FUNCTION CBK0 (X)
IMPLICIT DOUBLE COMPLEX (A-H,O-Z)
DOUBLE PRECISION PI,E,FACT1,Z1
CBK0=(0.0,0.0)
E=0.577215664901533
PI=3.14159265
IF(CDABS(X).LE.1.0E-03) GOTO 200
IF(CDABS(X).GT.50.0) GOTO 99
IF(CDABS(X).GT.5.0) GOTO 100
X2=X/2.0
X3=X*X/4.0
XX=X3
```

```
! SUM1 ADDS TO I0(X)
```

```
SUM1=DCMPLX(1.0,0.0)
SUM2=DCMPLX(0.0,0.0)
SUM3=DCMPLX(0.0,0.0)
FACT1=1.0
N=0
10 N=N+1
Z1=FLOAT(N)
FACT1=FACT1*Z1
TERM1=XX/(FACT1*FACT1)
SUM3=SUM3+1.0/Z1
SUM1=SUM1+TERM1
RUNTRM=TERM1*SUM3
SUM2=SUM2+RUNTRM
XX=XX*X3
IF(CDABS(RUNTRM/SUM2).LT.1.0E-06) GOTO 20
GOTO 10
20 CBI0=SUM1
CBK0=-(CDLOG(X2)+E)*CBI0+SUM2
GOTO 99
```

```
! LARGE X
```

```
100 Z=CDSQRT(X)
CBK0=CDEXP(-X)/Z*DSQRT(PI/2.0)
GOTO 99
```

```
! SMALL X
```

```

200      U=X/2.0
          CBI0=1.00+U*U
          CBK0=-CDLOG(U)*CBI0-E
99      CONTINUE
          RETURN
END

!      MODIFIED BESSEL FUNCTION K1(X)

!      SEE CARSLAW & JAEGER, PG. 489, EQUATION (10) FOR K1 SERIES.
!      SEE GRADSHTEYN & RYZHIK, PG. 961, EQUATION 8.477.2 FOR I1.

!      PROGRAMMED BY: E.A. SUDICKY,
!                      INSTITUTE FOR GROUNDWATER RESEARCH,
!                      UNIVERSITY OF WATERLOO,
!                      WATERLOO, ONTARIO, N2L SG1
!                      JANUARY, 1987.
!
!      UPDATE FOR COMPLEX: F.W.LETNIOWSKI
!                      MAY, 1987.

DOUBLE COMPLEX FUNCTION CBK1(X)

      IMPLICIT DOUBLE COMPLEX(A-H,O-Z)
      DOUBLE PRECISION PI,E,FACT,Z1,Z2

      CBK1=DCMPLX(0.0,0.0)
      E=0.577215665
      PI=3.14159265
      IF(CDABS(X).LE.1.0E-03) GOTO 200
      IF(CDABS(X).GT.50.0) GOTO 99
      IF(CDABS(X).GT.5.0) GOTO 100

      X2=X/2.0
      X3=X*X/4.0
      XX=X2*X3

!      SUM1 ADDS TO I1(X)

      SUM1=X2
      SUM2=SUM1
      SUM3=DCMPLX(0.0,0.0)
      FACT=1.0
      N=0
10     N=N+1
          Z1=FLOAT(N)
          Z2=FLOAT(N+1)
          FACT=FACT*Z1*Z2
          TERM1=XX/FACT
          SUM3=SUM3+1.0/Z1

```

```

SUMI=2.0*SUM3+1.0/Z2
SUM1=SUM1+TERM1
SUM2=SUM2+TERM1*SUMI
XX=XX*X3
IF (CDABS (TERM1*SUM1/SUM2) .LT.1.0E-06) GOTO 20
GOTO 10
20    CBI1=SUM1
      CBK1=(CDLOG (X2)+E) *CBI1-0.5*SUM2+1.0/X
      GOTO 99

!     LARGE X

100   Z=CDSQRT (X)
      CBK1=CDEXP (-X) /Z*DSQRT (PI/2.0) *(1.0+3.0/(8.0*X))
      GOTO 99

!     SMALL X

200   U=X/2.0
      CBK1=1.0/X+U* (CDLOG (U)+E) -X/4.0
99    CONTINUE

RETURN
END

!     MODIFIED BESSEL FUNCITON I1(X)

!     SEE CARSLAW & JAEGER, PG. 489, EQUATION (10) FOR K1 SERIES.
!     SEE GRADSHTEYN & RYZHIK, RG. 961, EQUATION 8.447.2 FOR I1.

!     PROGRAMMED BY: E.A. SUDICKY,
!                   INSTITUTE FOR GROUNDWATER RESEARCH,
!                   UNIVERSITY OF WATERLOO,
!                   WATERLOO, ONTARIO, N2L 3G1
!                   JANUARY, 1987.

!     UPDATE FOR COMPLEX: F.W. LETNIEWSKI
!                   MAY, 1987

DOUBLE COMPLEX FUNCTION CBI1 (X)

      IMPLICIT DOUBLE COMPLEX (A-H, O-Z)
      DOUBLE PRECISION PI, E, FACT, Z1, Z2

      CBI1=DCMPLX (0.0, 0.0)
      E=0.577215665
      PI=3.14159265
      IF (CDABS (X) .LE.1.0E-03) GOTO 200
      IF (CDABS (X) .GT.50.0) GOTO 99
      IF (CDABS (X) .GT.5.0) GOTO 100

      X2=X/2.0
      X3=X*X/4.0

```

```

                XX=X2*X3

!      SUM1 ADDS TO I1(X)
!      SERIES EXPANSION

                SUM1=X2
                SUM2=SUM1
                SUM3=DCMPLX(0.0,0.0)
                FACT=1.0
                N=0
10             N=N+1
                Z1=FLOAT(N)
                Z2=FLOAT(N+1)
                FACT=FACT*Z1*Z2
                TERM1=XX/FACT
                SUM3=SUM3+1.0/Z1
                SUMI=2.0*SUM3+1.0/Z2
                SUM1=SUM1+TERM1
                SUM2=SUM2+TERM1*SUMI
                XX=XX*X3
                IF(CDABS(TERM1*SUM1/SUM2).LT.1.0E-06) GOTO 20
                GOTO 10
20             CBI1=SUM1
                GOTO 99

!      LARGE X
!      ASYMPTOTIC SERIES EXPANSION

100            Z=CDSQRT(X)
                CBI1=CDEXP(X)/Z*DSQRT(PI*2.0)*(1.0-3.0/(8.0*X))
                GOTO 99

!      SMALL X
!      POLYNOMIAL APPROXIMATION

200            U=X/2.0
                T=X/3.75
                CBI1=U+.87890594*T**2*X+.51498869*T**4*X+.15084934*T**6*X
99             CONTINUE

RETURN
END

!      MODIFIED BESSEL FUNCTION I0(X) FOR COMPLEX X

!      SEE ABOMOWITZ & STEGUN, HANDBOOK OF MATHEMATICAL FUNCTIONS
!      PAGE 375 FOR SERIES EXPANSION.

!      PROGRAMMED BY: E.A. SUDICKY,
!                      INSTITUTE FOR GROUNDWATER RESERACH,
!                      UNIVERSITY OF WATERLOO,
!                      WATERLOO, ONTARIO, N2L 3G1
!                      MARCH, 1987.

```

```

DOUBLE COMPLEX FUNCTION CBI0(X)
  IMPLICIT DOUBLE COMPLEX (A-H,O-Z)
  DOUBLE PRECISION PI,E,FACT1,Z1
  CBI0=(0.0,0.0)
  E=0.577215664901533
  PI=3.14159265
  IF(CDABS(X).LE.1.0E-03) GOTO 200
  IF(CDABS(X).GT.50.0) GOTO 99
  IF(CDABS(X).GT.5.0) GOTO 100
  X2=X/2.0
  X3=X*X/4.0
  XX=X3

!   SUM1 ADDS TO I0(X)

      SUM1=DCMPLX(1.0,0.0)
      SUM2=DCMPLX(0.0,0.0)
      SUM3=DCMPLX(0.0,0.0)
      FACT1=1.0
      N=0
10     N=N+1
      Z1=FLOAT(N)
      FACT1=FACT1*Z1
      TERM1=XX/(FACT1*FACT1)
      SUM3=SUM3+1.0/Z1
      SUM1=SUM1+TERM1
      RUNTRM=TERM1*SUM3
      SUM2=SUM2+RUNTRM
      XX=XX*X3
      IF(CDABS(RUNTRM/SUM2).LT.1.0E-06) GOTO 20
      GOTO 10
20     CBI0=SUM1
      GOTO 99

!   LARGE X

100    Z=CDSQRT(X)
      CBI0=CDEXP(X)/(Z*DSQRT(PI*2.0))
      GOTO 99

!   SMALL X

200    U=X/2.0
      CBI0=1.00+U*U
99     CONTINUE
      RETURN
END

```

Appendix D

Hydraulic parameter estimates from Fletcher Creek field site

Table D.1 Estimate of horizontal hydraulic conductivity from pumping test analysis.

Pumped well	Observation well	Pumping test					
		Moench solution	95% Confidence Limits		Model solution	95% Confidence Limits	
			lower	upper		lower	upper
FC-9	FC-1	4.9×10^{-6}	-5.2×10^{-7}	5.2×10^{-7}	1.3×10^{-5}	9.4×10^{-6}	1.6×10^{-5}
FC-9	FC-2	7.3×10^{-6}	(-)	(-)	1.5×10^{-5}	1.1×10^{-5}	1.9×10^{-5}
FC-9	FC-3	1.1×10^{-5}	(-)	(-)	2.3×10^{-5}	1.6×10^{-5}	3.1×10^{-5}
FC-9	FC-4	6.3×10^{-6}	(-)	(-)	2.5×10^{-5}	4.8×10^{-6}	4.5×10^{-5}
FC-9	FC-5	8.8×10^{-6}	(-)	(-)	1.5×10^{-5}	1.2×10^{-5}	1.8×10^{-5}
FC-9	FC-6	5.9×10^{-6}	(-)	(-)	2.1×10^{-5}	6.4×10^{-6}	3.6×10^{-5}
FC-9	FC-7	1.1×10^{-5}	-1.6×10^{-6}	1.6×10^{-6}	1.2×10^{-5}	7.9×10^{-6}	1.6×10^{-5}
FC-9	FC-8	7.8×10^{-6}	(-)	(-)	1.2×10^{-5}	7.5×10^{-6}	1.6×10^{-5}
FC-9	FC-9	4.2×10^{-6}	-9.0×10^{-9}	9.0×10^{-9}	1.8×10^{-5}	1.6×10^{-5}	1.9×10^{-5}
FC-7	FC-1	5.9×10^{-6}	(-)	(-)	7.3×10^{-6}	6.6×10^{-6}	8.1×10^{-6}
FC-7	FC-2	4.3×10^{-6}	(-)	(-)	3.9×10^{-6}	-2.5×10^{-5}	3.3×10^{-5}
FC-7	FC-3	6.8×10^{-6}	(-)	(-)	1.3×10^{-5}	1.2×10^{-5}	1.4×10^{-5}
FC-7	FC-4	5.0×10^{-6}	(-)	(-)	1.7×10^{-5}	1.6×10^{-5}	1.8×10^{-5}
FC-7	FC-5	9.7×10^{-6}	(-)	(-)	1.4×10^{-5}	1.3×10^{-5}	1.4×10^{-5}
FC-7	FC-6	9.5×10^{-6}	(-)	(-)	9.2×10^{-6}	8.4×10^{-6}	9.9×10^{-6}
FC-7	FC-7	1.0×10^{-5}	-1.3×10^{-7}	1.3×10^{-7}	1.4×10^{-5}	1.2×10^{-5}	1.6×10^{-5}
FC-7	FC-8	4.2×10^{-6}	(-)	(-)	6.3×10^{-6}	5.8×10^{-6}	6.8×10^{-6}
FC-7	FC-9	7.1×10^{-6}	(-)	(-)	7.2×10^{-6}	6.8×10^{-6}	7.7×10^{-6}
Site geometric mean		6.8×10^{-6}			1.2×10^{-5}		
Standard deviation		2.3×10^{-6}			5.8×10^{-6}		

Table D.2 Estimate of horizontal hydraulic conductivity from pulse interference test analysis.

Pumped well	Observation well	Pulse interference test					
		Test A	95% Confidence Limits		Test B	95% Confidence Limits	
			lower	upper		lower	upper
FC-9	FC-1	1.8×10^{-5}	(-)	(-)	1.6×10^{-5}	(-)	(-)
FC-9	FC-2	1.3×10^{-5}	(-)	(-)	5.4×10^{-6}	(-)	(-)
FC-9	FC-3	1.3×10^{-5}	(-)	(-)	7.1×10^{-6}	(-)	(-)
FC-9	FC-4	1.8×10^{-5}	(-)	(-)	1.8×10^{-5}	(-)	(-)
FC-9	FC-5	4.7×10^{-5}	(-)	(-)	4.6×10^{-5}	(-)	(-)
FC-9	FC-6	1.2×10^{-5}	(-)	(-)	1.1×10^{-5}	(-)	(-)
FC-9	FC-7	4.2×10^{-5}	(-)	(-)	2.6×10^{-5}	2.5×10^{-5}	2.7×10^{-5}
FC-9	FC-8	2.0×10^{-5}	(-)	(-)	2.7×10^{-5}	(-)	(-)
FC-9	FC-9	9.8×10^{-6}	(-)	(-)	2.9×10^{-5}	2.9×10^{-5}	3.0×10^{-5}
FC-7	FC-1	1.9×10^{-5}	-6.1×10^{-6}	4.5×10^{-5}	3.1×10^{-6}	(-)	(-)
FC-7	FC-2	4.3×10^{-6}	(-)	(-)	7.1×10^{-6}	(-)	(-)
FC-7	FC-3	9.6×10^{-6}	(-)	(-)	9.9×10^{-6}	(-)	(-)
FC-7	FC-4	5.8×10^{-6}	(-)	(-)	1.2×10^{-5}	(-)	(-)
FC-7	FC-5	2.6×10^{-5}	2.1×10^{-5}	3.0×10^{-5}	2.9×10^{-5}	(-)	(-)
FC-7	FC-6	5.6×10^{-6}	(-)	(-)	5.6×10^{-6}	(-)	(-)
FC-7	FC-7	1.3×10^{-5}	1.2×10^{-5}	1.4×10^{-5}	1.6×10^{-5}	1.5×10^{-5}	1.6×10^{-5}
FC-7	FC-8	1.3×10^{-5}	(-)	(-)	1.3×10^{-5}	(-)	(-)
FC-7	FC-9	2.3×10^{-5}	2.2×10^{-5}	2.4×10^{-5}	1.8×10^{-5}	(-)	(-)
Site geometric mean				1.4×10^{-5}			
Standard deviation				1.1×10^{-5}			

Table D.3 Estimate of horizontal hydraulic conductivity from constant head test data analysis.

Borehole	Vertical well depth (m)	Hydraulic Conductivity (m/s)
FC-1	32.18	2.9×10^{-6}
FC-2	28.11	7.0×10^{-6}
FC-3	19.77	5.5×10^{-6}
FC-4	18.70	1.6×10^{-5}
FC-5	21.44	6.6×10^{-6}
FC-6	19.70	4.9×10^{-6}
FC-7	28.46	3.5×10^{-6}
FC-8	28.64	1.2×10^{-6}
FC-9	28.45	3.9×10^{-6}
Geometric mean		4.6×10^{-6}
Standard deviation		4.2×10^{-6}

Table D.4 Estimate of specific storage from pumping test analysis.

Pumped well	Observation well	Pumping test					
		Moench solution	95% Confidence Limits		Model solution	95% Confidence Limits	
			lower	upper		lower	upper
FC-9	FC-1	1.7×10^{-7}	-6.6×10^{-9}	6.6×10^{-9}	2.7×10^{-7}	1.4×10^{-7}	3.9×10^{-7}
FC-9	FC-2	1.4×10^{-7}	(-)	(-)	2.8×10^{-7}	2.5×10^{-7}	3.1×10^{-7}
FC-9	FC-3	3.2×10^{-8}	(-)	(-)	4.4×10^{-7}	2.4×10^{-7}	6.5×10^{-7}
FC-9	FC-4	1.1×10^{-8}	(-)	(-)	4.6×10^{-7}	-1.4×10^{-7}	1.1×10^{-6}
FC-9	FC-5	5.4×10^{-9}	(-)	(-)	4.7×10^{-9}	-1.3×10^{-8}	2.3×10^{-8}
FC-9	FC-6	2.9×10^{-9}	(-)	(-)	1.0×10^{-6}	9.2×10^{-7}	1.1×10^{-6}
FC-9	FC-7	9.7×10^{-10}	-1.6×10^{-6}	1.6×10^{-6}	7.6×10^{-9}	-3.5×10^{-8}	5.0×10^{-8}
FC-9	FC-8	1.8×10^{-10}	(-)	(-)	4.5×10^{-8}	-2.9×10^{-8}	1.2×10^{-7}
FC-9	FC-9	1.6×10^{-9}	-6.0×10^{-11}	6.0×10^{-11}	1.2×10^{-8}	-4.9×10^{-8}	7.3×10^{-8}
FC-7	FC-1	3.2×10^{-7}	(-)	(-)	5.1×10^{-7}	4.5×10^{-7}	5.8×10^{-7}
FC-7	FC-2	8.1×10^{-6}	(-)	(-)	2.6×10^{-6}	2.3×10^{-6}	2.8×10^{-6}
FC-7	FC-3	1.5×10^{-6}	(-)	(-)	1.7×10^{-6}	1.6×10^{-6}	1.8×10^{-6}
FC-7	FC-4	3.5×10^{-7}	(-)	(-)	1.3×10^{-6}	1.1×10^{-6}	1.4×10^{-6}
FC-7	FC-5	7.8×10^{-11}	(-)	(-)	8.7×10^{-8}	-5.9×10^{-7}	7.6×10^{-7}
FC-7	FC-6	2.4×10^{-7}	(-)	(-)	5.1×10^{-10}	-4.8×10^{-8}	4.9×10^{-8}
FC-7	FC-7	1.2×10^{-6}	-2.1×10^{-9}	2.1×10^{-9}	1.3×10^{-9}	-4.1×10^{-7}	4.1×10^{-7}
FC-7	FC-8	1.6×10^{-7}	(-)	(-)	5.3×10^{-10}	-1.0×10^{-7}	1.0×10^{-7}
FC-7	FC-9	4.5×10^{-9}	(-)	(-)	3.2×10^{-6}	2.9×10^{-6}	3.4×10^{-6}
Site arithmetic mean		2.7×10^{-7}			6.6×10^{-7}		
Standard deviation		8.6×10^{-7}			9.5×10^{-7}		

Table D.5 Estimate of specific storage from pulse interference test analysis.

Pumped well	Observation well	Pulse interference test					
		Test A	95% Confidence Limits		Test B	95% Confidence Limits	
			lower	upper		lower	upper
FC-9	FC-1	3.1×10^{-7}	(-)	(-)	1.9×10^{-6}	(-)	(-)
FC-9	FC-2	2.9×10^{-7}	(-)	(-)	3.1×10^{-6}	(-)	(-)
FC-9	FC-3	1.4×10^{-7}	(-)	(-)	1.3×10^{-6}	(-)	(-)
FC-9	FC-4	1.1×10^{-8}	(-)	(-)	2.3×10^{-5}	(-)	(-)
FC-9	FC-5	1.4×10^{-7}	(-)	(-)	1.4×10^{-7}	(-)	(-)
FC-9	FC-6	2.4×10^{-6}	(-)	(-)	1.2×10^{-6}	(-)	(-)
FC-9	FC-7	1.1×10^{-6}	(-)	(-)	3.8×10^{-7}	-4.6×10^{-5}	4.6×10^{-5}
FC-9	FC-8	1.0×10^{-6}	(-)	(-)	5.6×10^{-7}	(-)	(-)
FC-9	FC-9	1.1×10^{-8}	(-)	(-)	1.8×10^{-7}	1.5×10^{-7}	2.0×10^{-7}
FC-7	FC-1	1.0×10^{-6}	6.6×10^{-7}	1.4×10^{-6}	6.8×10^{-8}	(-)	(-)
FC-7	FC-2	4.7×10^{-6}	(-)	(-)	1.5×10^{-5}	(-)	(-)
FC-7	FC-3	3.0×10^{-6}	(-)	(-)	3.1×10^{-6}	(-)	(-)
FC-7	FC-4	3.2×10^{-7}	(-)	(-)	4.6×10^{-7}	(-)	(-)
FC-7	FC-5	4.3×10^{-7}	1.9×10^{-7}	6.7×10^{-7}	4.3×10^{-7}	(-)	(-)
FC-7	FC-6	1.1×10^{-7}	(-)	(-)	1.1×10^{-7}	(-)	(-)
FC-7	FC-7	9.9×10^{-8}	8.1×10^{-8}	1.2×10^{-7}	4.9×10^{-7}	4.6×10^{-7}	5.1×10^{-7}
FC-7	FC-8	2.2×10^{-6}	(-)	(-)	1.6×10^{-6}	(-)	(-)
FC-7	FC-9	5.3×10^{-8}	-4.1×10^{-5}	4.1×10^{-5}	9.5×10^{-8}	(-)	(-)
Site arithmetic mean				2.3×10^{-6}			
Standard deviation				4.7×10^{-6}			

Table D.6 Estimate of specific yield from pumping test analysis.

Pumped well	Observation well	Pumping test					
		Moench solution	95% Confidence Limits		Model solution	95% Confidence Limits	
			lower	upper		lower	upper
FC-9	FC-1	5.6×10^{-4}	-4.5×10^{-4}	4.5×10^{-4}	1.2×10^{-7}	-3.9×10^{-6}	4.1×10^{-6}
FC-9	FC-2	1.1×10^{-6}	(-)	(-)	1.2×10^{-6}	1.6×10^{-7}	2.2×10^{-6}
FC-9	FC-3	1.0×10^{-5}	(-)	(-)	9.74E-10	-4.1×10^{-6}	4.1×10^{-6}
FC-9	FC-4	7.4×10^{-6}	(-)	(-)	1.2×10^{-7}	-1.1×10^{-5}	1.1×10^{-5}
FC-9	FC-5	5.9×10^{-6}	(-)	(-)	1.0×10^{-6}	5.3×10^{-7}	1.5×10^{-6}
FC-9	FC-6	1.0×10^{-5}	(-)	(-)	7.6×10^{-7}	-6.8×10^{-7}	2.2×10^{-6}
FC-9	FC-7	1.0×10^{-5}	-4.8×10^{-2}	4.8×10^{-2}	1.8×10^{-5}	1.6×10^{-5}	2.0×10^{-5}
FC-9	FC-8	1.0×10^{-6}	(-)	(-)	2.1×10^{-5}	1.7×10^{-5}	2.5×10^{-5}
FC-9	FC-9	1.6×10^{-6}	-1.1×10^{-7}	1.1×10^{-7}	7.9×10^{-8}	-3.1×10^{-2}	3.1×10^{-2}
FC-7	FC-1	1.4×10^{-6}	(-)	(-)	9.5×10^{-7}	-5.5×10^{-7}	2.4×10^{-6}
FC-7	FC-2	6.4×10^{-6}	(-)	(-)	6.9×10^{-6}	4.5×10^{-6}	9.3×10^{-6}
FC-7	FC-3	1.0×10^{-6}	(-)	(-)	2.2×10^{-6}	1.3×10^{-6}	3.2×10^{-6}
FC-7	FC-4	1.0×10^{-5}	(-)	(-)	3.2×10^{-6}	1.4×10^{-6}	5.0×10^{-6}
FC-7	FC-5	3.0×10^{-7}	(-)	(-)	1.3×10^{-7}	-1.4×10^{-5}	1.4×10^{-5}
FC-7	FC-6	3.3×10^{-4}	(-)	(-)	9.3×10^{-5}	8.9×10^{-5}	9.6×10^{-5}
FC-7	FC-7	1.0×10^{-7}	-6.9×10^{-5}	6.9×10^{-5}	1.0×10^{-7}	-5.3×10^{-3}	5.3×10^{-3}
FC-7	FC-8	4.2×10^{-4}	(-)	(-)	9.3×10^{-5}	8.8×10^{-5}	9.7×10^{-5}
FC-7	FC-9	2.3×10^{-2}	(-)	(-)	3.7×10^{-4}	3.1×10^{-4}	4.2×10^{-4}
Site arithmetic mean		8.6×10^{-5}			1.5×10^{-5}		
Standard deviation		1.8×10^{-4}			8.8×10^{-5}		

Table D.7 Estimate of specific yield from pulse interference test analysis.

Pumped well	Observation well	Pulse interference test					
		Test A	95% Confidence Limits		Test B	95% Confidence Limits	
			lower	upper		lower	upper
FC-9	FC-1	6.9×10^{-5}	(-)	(-)	2.2×10^{-5}	(-)	(-)
FC-9	FC-2	3.1×10^{-8}	(-)	(-)	3.4×10^{-6}	(-)	(-)
FC-9	FC-3	5.0×10^{-4}	(-)	(-)	4.6×10^{-5}	(-)	(-)
FC-9	FC-4	6.7×10^{-5}	(-)	(-)	6.0×10^{-5}	(-)	(-)
FC-9	FC-5	5.0×10^{-4}	(-)	(-)	4.0×10^{-5}	(-)	(-)
FC-9	FC-6	6.0×10^{-5}	(-)	(-)	1.0×10^{-4}	(-)	(-)
FC-9	FC-7	2.1×10^{-5}	(-)	(-)	3.9×10^{-6}	-1.3×10^{-3}	1.3×10^{-3}
FC-9	FC-8	9.5×10^{-5}	(-)	(-)	9.0×10^{-5}	(-)	(-)
FC-9	FC-9	(-)	(-)	(-)	(-)	(-)	(-)
FC-7	FC-1	1.2×10^{-4}	-1.7×10^{-1}	1.7×10^{-1}	1.9×10^{-5}	(-)	(-)
FC-7	FC-2	3.0×10^{-4}	(-)	(-)	1.7×10^{-5}	(-)	(-)
FC-7	FC-3	1.5×10^{-4}	(-)	(-)	1.3×10^{-4}	(-)	(-)
FC-7	FC-4	1.5×10^{-4}	(-)	(-)	1.1×10^{-4}	(-)	(-)
FC-7	FC-5	5.0×10^{-4}	-3.3	3.3	5.0×10^{-4}	(-)	(-)
FC-7	FC-6	1.9×10^{-5}	(-)	(-)	6.0×10^{-4}	(-)	(-)
FC-7	FC-7	(-)	(-)	(-)	(-)	(-)	(-)
FC-7	FC-8	2.1×10^{-4}	(-)	(-)	1.9×10^{-5}	(-)	(-)
FC-7	FC-9	1.4×10^{-5}	-1.2×10^{-3}	1.2×10^{-3}	2.0×10^{-5}	(-)	(-)
Site arithmetic mean				1.3×10^{-4}			
Standard deviation				1.8×10^{-4}			

Table D.8 Estimate of specific yield from constant head test analysis.

Borehole	Total T (m ² /s)	2b _{eq} (m)	Tested borehole length (m)	S _y (-)
FC-1	9.3 x 10 ⁻⁵	5.4 x 10 ⁻⁴	22.68	2.4 x 10 ⁻⁵
FC-2	2.0 x 10 ⁻⁴	7.0 x 10 ⁻⁴	21.08	3.3 x 10 ⁻⁵
FC-3	1.1 x 10 ⁻⁴	5.7 x 10 ⁻⁴	15.96	3.6 x 10 ⁻⁵
FC-4	3.0 x 10 ⁻⁴	8.0 x 10 ⁻⁴	13.76	5.8 x 10 ⁻⁵
FC-5	1.4 x 10 ⁻⁴	6.2 x 10 ⁻⁴	8.46	7.3 x 10 ⁻⁵
FC-6	9.6 x 10 ⁻⁵	5.5 x 10 ⁻⁴	9.41	5.8 x 10 ⁻⁵
FC-7	9.9 x 10 ⁻⁵	5.5 x 10 ⁻⁴	9.19	6.0 x 10 ⁻⁵
FC-8	3.4 x 10 ⁻⁵	3.9 x 10 ⁻⁴	12.18	3.2 x 10 ⁻⁵
Site arithmetic mean				4.4 x 10 ⁻⁵
Standard deviation				1.8 x 10 ⁻⁵

Table D.9 Estimate of vertical hydraulic conductivity from pumping test analysis.

Pumped well	Observation well	Pumping test					
		Moench solution	95% Confidence limits		Model solution	95% Confidence limits	
			lower	upper		lower	upper
FC-9	FC-1	6.8 x 10 ⁻⁶	(-)	(-)	1.4 x 10 ⁻⁶	-9.8 x 10 ⁻³	9.8 x 10 ⁻³
FC-9	FC-2	4.9 x 10 ⁻⁶	(-)	(-)	2.0 x 10 ⁻⁵	-1.9 x 10 ⁻⁴	2.3 x 10 ⁻⁴
FC-9	FC-3	3.4 x 10 ⁻⁵	(-)	(-)	8.9 x 10 ⁻⁶	-5.8 x 10 ⁻⁴	6.0 x 10 ⁻⁴
FC-9	FC-4	5.9 x 10 ⁻⁶	(-)	(-)	1.0 x 10 ⁻⁵	-9.6 x 10 ⁻⁵	1.2 x 10 ⁻⁴
FC-9	FC-5	5.9 x 10 ⁻⁶	(-)	(-)	1.4 x 10 ⁻⁵	-9.7 x 10 ⁻⁶	3.9 x 10 ⁻⁵
FC-9	FC-6	5.9 x 10 ⁻⁶	(-)	(-)	7.6 x 10 ⁻⁶	5.6 x 10 ⁻⁶	9.6 x 10 ⁻⁶
FC-9	FC-7	7.4 x 10 ⁻⁶	(-)	(-)	2.7 x 10 ⁻⁵	2.3 x 10 ⁻⁵	3.0 x 10 ⁻⁵
FC-9	FC-8	5.6 x 10 ⁻⁶	(-)	(-)	3.3 x 10 ⁻⁵	2.7 x 10 ⁻⁵	3.9 x 10 ⁻⁵
FC-9	FC-9	4.2 x 10 ⁻⁶	(-)	(-)	1.0 x 10 ⁻⁵	-3.0	3.0
FC-7	FC-1	(-)	(-)	(-)	(-)	(-)	(-)
FC-7	FC-2	3.6 x 10 ⁻⁶	(-)	(-)	1.1 x 10 ⁻⁵	-5.8 x 10 ⁻⁶	2.7 x 10 ⁻⁵
FC-7	FC-3	6.8 x 10 ⁻⁶	(-)	(-)	1.4 x 10 ⁻⁵	6.3 x 10 ⁻⁶	2.1 x 10 ⁻⁵
FC-7	FC-4	5.0 x 10 ⁻⁶	(-)	(-)	3.9 x 10 ⁻⁵	3.2 x 10 ⁻⁵	4.5 x 10 ⁻⁵
FC-7	FC-5	9.7 x 10 ⁻⁶	(-)	(-)	1.1 x 10 ⁻⁴	-5.7 x 10 ⁻²	5.8 x 10 ⁻²
FC-7	FC-6	9.9 x 10 ⁻⁶	(-)	(-)	1.0 x 10 ⁻⁴	-5.8 x 10 ⁻⁴	7.8 x 10 ⁻⁴
FC-7	FC-7	6.5 x 10 ⁻⁶	(-)	(-)	6.5 x 10 ⁻⁶	-9.8 x 10 ⁻²	9.8 x 10 ⁻²
FC-7	FC-8	4.2 x 10 ⁻⁶	(-)	(-)	1.0 x 10 ⁻⁴	-2.7 x 10 ⁻⁵	2.3 x 10 ⁻⁴
FC-7	FC-9	4.0 x 10 ⁻⁶	(-)	(-)	5.0 x 10 ⁻⁶	4.2 x 10 ⁻⁶	5.8 x 10 ⁻⁶
Geometric mean		6.4 x 10 ⁻⁶			1.7 x 10 ⁻⁵		
Standard deviation		6.9 x 10 ⁻⁶			3.7 x 10 ⁻⁵		

Table D.10 Estimate of vertical hydraulic conductivity from pulse interference test analysis.

Pumped well	Observation well	Pulse interference test					
		Test A	95% Confidence limits		Test B	95% Confidence limits	
			lower	upper		lower	upper
FC-9	FC-1	8.7×10^{-6}	(-)	(-)	4.4×10^{-6}	(-)	(-)
FC-9	FC-2	5.7×10^{-6}	(-)	(-)	1.8×10^{-6}	(-)	(-)
FC-9	FC-3	7.0×10^{-8}	(-)	(-)	1.2×10^{-7}	(-)	(-)
FC-9	FC-4	1.0×10^{-5}	(-)	(-)	1.0×10^{-7}	(-)	(-)
FC-9	FC-5	2.9×10^{-6}	(-)	(-)	3.1×10^{-6}	(-)	(-)
FC-9	FC-6	6.5×10^{-10}	(-)	(-)	3.1×10^{-8}	(-)	(-)
FC-9	FC-7	7.7×10^{-5}	(-)	(-)	8.2×10^{-5}	-1.6×10^{-2}	1.6×10^{-2}
FC-9	FC-8	1.0×10^{-5}	(-)	(-)	6.6×10^{-6}	(-)	(-)
FC-9	FC-9	(-)	(-)	(-)	(-)	(-)	(-)
FC-7	FC-1	3.2×10^{-9}	-5.3×10^{-9}	1.2×10^{-8}	6.7×10^{-8}	(-)	(-)
FC-7	FC-2	6.1×10^{-6}	(-)	(-)	4.2×10^{-7}	(-)	(-)
FC-7	FC-3	7.0×10^{-6}	(-)	(-)	7.0×10^{-6}	(-)	(-)
FC-7	FC-4	7.0×10^{-6}	(-)	(-)	7.0×10^{-6}	(-)	(-)
FC-7	FC-5	4.1×10^{-10}	9.2×10^{-11}	7.2×10^{-10}	4.1×10^{-8}	(-)	(-)
FC-7	FC-6	6.7×10^{-8}	(-)	(-)	6.7×10^{-8}	(-)	(-)
FC-7	FC-7	(-)	3.6×10^{-10}	4.5×10^{-10}	(-)	4.0×10^{-10}	4.8×10^{-10}
FC-7	FC-8	1.3×10^{-7}	(-)	(-)	2.3×10^{-7}	(-)	(-)
FC-7	FC-9	9.8×10^{-6}	-5.7×10^{-4}	5.9×10^{-4}	5.0×10^{-6}	(-)	(-)
Geometric mean				7.3×10^{-7}			
Standard deviation				1.9×10^{-5}			

Table D.11 Estimate of vertical hydraulic conductivity from isolated zone pumping test and constant head test analysis.

Isolated vertical fractures	Isolated zone pumping test	Constant head test
FC1-2	1.3×10^{-5}	5.7×10^{-7}
FC1-3	8.8×10^{-8}	1.5×10^{-7}
FC2-1	1.5×10^{-7}	5.0×10^{-7}
FC3-1	2.7×10^{-7}	2.3×10^{-7}
FC3-2	5.7×10^{-8}	9.4×10^{-8}
FC5-1	1.9×10^{-7}	8.1×10^{-7}
FC6-2	4.8×10^{-5}	1.6×10^{-6}
Site geometric mean	5.8×10^{-7}	3.8×10^{-7}
Standard deviation	1.8×10^{-5}	5.2×10^{-7}

Table D.12 Estimate of vertical specific storage from pumping analysis.

Pumped well	Observation well	Pumping test		
		Model solution	95% Confidence limits	
			lower	upper
FC-9	FC-1	2.2×10^{-8}	-2.6×10^{-7}	3.0×10^{-7}
FC-9	FC-2	4.0×10^{-7}	1.0×10^{-7}	7.0×10^{-7}
FC-9	FC-3	5.8×10^{-8}	-2.2×10^{-7}	3.4×10^{-7}
FC-9	FC-4	7.2×10^{-8}	-5.0×10^{-7}	6.4×10^{-7}
FC-9	FC-5	1.2×10^{-7}	-2.2×10^{-8}	2.5×10^{-7}
FC-9	FC-6	8.1×10^{-8}	-3.7×10^{-7}	5.3×10^{-7}
FC-9	FC-7	9.9×10^{-7}	4.2×10^{-7}	1.6×10^{-6}
FC-9	FC-8	1.4×10^{-6}	1.1×10^{-6}	1.6×10^{-6}
FC-7	FC-1	1.3×10^{-6}	-3.2×10^{-6}	3.2×10^{-6}
FC-7	FC-2	3.1×10^{-6}	9.0×10^{-7}	1.8×10^{-6}
FC-7	FC-3	3.3×10^{-6}	2.3×10^{-6}	3.9×10^{-6}
FC-7	FC-4	6.9×10^{-7}	3.0×10^{-6}	3.6×10^{-6}
FC-7	FC-5	1.8×10^{-7}	5.7×10^{-7}	8.1×10^{-7}
FC-7	FC-6	1.2×10^{-9}	-2.3×10^{-8}	3.8×10^{-7}
FC-7	FC-8	8.7×10^{-11}	-8.9×10^{-7}	8.9×10^{-7}
FC-7	FC-9	1.0×10^{-5}	-8.1×10^{-6}	8.1×10^{-6}
Site arithmetic mean		1.4×10^{-6}		
Standard deviation		2.6×10^{-6}		

Table D.13 Estimate of vertical specific storage from pulse interference test analysis.

Pumped well	Observation well	Pulse interference test					
		Test A	95% Confidence limits		Test B	95% Confidence limits	
			lower	upper		lower	upper
FC-9	FC-1	1.5×10^{-5}	(-)	(-)	1.1×10^{-5}	(-)	(-)
FC-9	FC-2	1.2×10^{-4}	(-)	(-)	5.8×10^{-5}	(-)	(-)
FC-9	FC-3	5.0×10^{-4}	(-)	(-)	6.9×10^{-5}	(-)	(-)
FC-9	FC-4	6.8×10^{-6}	(-)	(-)	3.5×10^{-8}	(-)	(-)
FC-9	FC-5	1.3×10^{-7}	(-)	(-)	1.0×10^{-6}	(-)	(-)
FC-9	FC-6	2.5×10^{-6}	(-)	(-)	2.0×10^{-5}	(-)	(-)
FC-9	FC-7	4.0×10^{-5}	(-)	(-)	1.0×10^{-5}	5.6×10^{-6}	1.5×10^{-5}
FC-9	FC-8	5.4×10^{-6}	(-)	(-)	9.6×10^{-6}	(-)	(-)
FC-7	FC-1	2.7×10^{-8}	(-)	(-)	3.6×10^{-6}	8.5×10^{-6}	1.0×10^{-5}
FC-7	FC-2	3.0×10^{-10}	-1.1×10^{-6}	1.2×10^{-6}	8.3×10^{-6}	(-)	(-)
FC-7	FC-3	3.8×10^{-8}	(-)	(-)	1.5×10^{-7}	(-)	(-)
FC-7	FC-4	1.1×10^{-7}	(-)	(-)	2.3×10^{-8}	(-)	(-)
FC-7	FC-5	5.3×10^{-7}	(-)	(-)	5.3×10^{-7}	(-)	(-)
FC-7	FC-6	3.6×10^{-6}	-1.6×10^{-6}	2.7×10^{-6}	2.8×10^{-6}	(-)	(-)
FC-7	FC-8	1.1×10^{-10}	(-)	(-)	2.3×10^{-7}	(-)	(-)
FC-7	FC-9	5.7×10^{-6}	2.1×10^{-7}	7.9×10^{-7}	4.0×10^{-6}	5.4×10^{-6}	7.2×10^{-6}
Site arithmetic mean				1.3×10^{-6}			
Standard deviation				9.0×10^{-5}			

Appendix E

Sensitivity of model parameters to pumping test response

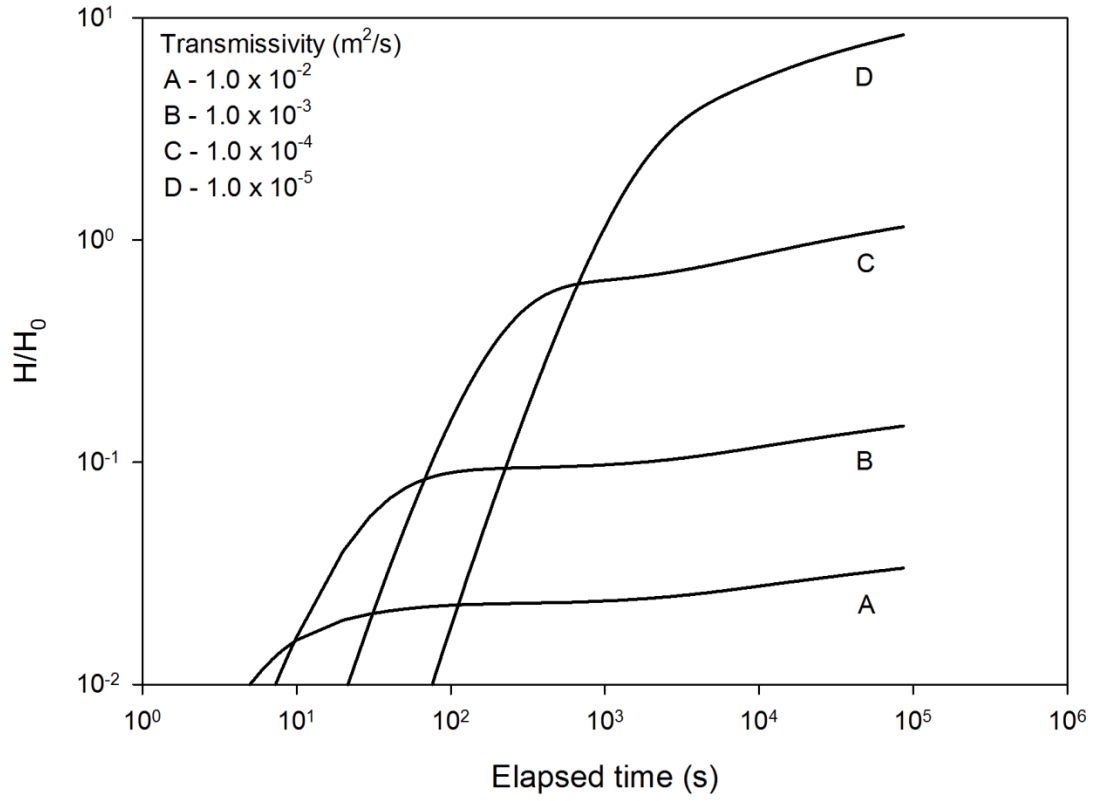


Figure E.1 Effect of transmissivity on the pumping test response in an observation well.

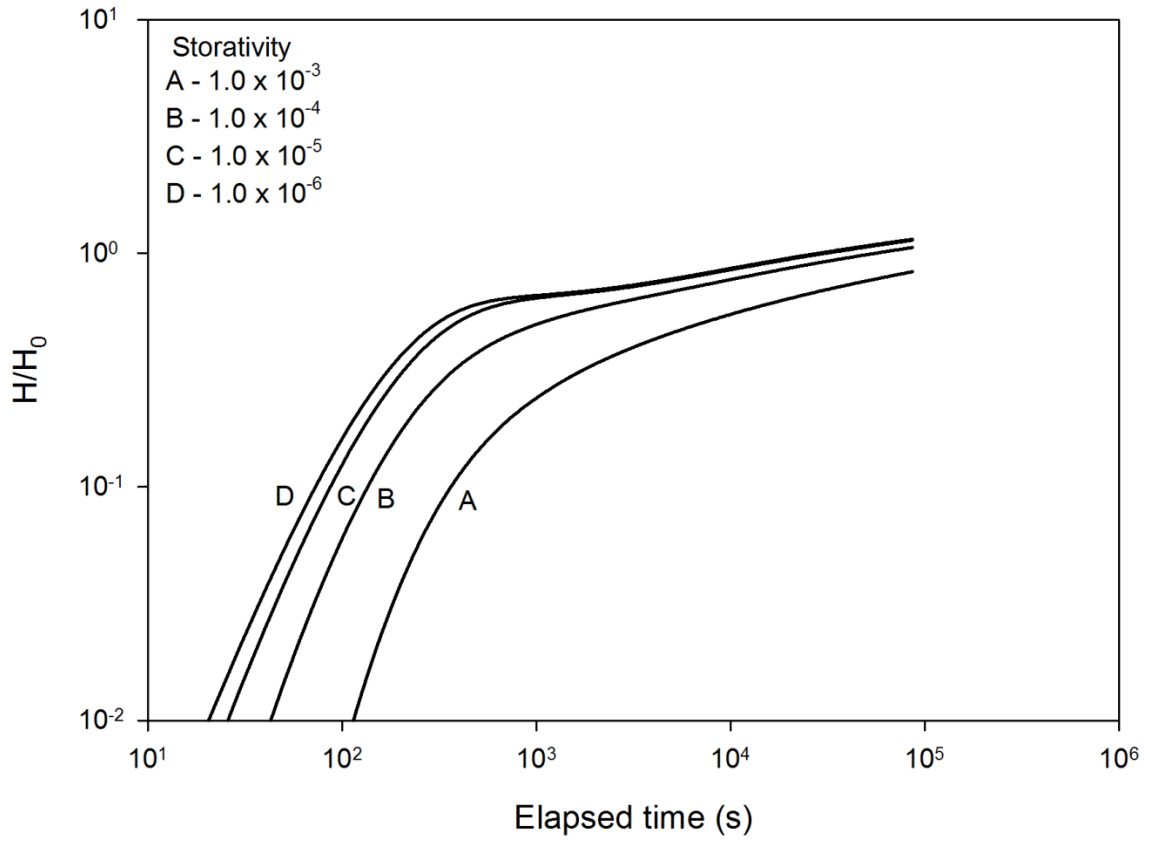


Figure E.2 Effect of storativity on the pumping test response in an observation well.

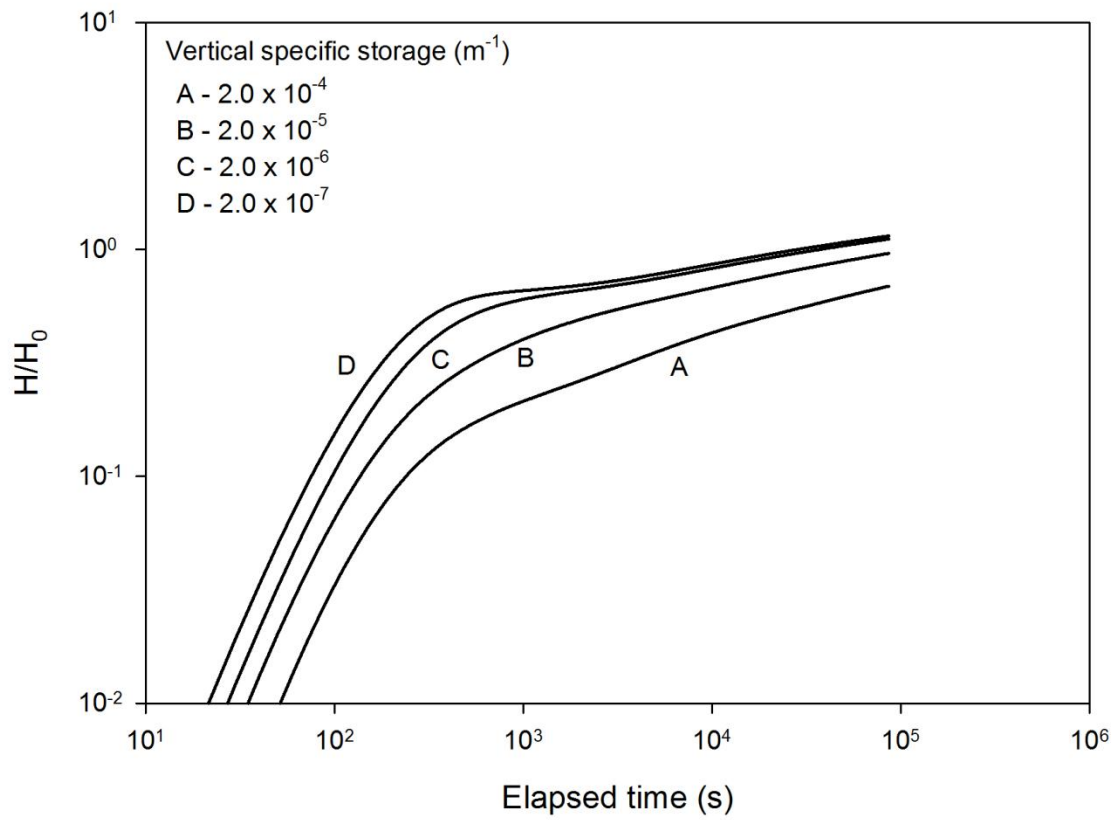


Figure E.3 Effect of vertical specific storage on the pumping test response in an observation well.

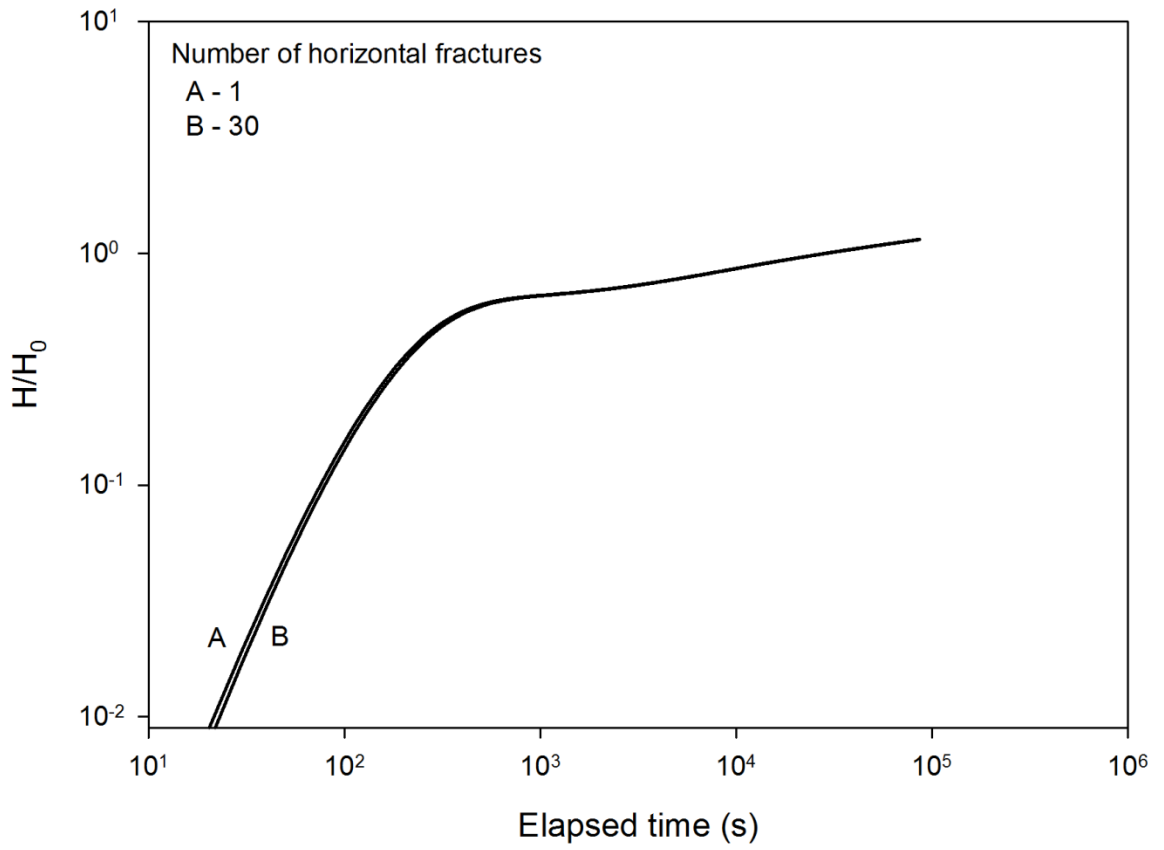


Figure E.4 Effect of number of horizontal fractures on pumping test response in an observation well.

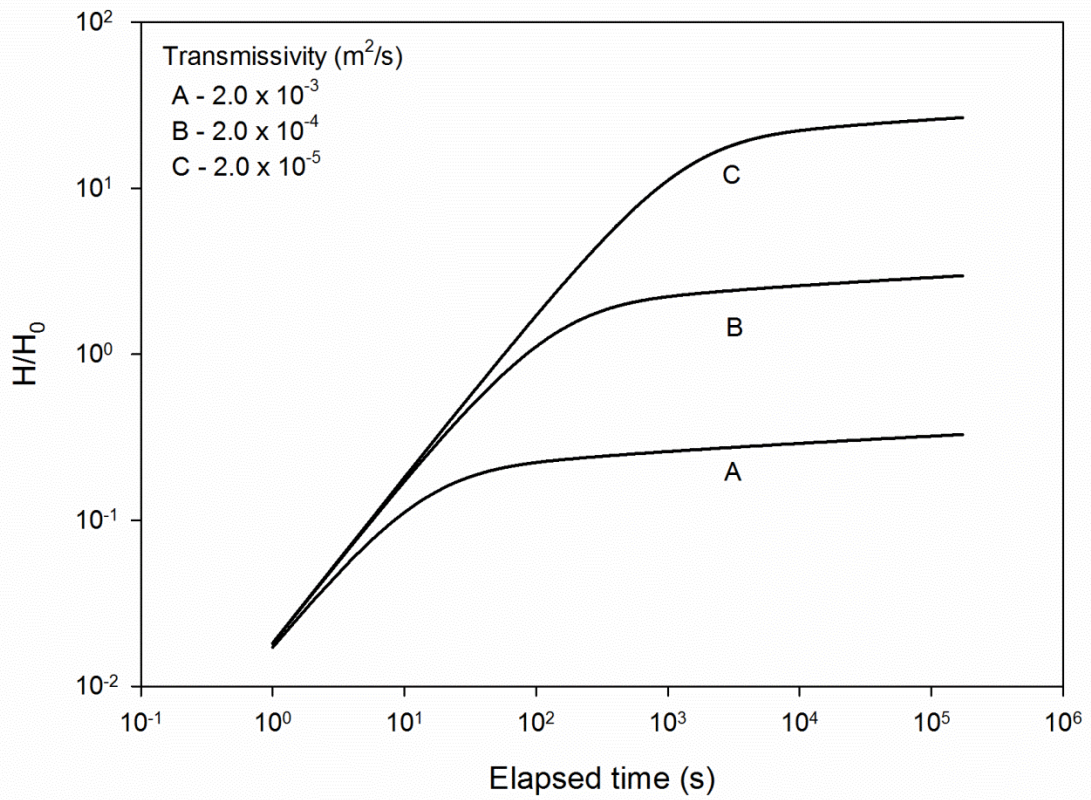


Figure E.5 Effect of transmissivity on pumping test source well response.

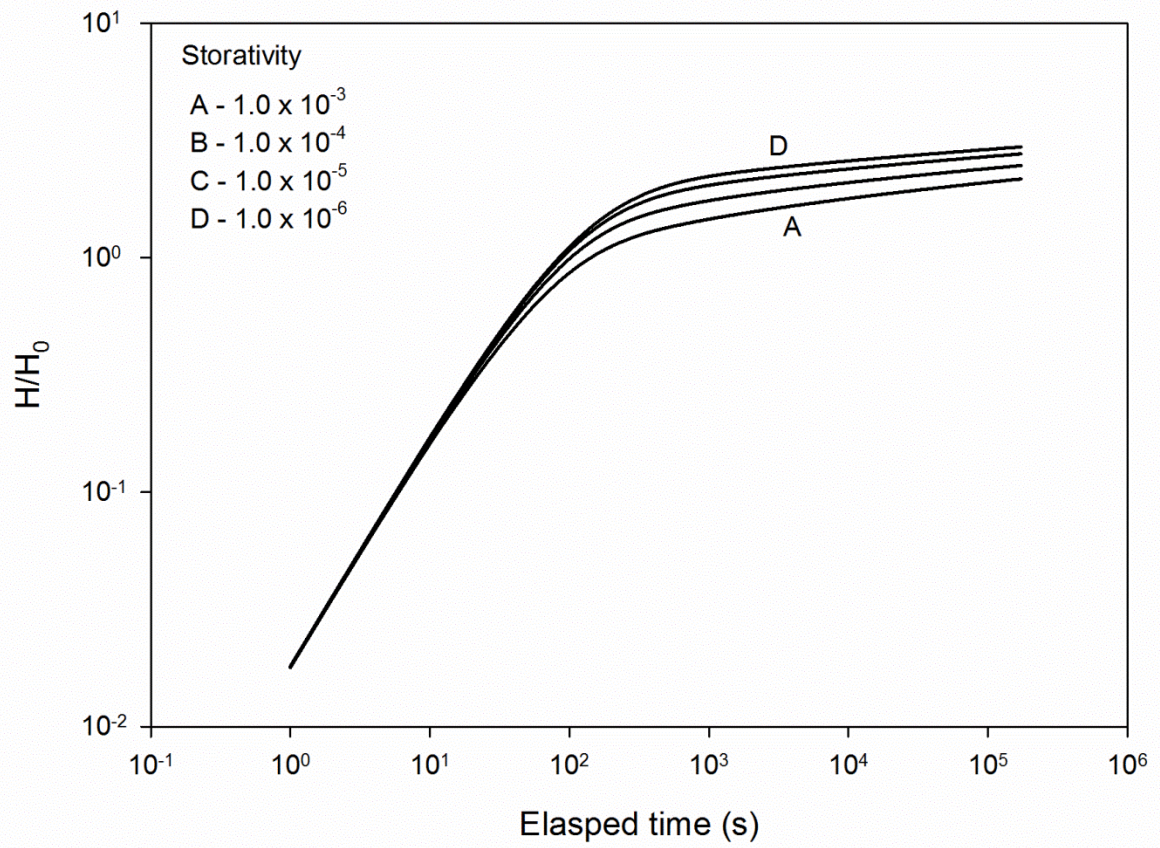


Figure E.6 Effect of storativity on pumping test source well response.

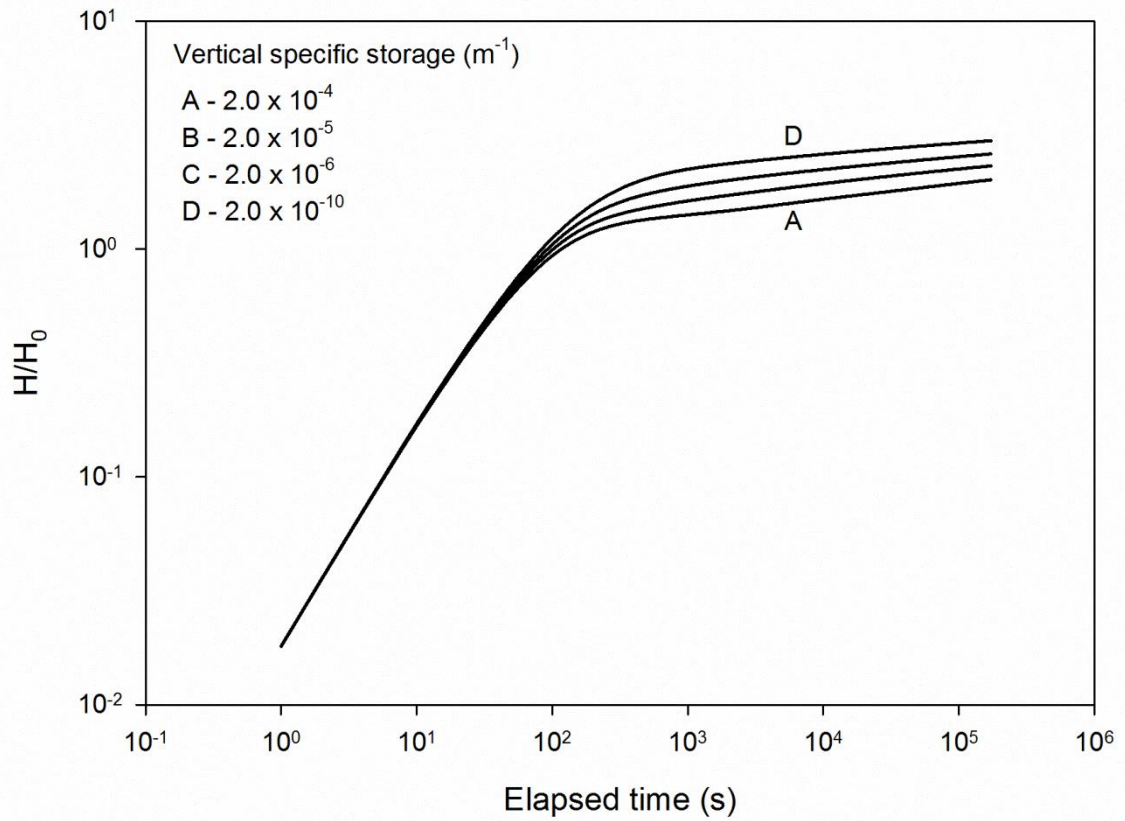


Figure E.7 Effect of vertical specific storage on pumping test source well response.

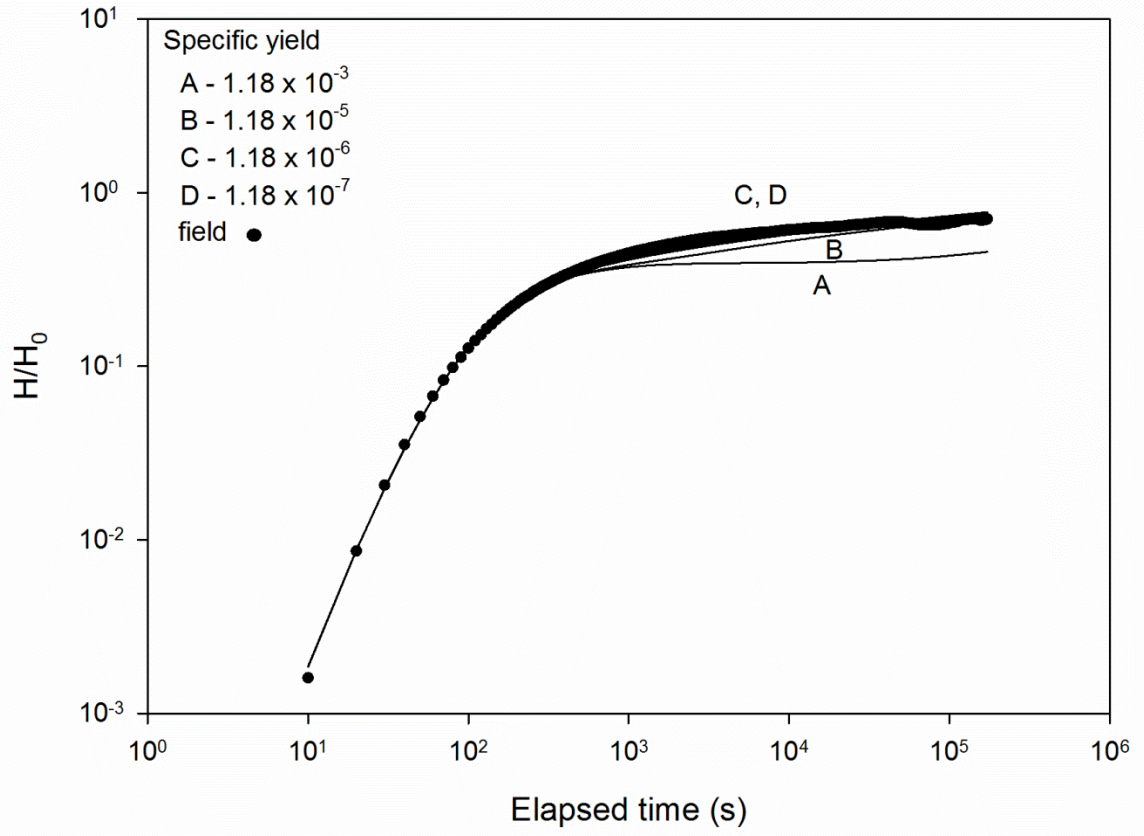


Figure E.8 Pumping test response in FC-1 to pumping in FC-9 by holding K' fixed and varying values of S_y .

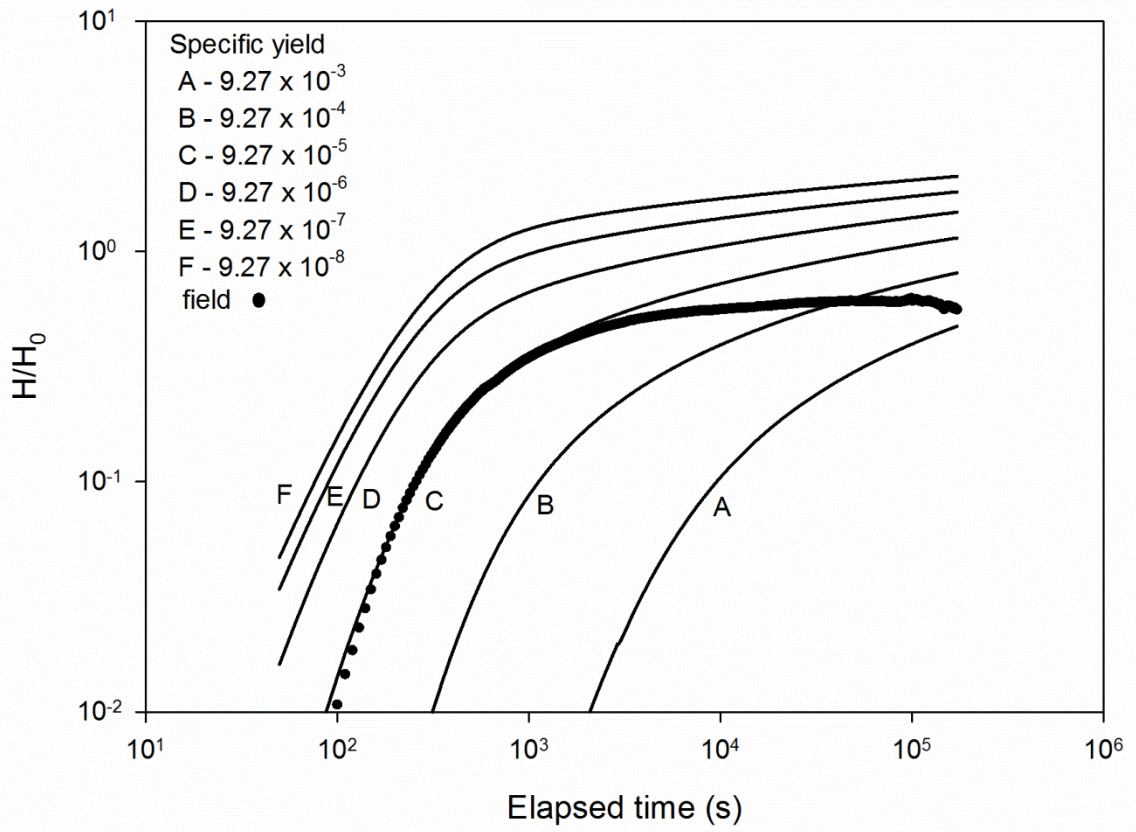


Figure E.9 Pumping test response in FC-6 to pumping in FC-7 by holding K' fixed and varying values of S_y .

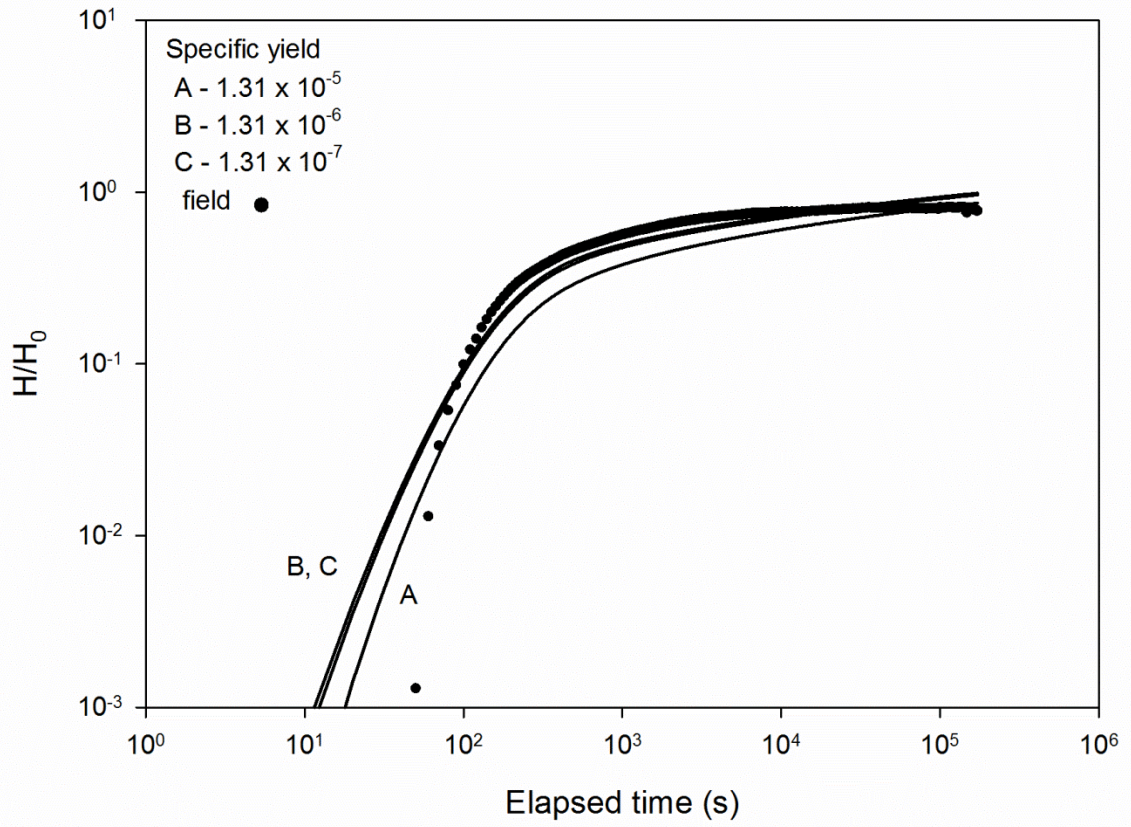


Figure E.10 Pumping test response in FC-5 to pumping in FC-7 by holding K' fixed and varying values of S_y .

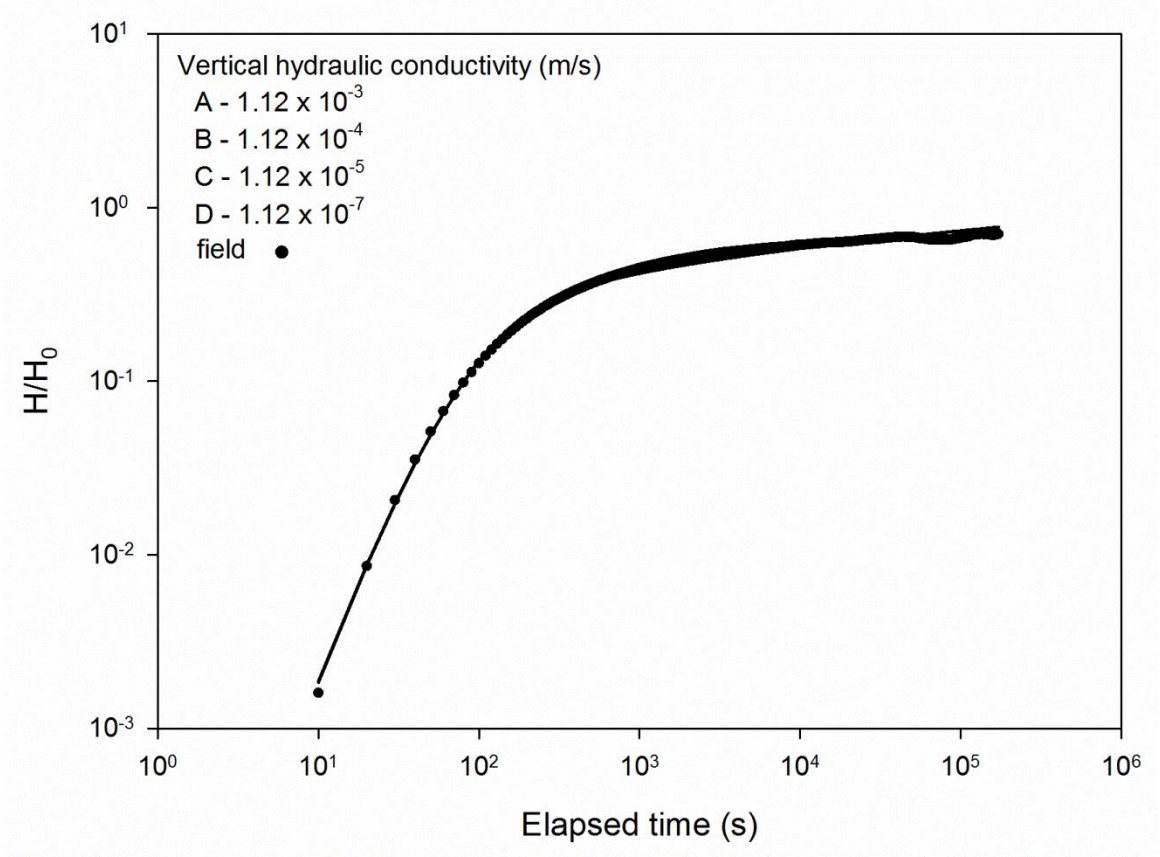


Figure E.11 Pumping test response in FC-1 to pumping in FC-9 by holding S_y fixed and varying values of K' .

Appendix F

Sensitivity of the source and interference responses to the Elmhirst and Novakowski (2012) solution for a pulse interference test

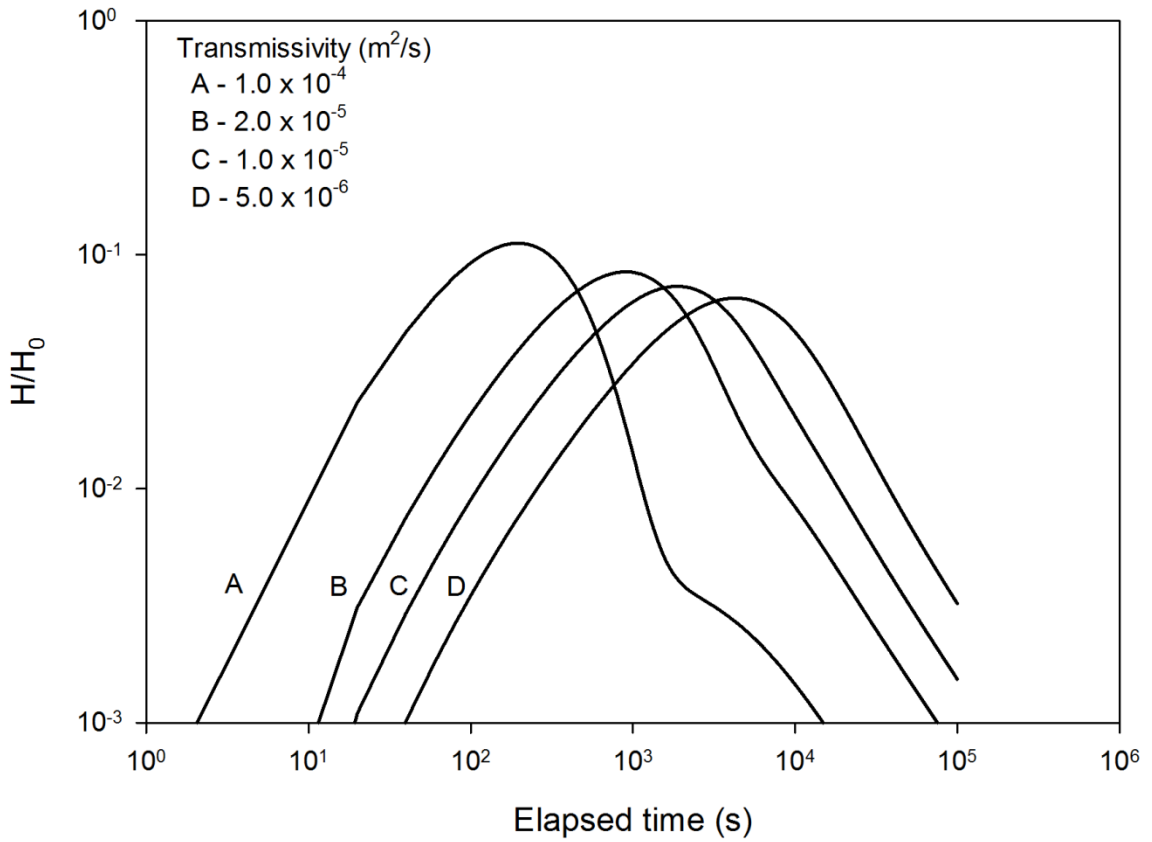


Figure F.1 Effect of transmissivity on the pulse interference test response for an observation well.

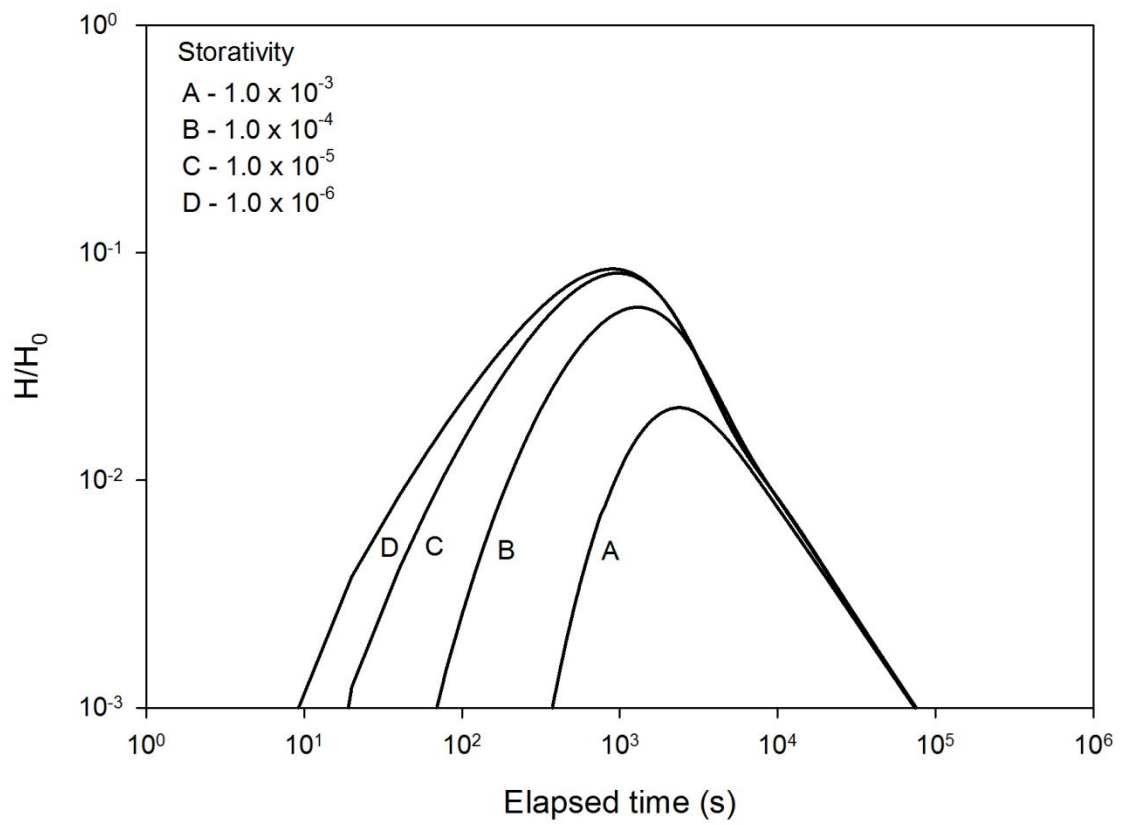


Figure F.2 Effect of storativity on the pulse interference test response for an observation well.

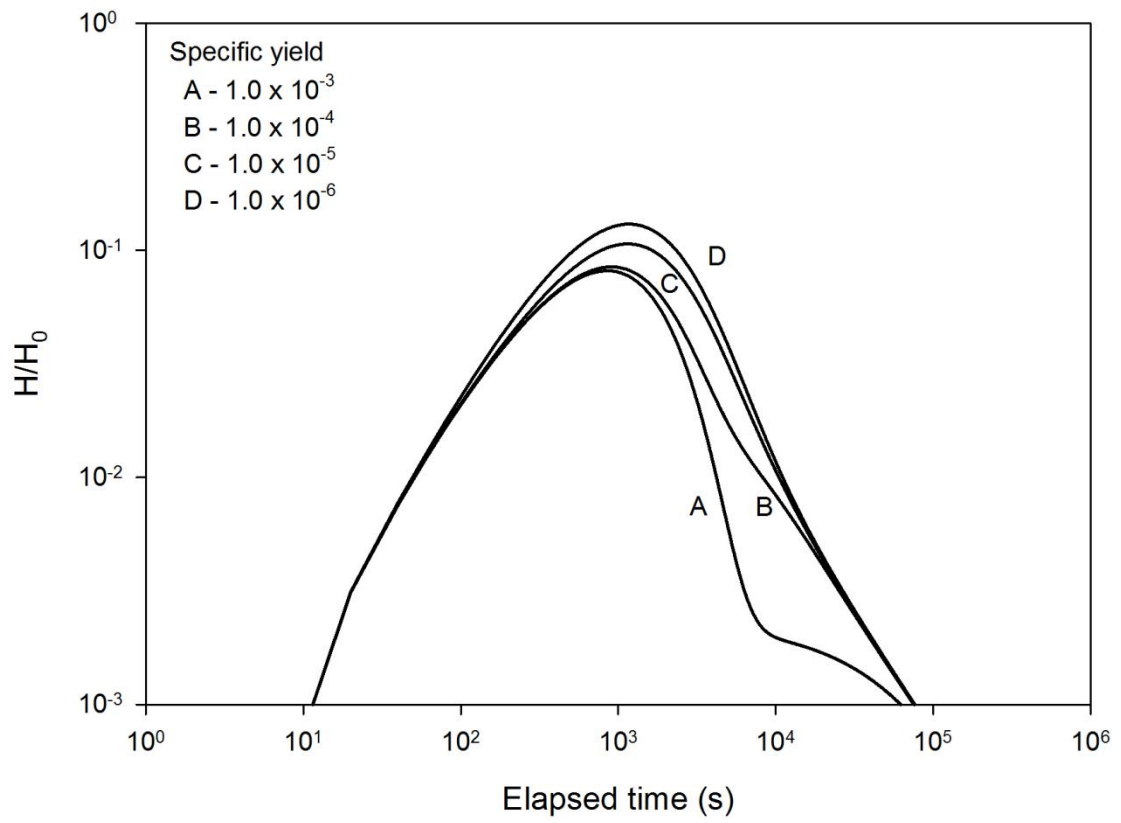


Figure F.3 Effect of specific yield on the pulse interference test response for an observation well.

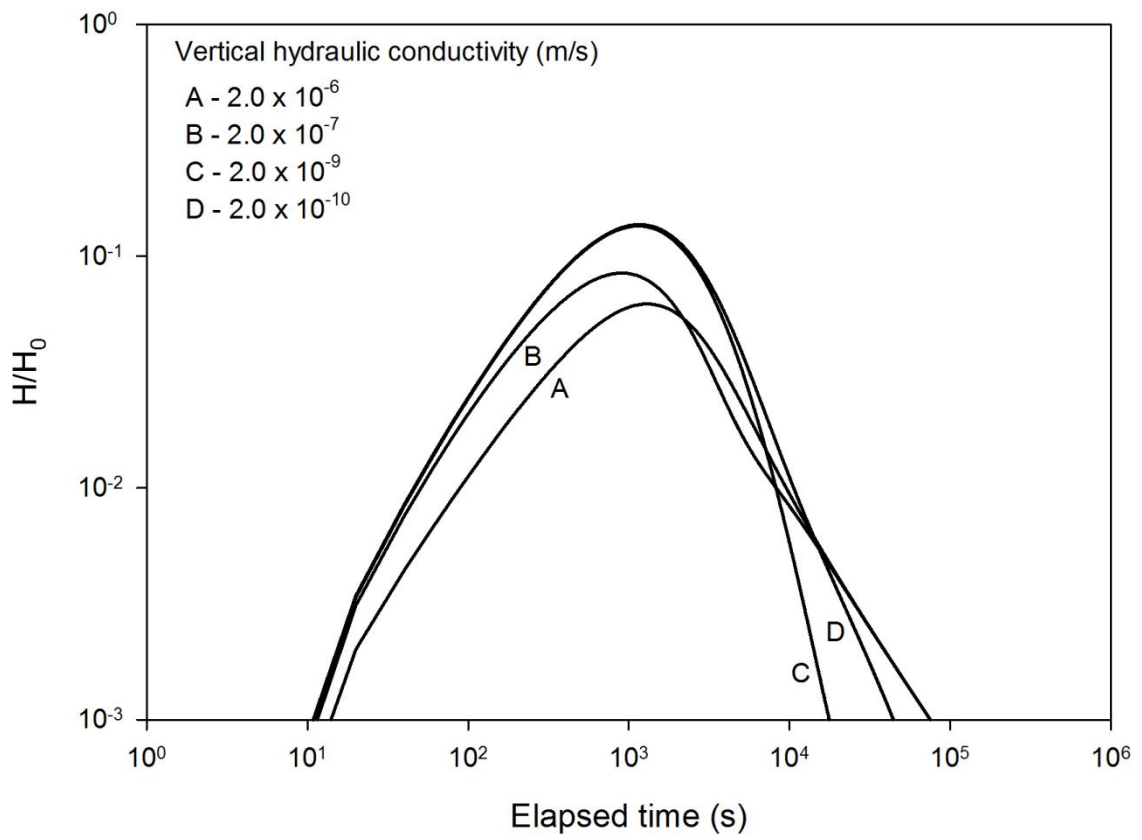


Figure F.4 Effect of vertical hydraulic conductivity on the pulse interference test response for an observation well.

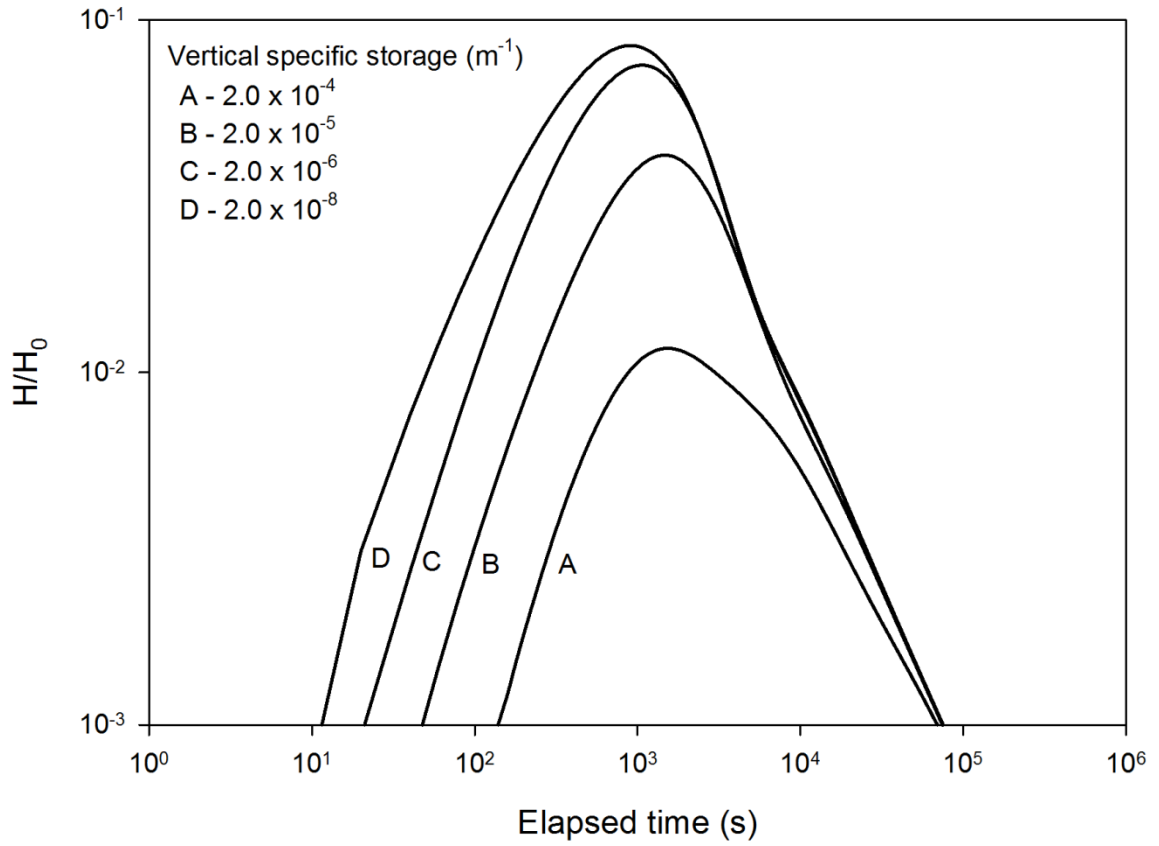


Figure F.5 Effect of vertical specific storage on the pulse interference test response for an observation well.

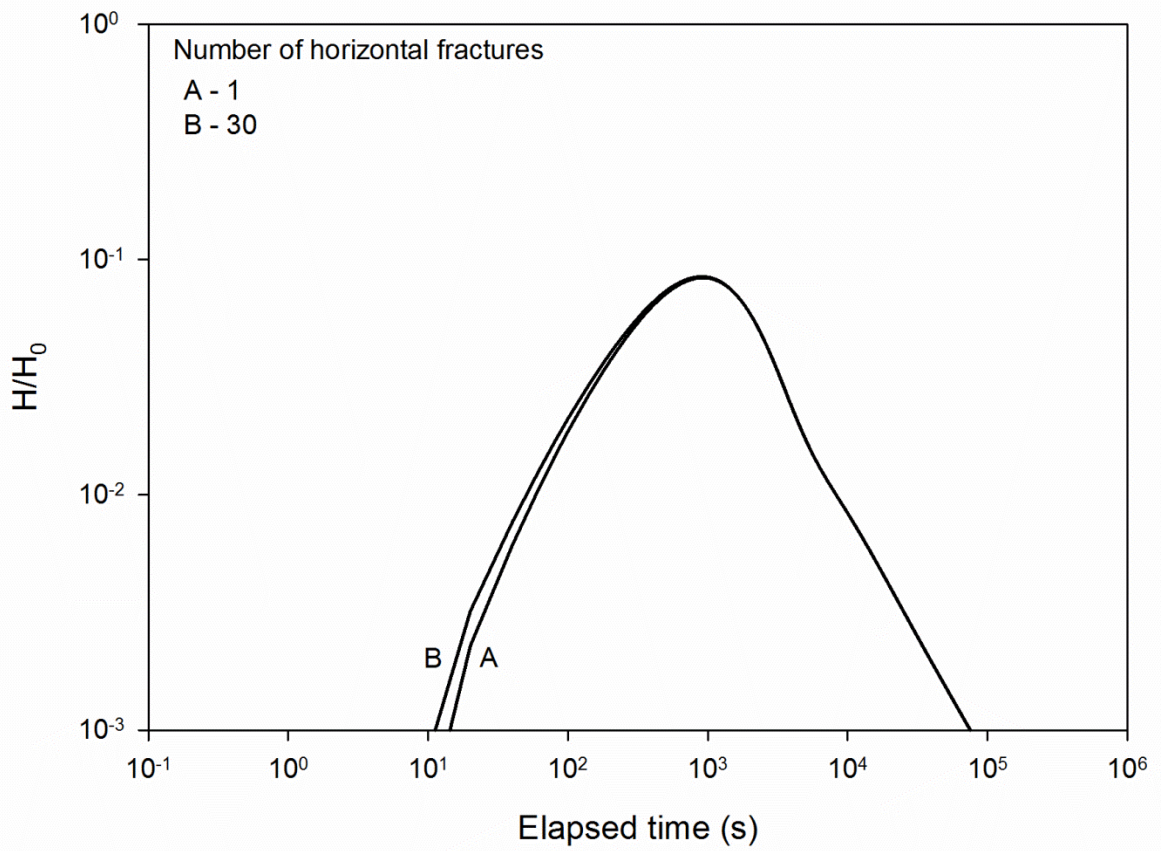


Figure F.6 Effect of number of horizontal fractures on the pulse interference test response for an observation well.

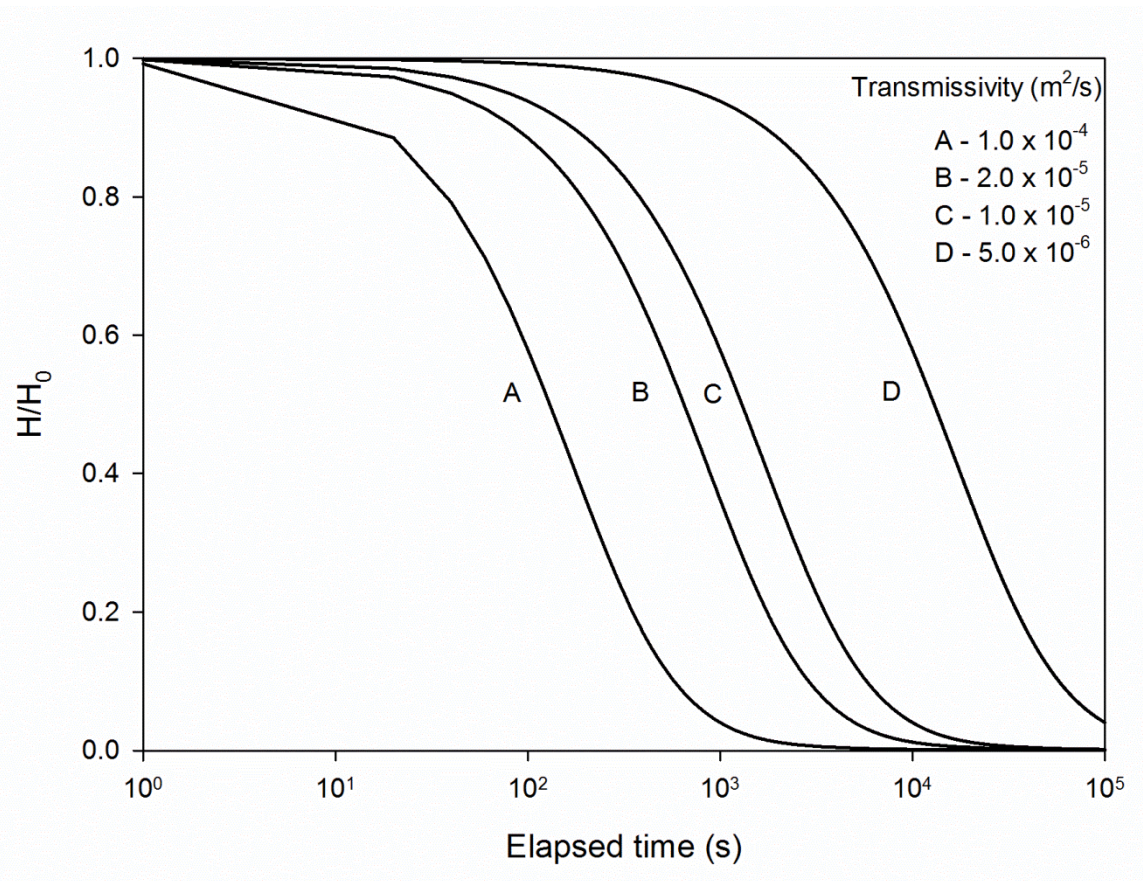


Figure F.7 Effect of transmissivity on the pulse interference test source well response.

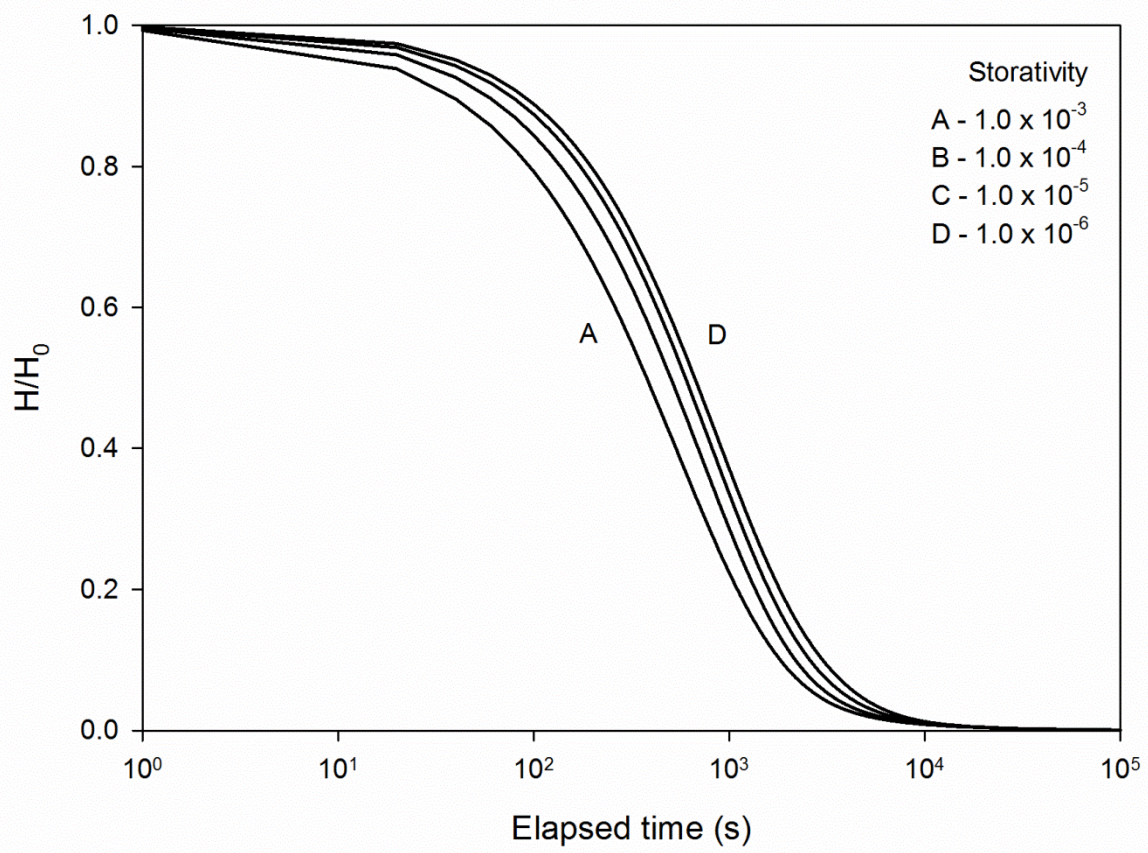


Figure F.8 Effect of storativity on the pulse interference test source well response.

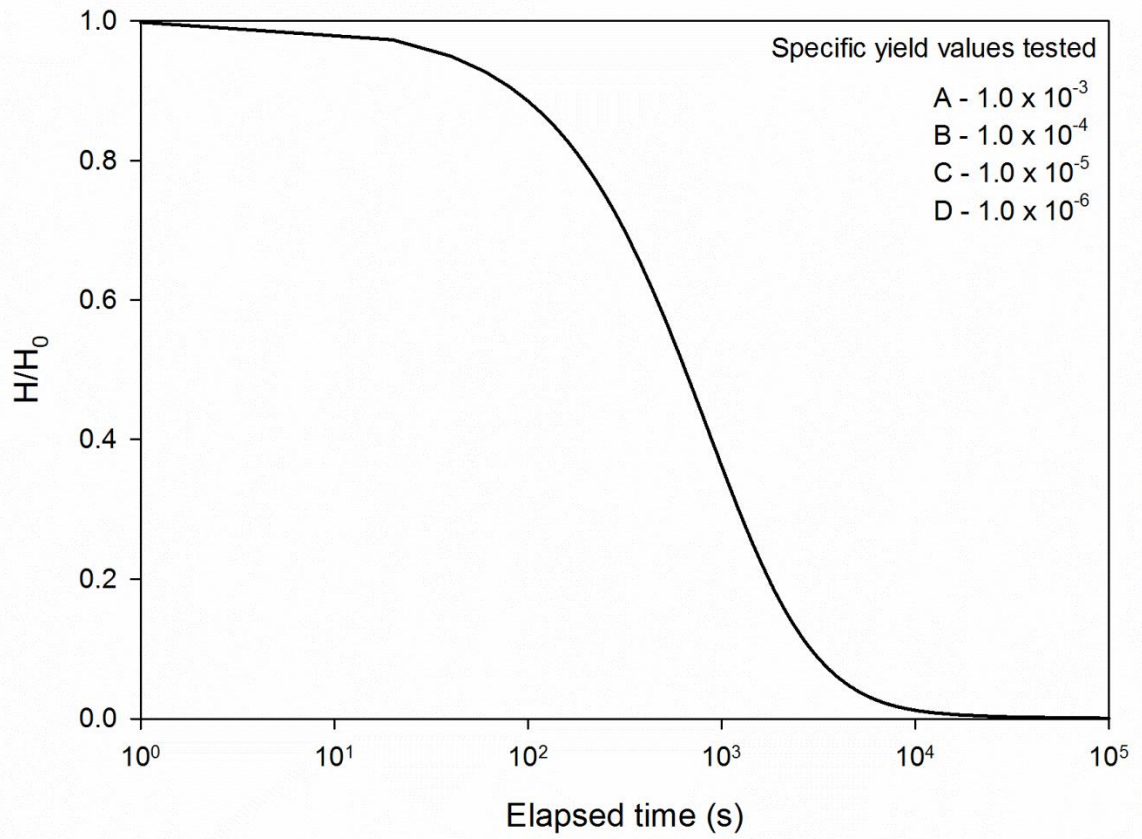


Figure F.9 Effect of specific yield on the pulse interference test source well response.

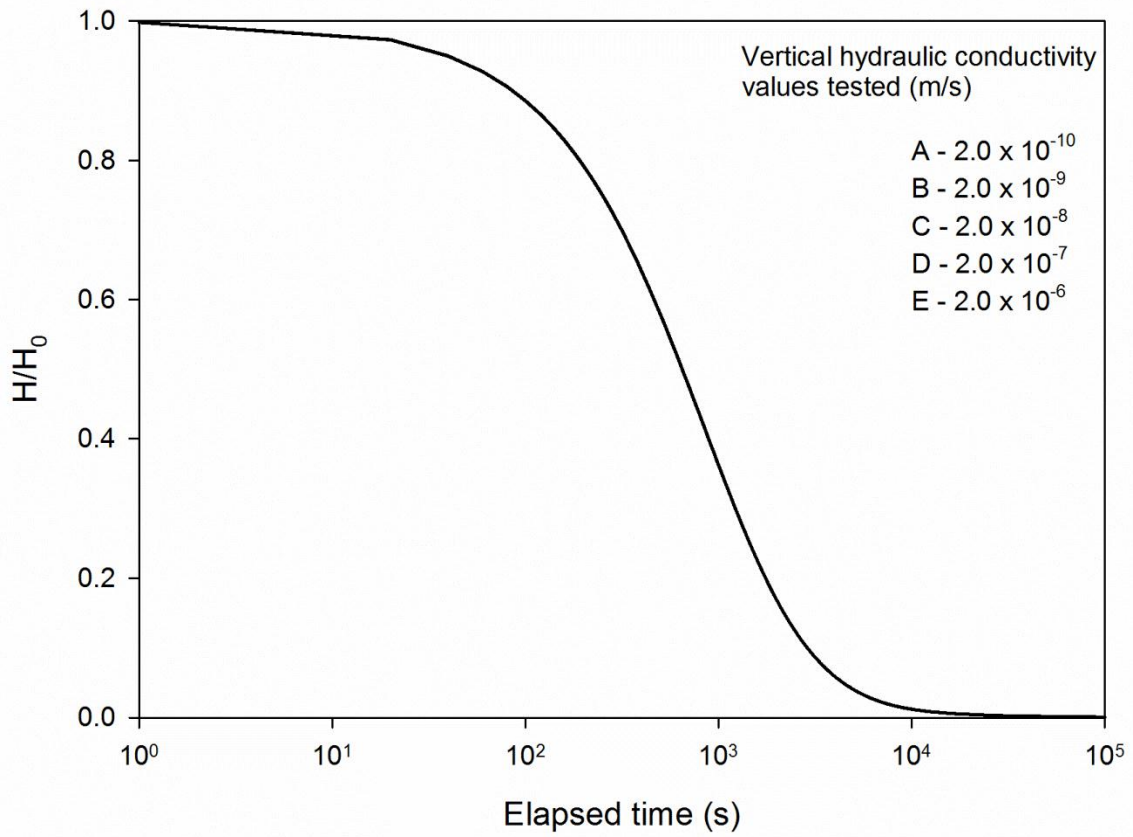


Figure F.10 Effect of vertical hydraulic conductivity on the pulse interference test source well response.

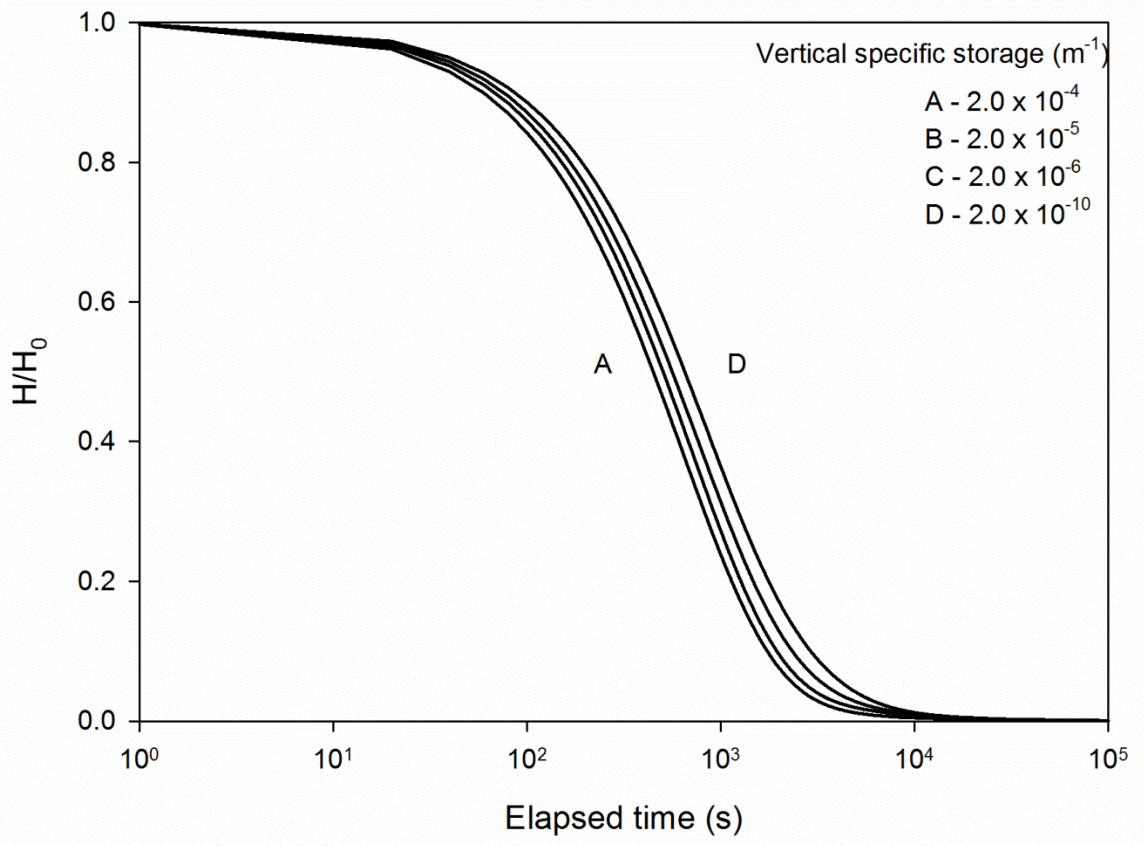


Figure F.11 Effect of vertical specific storage on the pulse interference test source well response.

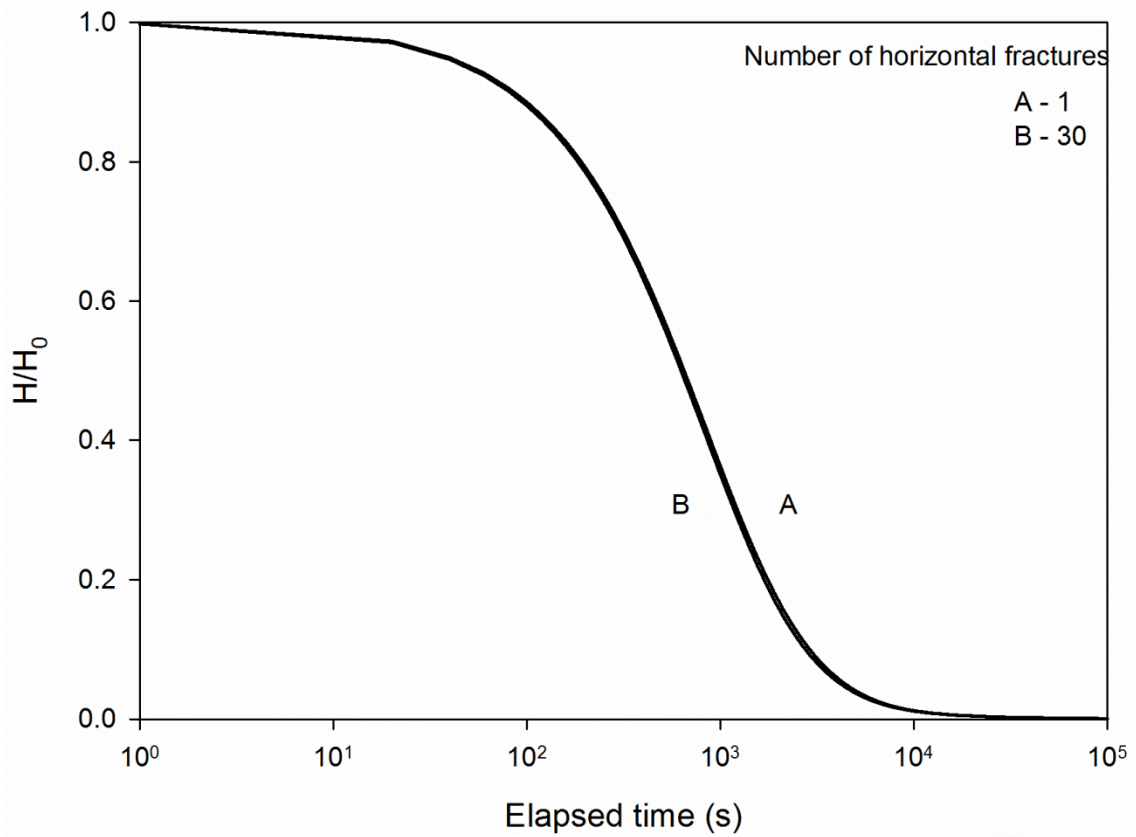


Figure F.12 Effect of number of horizontal fractures on the pulse interference test source well response.